INVESTIGATION OF STANDARD TEST PROCEDURES FOR INTEGRAL STORAGE SOLAR DOMESTIC HOT WATER SYSTEMS

by

Russell Charles Lindsay

Thesis submitted to the Faculty of the

Virginia Polytechnic Institute and State University

in partial fulfillment of the requirements for the degree of

MASTER OF SCIENCE

in

Mechanical Engineering

APPROVED:

William C. Thomas
W. C. Thomas, Chairman

F J Pierce
F. J. Pierce

David H. Vaughan
D. H. Vaughan

July, 1983

Blacksburg, Virginia

ACKNOWLEDGEMENTS

The author would like to express his gratitude to Dr. William C. Thomas for his patience and support throughout this research effort. Thanks are also extended to fellow students and faculty members at VPI&SU for their help and encouragement. The National Bureau of Standards is also gratefully acknowledged for providing the financial support for this investigation.

Finally, a special thanks is extended to his parents, for their support and encouragement throughout his education, and to Paula, whose patience and inspiration made this achievement possible.

TABLE OF CONTENTS

TABLE OF CONTENTS (cont'd)

Page

LIST OF FIGURES

LIST OF TABLES

NOMENCLATURE

A_a	Collector aperture area, m^2
A_c	Cover area, m^2
A_r	Reflector surface area, m^2
A_t	Tank (absorber) surface area, m^2
b_c	Bottom clearance between tank and reflector, m
C_e	Effective specific heat of the tank and fluid, kJ/(kg C)
C_f	Specific heat of the fluid, kJ/(kg C)
d	Cover plate spacing, m
E_{bc1}	Blackbody emissive power of cover 1 (σT_{c1}^4), W/m^2
E_{br}	Blackbody emissive power of reflector (σT_r^4), W/m^2
E_{bt}	Blackbody emissive power of tank (σT_t^4), W/m^2
E_{bsky}	Blackbody emissive power of sky (σT_{sky}^4), W/m^2
F_{mn}	Radiation shape factor from surface m to n
G_T^T	Total (global) irradiance in the tilted (aperture) plane, W/m^2
G_b	Beam irradiance, W/m^2
G_b^T	Beam irradiance normal to the tilted (aperture) plane, W/m^2
G_d^T	Diffuse irradiance in the tilted (aperture) plane, W/m^2
h_{cg}	Free convection coefficient between the inside cover and the gas (air) in the enclosure, $W/(m^2\ C)$
h_{rg}	Free convection coefficient between the reflector and the air in the enclosure, $W/(m^2\ C)$

h_{tg}	Free convection coefficient between the tank and the air in the enclosure, $W/(m^2\ C)$
h_{21}	Free convection coefficient between covers 1 and 2, $W/(m^2\ C)$
h_{23}	Free convection coefficient between covers 2 and 3, $W/(m^2\ C)$
h_w	Forced convection coefficient between the outside cover and ambient air (wind), $W/(m^2\ C)$
$\hat{J}_j$	Solar diffuse radiosity, jth surface, W/m^2
J_j	Longwave diffuse radiosity, jth surface, W/m^2
k	Thermal conductivity of air, W/(m C)
L	Cover thickness, mm
m_e	Effective mass of the tank and fluid, kg
$\dot{m}_d$	Mass flowrate of hot water draw, kg/s
Nu	Nusselt number, dimensionless
n_1	Index of reflection of air, dimensionless
n_2	Index of reflection of cover, dimensionless
Pr	Prandtl Number, dimensionless
$Q_{absorbed}$	Solar radiation absorbed by the tank and fluid, W
Q_{loss}	Energy lost by the tank and fluid by convection and longwave diffuse radiation, W
Q_{sra}	Solar radiation absorbed by the reflector, W
R_a	Rayleigh number, dimensionless
R_t	Radius of the tank, m
r_m	Reflectance for radiation polarized perpendicular to the plane of incidence

r_n	Reflectance for radiation polarized parallel to the plane of incidence
r	Number of reflections for a single ray
S_m	Mean solar flux on the tank (beam and diffuse), W/m^2
$S_{b,D}$	Direct component of the beam solar flux on the tank, W/m^2
S_{bm}	Mean beam solar flux on the tank, W/m^2
S_{br}	Beam solar radiation flux absorbed by the tank, W/m^2
S_{dm}	Mean diffuse solar flux on the tank, W/m^2
S_r	Reflected component of the beam solar flux on the tank, average of right and left sides, W/m^2
$S_{r,L}$	Left-side reflected component of the beam solar flux on the tank, W/m^2
$S_{r,R}$	Right-side reflected component of the beam solar flux on the tank, W/m^2
T_a	Ambient air temperature, K
T_{c1}	Temperature of cover 1, K
T_d	Average temperature of a hot water draw, K
T_g	Temperature of the gas (air) inside the collector enclosure, K
T_{in}	Inlet temperature of the fluid during a draw, K
T_r	Temperature of the reflector, K
T_{sky}	Effective blackbody temperature of the sky, K
T_t	Temperature of the tank (and fluid), K
T_{t_o}	Initial temperature of the tank (and fluid), K

U_L Overall heat loss coefficient based on tank surface area, $W/(m^2\ C)$

U_{LC} Overall heat loss coefficient based on cover area, $W/(m^2\ C)$

V_w Wind speed, m/s

W_a Aperture width, m

W_r Reflector surface width, m

Z_{max} Outer limit for reflector shading, m

Z_{min} Inner limit for reflector shading, m

Greek Symbols

α Absorptance, longwave

$\hat{\alpha}$ Absorptance, solar

β Collector slope, degrees

δ Declination, degrees

ε Emittance

ζ Projected incidence angle in an east-west plane normal to the aperture plane, degrees

η_c Daily collection efficiency

η_o Optical efficiency

θ Incidence angle of beam radiation, degrees

θ_Z Zenith angle, degrees

θ_2 Refracted angle, degrees

κ Extinction coefficient, mm^{-1}

ρ Reflectance, longwave

$\hat{\rho}$ Reflectance, solar

τ	Transmittance, longwave
$\hat{\tau}$	Transmittance, solar
$\hat{\tau}_{bc}$	Effective beam solar transmittance of the cover system
ϕ	Latitude, degrees
ψ	Projected incidence angle in a north-south plane normal to the aperture plane, degrees
ω	Hour angle, degrees

Subscripts

a	Ambient
b	Beam
c	Cover
c1	Cover 1
c2	Cover 2
c3	Cover 3
D	Direct
d	Diffuse
l	Left side
r	Reflector, right side
T	Total
t	Tank

Superscripts

T	Tilted
^	Solar wavelength
R	Average number of reflections for beam radiation

I. INTRODUCTION

The purpose of this investigation is to provide the experimental and analytical basis for the evaluation of possible test methods for a specific class of solar domestic hot water (SDHW) systems, namely integral storage collectors (ISC). Such systems generally consist of a relatively large water tank placed inside an insulated enclosure which has glazing on one or more sides to admit solar radiation. These systems, commonly called "breadbox" systems because some designs resemble a large breadbox, are an important class of SDHW system and are primarily used as a preheater for a conventional domestic hot water system. They are currently sold by a variety of manufacturers and possess several distinctive features which set them apart from other SDHW systems. ISC systems are constructed as a single unit, with the collection and storage functions combined. These systems are also truly "passive" since no pumps, controls, or tracking mechanisms are required in normal operation. All fluid circulation in the collector-storage unit is by thermosyphon action.

Consistent and repeatable test methods are needed to produce results which can be used to compare various ISC systems and estimate the economic benefits of different designs for specific applications. Such test methods should give reliable results at a reasonable cost and cover a wide range of ISC system designs. Presently, the only accepted consensus test standard for this class of SDHW systems requires the use of a solar irradiance simulator. Consequently,

testing of ISC systems for rating purposes is expensive and may be subject to credibility questions since artificial sunlight is used. The present investigation is concerned with evaluating experimental techniques for measuring the performance of ISC systems and developing analysis techniques useful toward the development of a test method which does not require the use of a solar irradiance simulator. Several possible test approaches are considered and evaluated based on the results of the experimental and analytical work.

1.1 Scope

Two commercial ISC's of very different designs were experimentally evaluated to obtain performance data for comparison purposes and to determine thermal stratification characteristics, transient characteristics, and response to varying environmental conditions. An experimental technique for measuring the instantaneous energy stored in the system was evaluated. The effects of draw schedule and forced circulation in the storage tank were also experimentally evaluated.

In addition to the experimental work, the functional elements of one of the systems from which experimental results were available were mathematically modeled. The analysis was designed to show whether it is feasible to simulate the collection process which occurs in ISC systems using a simplified theory and test-derived collector parameters.

1.2 Background

An industry consensus standard test method, ASHRAE Standard 95 (1), has recently evolved for SDHW systems. The systematic and uniform test procedures specified under ASHRAE Standard 95 are intended to give results which can be used to compare various SDHW systems and to estimate the economic benefits of different designs in different applications. This standard allows system testing using either a solar irradiance simulator or an in-line heat source. Outdoor testing using natural sunlight is not allowed because of repeatability problems caused by the variability and location dependence of daily irradiance profiles and ambient conditions. A test of the complete system is necessary to determine the dynamic interaction of the components and the effects on system performance. The rationale for adopting a mandatory test of the complete system and several possible approaches has been discussed in detail in references 2 through 4. These discussions stress the need for a test method which avoids the use of either extensive mathematical modeling or solar simulators to approximate the solar radiation spectrum.

When using the in-line heat source approach, the ASHRAE standard specifies the procedures to be followed to determine the thermal performance of the collector component in a separate test. Then, characteristics such as the collector thermal efficiency and incident angle modifier (IAM), along with a specified irradiance profile and ambient conditions, are used to program a conventional heat source

inserted in the system fluid loop to provide the energy input for carefully controlled nonirradiated tests of the complete system.

The present investigation is concerned with extending ASHRAE Standard 95 to include ISC systems using an in-line heat source approach. Several limitations become obvious when attempting to apply the current heat source method to ISC systems. The use of a conventional heat source in testing the system requires that the thermal performance of the collector portion of the system be available in terms of the prevailing environmental and operating conditions in accordance with ASHRAE Standard 93-77 (5). This requirement complicates testing ISC systems since the collector element is integral to the storage element and may not be readily removed and tested separately as for other types of SDHW systems. And in general, the performance of ISC systems is more strongly dependent on the weather conditions, especially the fraction of diffuse (scattered and reflected) solar irradiance, than that of a flat-plate collector. This results, in part, from the fact that ISC systems typically are designed with reflective features which are intended to concentrate the radiative flux onto the tank. Thermal stratification in the stored fluid also appears to be more critical in integral systems since the degree of stratification has been shown to have a strong effect on storage capacity (6, 7) and the thermal energy delivered. Because of these additional limitations, ASHRAE Standard 95 currently mandates the use of a solar irradiance simulator for the testing of ISC systems. The present investigation attempts to evaluate

procedures which may allow the in-line heat source approach to be used with ISC systems because solar simulators are expensive to build and operate, availability is limited, and questions remain on their credibility.

The present investigation resulted in all-day performance data for two ISC's under a range of operating, environmental, and irradiance conditions and a detailed analytical model for one ISC. A separate current research effort at VPI&SU is underway to characterize the collector subsystems of the same two ISC's. Then the two systems will be equipped with appropriate heat sources to determine if the measured outdoor results of the present investigation can be reasonably duplicated indoors using ASHRAE Standard 95 procedures. The latter experiments are to be conducted in the ASHRAE 95 test facility at the National Bureau of Standards. The ultimate objective is to recommend test procedures for this type of SDHW system for inclusion in ASHRAE Standard 95.

1.3 Literature Review

The body of literature dealing with SDHW systems includes very little pertaining to the standard testing of ISC systems. The New Mexico Solar Energy Association (NMSEA) has performed several comparisons of different ISC designs based on outdoor side-by-side tests of the systems (8, 9). This is similar to the "reference system" approach which Cooper and Lacey found to be unsatisfactory for systems with conventional flat-plate collectors (4). Several other studies

have been carried out in attempts to optimize the design of ISC systems (10, 11, 12), but few take into account the effects (positive or negative) that tank stratification has on the performance of integral storage collectors. Garg and Rani have shown that the tank geometry does indeed have a marked effect on thermal stratification which, in turn, affects the overall performance of the system (13). Koldhekar (7) and Fanney, et al. (6) have shown that storage tank stratification has a significant effect on the energy delivered and storage capacity of a thermal storage system. The transient simulation code TRNSYS (14) accounts for stratification in the storage tank of flat-plate SDHW systems by dividing the storage tank into a number of fully-mixed equal volume segments. Fluid entering the tank is assumed to be added to the segment (node) that most closely matches its temperature. Natural convection, entrainment, and conduction effects inside the tank are neglected. This model has not yet been extended to apply to ISC systems. Reichmuth and Robison have presented a simple transient model which uses test-derived parameters to predict the performance of ISC systems under a range of conditions assuming that the ISC is a single-node transient system, i.e. no stratification (15). The Reichmuth and Robison procedure, however, relies heavily on mathematical modeling and would likely not be acceptable as a means of calculating performance ratings for ISC systems under ASHRAE 95. In fact, none of these studies has resulted in an alternate test method which would meet the criteria of ASHRAE Standard 95 for integral storage systems.

II. EXPERIMENTAL APPARATUS AND PROCEDURES

2.1 Objectives

The main objectives for developing the experimental apparatus used in this investigation were to obtain all-day thermal performance data for comparison purposes and to determine whether stratification or forced circulation has a significant effect on the daily performance or delivered energy of the system. The experimental technique of estimating the instantaneous stored energy in the system from measured temperatures in the stored fluid was also evaluated. To accomplish the above tasks, special probes were constructed and an existing outdoor solar collector test facility was used.

2.2 Experimental Apparatus

The outdoor test facility was used to obtain performance data for two different commercial integral storage SDHW systems. Two ISC's of different geometries were used in this investigation in order to cover a wide range of design configurations with a minimum effort and to reduce the likelihood of making generalizations based on a single system. System A, manufactured by Tao-Starr, has a single Plexiglas^{TM} cover and a semicircular reflector surrounding a 304.8 mm (12 in.) diameter tank. System A has no insulation and is designed for installation with the axis of the tank along a north-south line in a tilted plane. System B, manufactured by Cornell Energy, has reflective polyisocyanurate insulation with one glass and two fiberglass covers

and is designed for installation with the axis of the 355.6 mm (14 in.) diameter tank along an east-west line in the horizontal plane. System A and B are shown in Figs. 1 and 2, respectively, and the dimensions and materials for these two systems are tabulated in Table 1.

Integrated systems A and B were mounted on an adjustable-tilt test rack set at 45 degrees. The test rack faces south and is located at a latitude of 37.23 degrees north. The necessary instrumentation and data recording equipment were located in a separate instrumentation room.

Instrumentation was available to measure the total (global) irradiance, beam irradiance, effective blackbody sky temperature, ambient temperature, wind speed, and tank fluid temperatures. The total solar radiation and infrared sky radiation were measured normal to the aperture plane of the ISC system using an Eppley model PSP pyranometer and an Eppley model PIR pyrgeometer, respectively. An Eppley model NIP pyrheliometer was used to measure the beam solar radiation and a three-cup model W103B Weathermeasure anemometer was used to measure wind speed. A type T thermocouple was mounted in a small, white, ventilated box near the test stand to measure the ambient air temperature.

One of the primary objectives of this investigation required measurement of the thermal stratification of the fluid inside the storage component of these systems. Therefore, probes were constructed for measuring the temperature of the fluid at five vertical

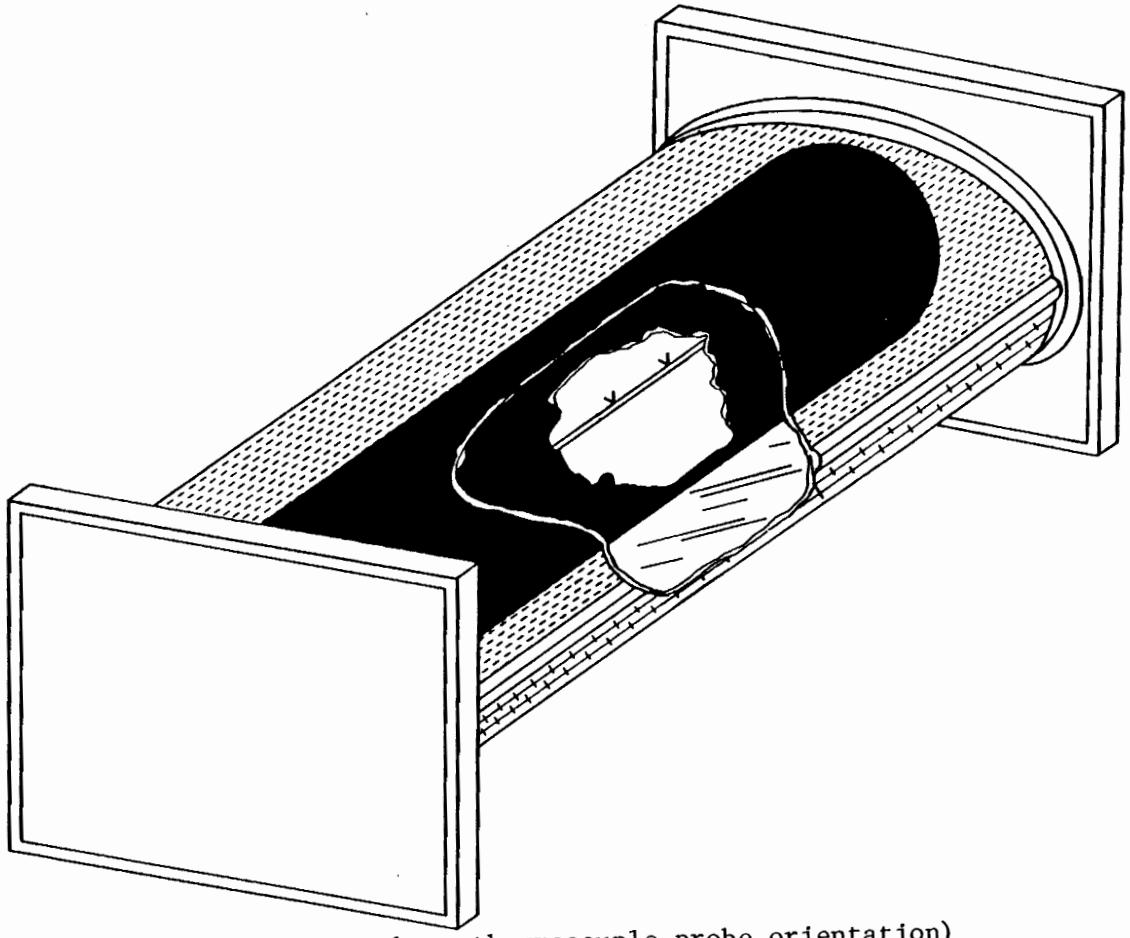

Figure 1. ISC System A (Cutaway shows thermocouple probe orientation)

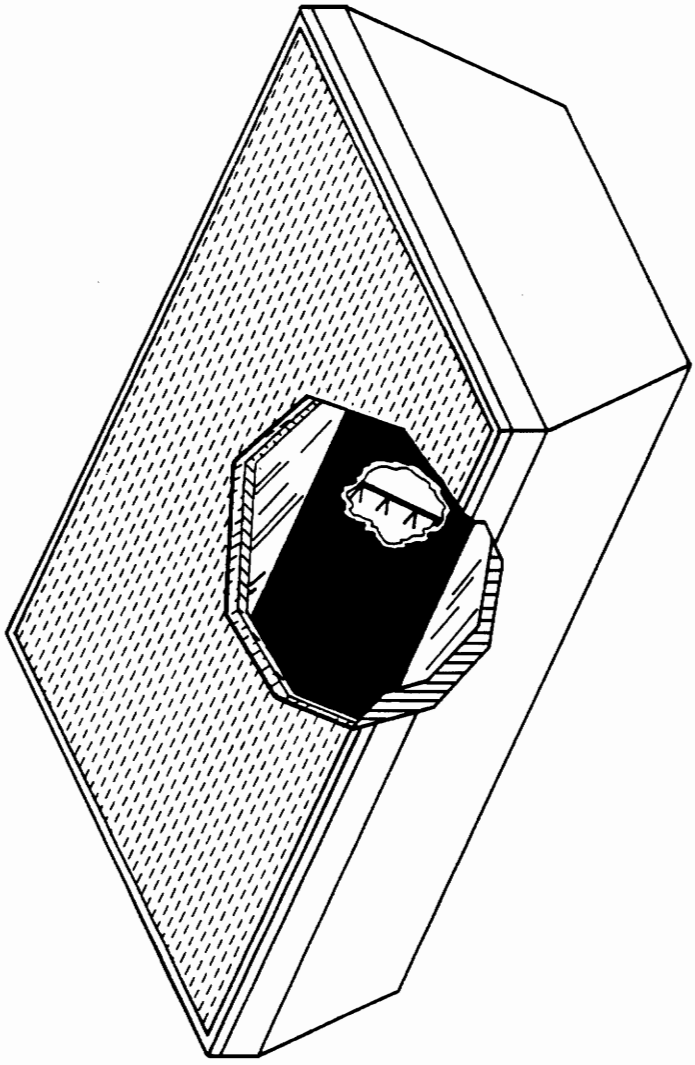

Figure 2. ISC System B (Cutaway shows thermocouple probe orientation)

Table 1

SPECIFICATION	ISC 'A'	ISC 'B'
Nominal Capacity (cu m)	0.121	0.121
Aperture Area (sq m)	0.846	1.317
Length (m)	1.63	1.62
Width (m)	0.52	1.04
Tank Diameter (mm)	304.8	355.6
Covers	Plexiglas	Low Iron Glass (1, outer) Fiberglass Acrylic (2, inner)
Insulation	None	Reflective Polyisocyanurate

heights inside each tank. These probes and their position inside each tank can be seen in Figs. 1 and 2. The junctions of these type T thermocouple probes were electrically insulated from the water (and each other) using silicone rubber sealant and heat shrink tubing to prevent the occurrence of ground loops.

Instantaneous values for the solar radiation and wind speed can change significantly in a few seconds. Therefore, these measurements, as well as the ambient temperature and the measured fluid temperatures and flowrates were integrated over five-minute periods by electronic integrators, manufactured by AGM, Incorporated. Average values for each five-minute interval were then input to a TRS-80^{TM} Model III microcomputer which converted signals to "real" quantities using stored calibration data. The microcomputer displayed the measured quantities, produced a printed record of each measurement, and calculated hourly averages for each measurement. At the end of each test, the microcomputer stored the hourly averages on a cassette tape for transfer to the VPI&SU mainframe computer and permanent storage. The data acquisition system using the microcomputer is described in more detail in Appendix A. The infrared sky temperature was recorded on a Westronics model LD11D strip chart recorder.

A schematic of the piping used in this investigation is shown in Fig. 3. The pump and "bypass loop" were needed for two purposes: to validate the method of averaging measured tank stratified temperatures to estimate instantaneous system energy and to minimize stratification in the tank to determine the effect of stratification on ISC system

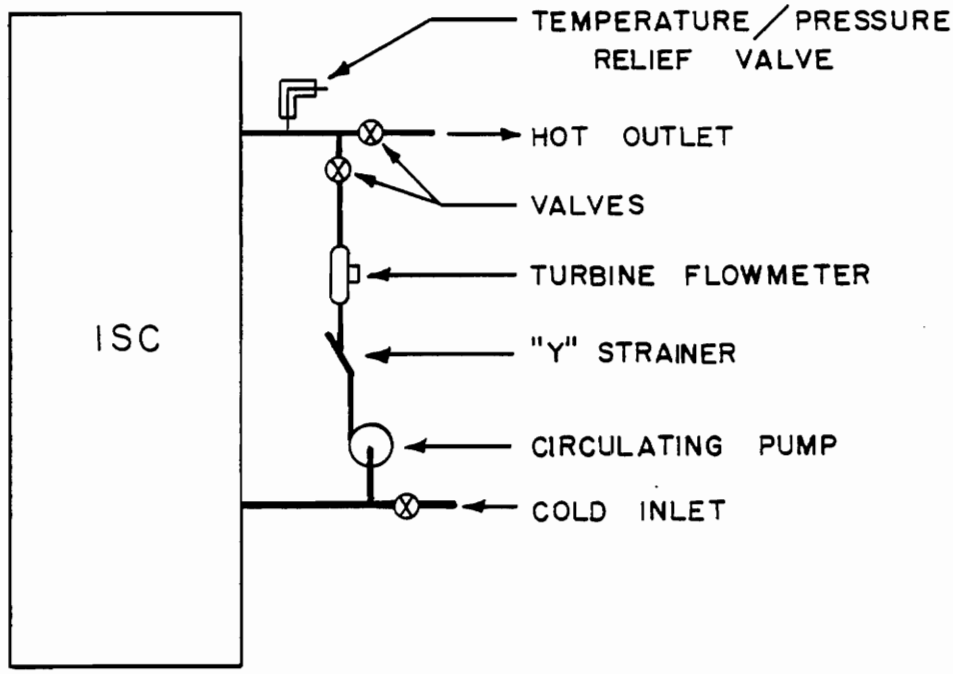

Figure 3. Piping Schematic for the ISC Tests

performance. The same arrangement was used for the tests on both ISC systems A and B, but the different system geometries required the use of slightly different physical layouts for the two systems. Flowrates through the circulation loop were measured using a Flow Technology model FT-8M3-LB Turbine Flowmeter. The flowmeter pulses were counted for each five-minute period and input to the microcomputer data acquisition system.

Also required for this experimental investigation was a method for accurately measuring the thermal energy contained in hot water draws which were taken from the ISC systems during some tests. Therefore, an "adiabatic" box was constructed which could contain 0.1168 m^3 (4.125 ft^3) of withdrawn water and maintain its temperature while the mass and mixed temperature of the water were measured. This box was constructed of plywood, insulated on the inside with 50.8 mm (2 in.) thick polystyrene rigid insulation, and lined with a polyethylene liner to contain the water and is shown in Fig. 4. This type of construction was chosen so that the effective thermal mass of the container was minimized by putting bulky structural materials outside, insulated from the water mass by a low density insulation, thus reducing inaccuracies caused by the heat capacity of the container.

2.3 Experimental Procedures

The realization of the objectives of this experimental investigation requried three types of all-day tests on the two integral systems. All of the tests were performed for both system A and B and

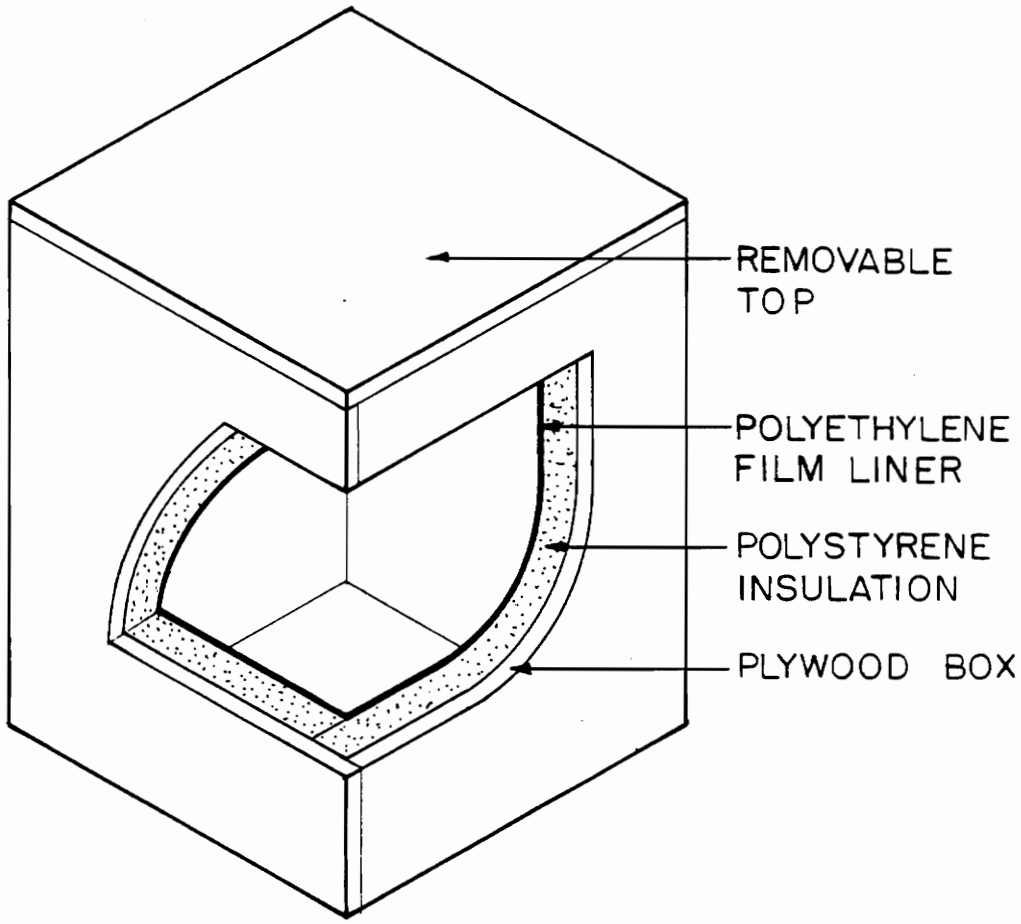

Figure 4. "Adiabatic" Box to Contain Heated Water Withdrawn from ISC's

were begun with the system filled with water at a uniform temperature. Prevailing environmental conditions and tank fluid temperatures were measured continuously throughout each test.

The first type of test was an all-day test with no withdrawal of heated water during the day and without circulation of fluid through the collector. The bypass valve at the pump outlet remained closed throughout the test. This flow configuration eliminated the possibility of any fluid circulation which might be caused by thermosyphon action in the tank. At the end of the test period, after which the stratified fluid temperatures were recorded, the bypass valve was opened and the pump turned on to mix the fluid thoroughly. When the resulting temperature readings from the five thermocouples in the tank were approximately equal (and not changing) the tank was assumed to be fully mixed. This "mixed" temperature was compared with the stratified average temperature to verify the accuracy of the technique of estimating the instantaneous energy in the tank using the measured stratified temperatures. This series of tests should give a conservative estimate of the accuracy of this technique since the maximum stratification should occur under the no draw, no circulation conditions. This no draw, no circulation test will be referred to in later sections as a type I test.

The second type of test performed was an all-day test with a single draw of approximately half the volume of the system capacity taken at solar noon. The bypass valve was also closed as for the type I test. The draw was accomplished by manually opening the discharge

valve of the system and allowing the pressure of the water main to force hot water from the collector. This heated water was collected in the adiabatic box described previously until the target draw mass was reached. Then the discharge valve was closed and the net weight of the draw determined by measuring the gross weight of the box and subtracting the tare weight of the box. The temperature of the draw was determined by measuring the mixed water temperature with a mercury-in-glass thermometer. The energy supplied to the system from the inlet water was determined by averaging the measured temperatures of the water supply before and after the draw. This test was terminated in the same manner as the type I tests where the energy in the tank was determined both from averaging the stratified temperatures and from the "mixed" temperature. This type of test will be referred to as a type II test.

The final type of test which was performed in this investigation was an all-day test during which the bypass valve was open and the circulating pump running slowly, providing a mixing effect, for the duration of the test. This test was designed to give some indication of the effects of operating under forced flow conditions instead of natural convection. The stratification of the storage tank was expected to be minimal for this test so that the instantaneous energy of the tank was easy to determine from the measured temperatures in the tank. This test was performed to help evaluate the possible method of using an external heat source in series with the collector/storage system in an ASHRAE 95-type test. This test was

also used to determine whether thermal stratification has a significant effect on the daily energy collected in an ISC system. Two nominal flowrates were used for this test to determine the extent to which circulation rate affects the degree of stratification. This type of test will be referred to as a type III test.

III. ANALYSIS

3.1 Objectives

A mathematical model was needed to correlate test results and evaluate the applicability of any proposed test method to other ISC designs. The objective of the analysis was to obtain a tractable mathematical expression for the simulation of solar energy collected in an ISC system. An attempt was made to determine whether the solar collection process can be accurately simulated using a simplified theory and test-derived parameters for the collector elements, thereby avoiding the mandatory use of a solar irradiance simulator for the standard test. A detailed analysis was carried out for system B, but a similar analysis could be carried out for system A or any other system with slight changes to account for different geometries.

3.2 Assumptions

The following simplifying assumptions were used in the analysis:

1. Heat transfer through the covers and back-side insulation is one-dimensional.
2. Thermal conduction resistances through the absorber (tank) and individual covers are negligible compared to radiation and convection resistances.
3. Cover surfaces obey ideal optical laws.
4. Component surface properties and thermal properties are not temperature dependent.

5. Radiation exchange can be divided into three types:
    a) Diffuse-gray long wave (infrared) radiation
    b) Diffuse-gray short wave (solar) radiation
    c) Specular (beam) solar radiation

    Wavelength- and directional-dependence of surface properties can be approximated for these three types of radiation exchange.
6. All solar radiation reflected from the absorber (tank) is diffuse.
7. Fluid temperature in the tank is uniform, i.e. no thermal stratification.
8. Heat capacity of the reflector and covers is negligible with respect to that of the tank, i.e. only the time response of the tank (and fluid) need be considered and all other components can be assumed to be in thermal equilibrium at all times.
9. An effective length can be used to account for end effects.
10. The air in the collector is a nonparticipating medium for radiation heat transfer.
11. The solar flux distribution on the absorber (tank) can be treated as a mean flux because of the high thermal conductivity of the steel tank.

3.3 Absorber-tank Transient Analysis

A single-node transient analysis was performed for the absorber-tank and the average hourly temperature calculated based on the measured environmental conditions. An overall loss coefficient based on the absorber temperature was defined analogous to that used in flat-plate collector analyses.

$$Q_{loss} = U_{LC} A_c (T_t - T_a) \qquad 3.1$$

An optical efficiency was also defined as the solar radiation which reaches the absorber divided by that incident on the aperture plane of the collector.

$$\eta_o = \frac{Q_{absorbed}}{A_c G_T} \qquad 3.2$$

Using the above definitions, an energy balance on the tank yields the differential equation

$$dQ = m_e C_e dT_t = \dot{m}_d C_f [T_{in} - T_t] + A_c \{G_T \eta_o - U_{LC} [T_t - T_a]\} \qquad 3.3$$

where m_e and C_e are the effective mass and specific heat of the tank, respectively, and $\dot{m}_d$ is the mass flowrate of a hot water draw. This equation also applies when there is no draw if $\dot{m}_d$ is set equal to zero. After integration, equation 3.3 can be solved for the tank temperature, T_t, after an interval τ with an initial tank temperature, T_{t_o}.

$$T_t = T_{t_o} \exp\left(-\frac{\dot{m}_d C_f + U_{LC}A_c}{m_e C_e}\tau\right)$$

$$+ \left[\frac{\dot{m}_d C_f T_{in} + A_c(G_T\eta_o + U_{LC}T_a)}{\dot{m}_d C_f + U_{LC}A_c}\right]\left[1 - \exp\left(-\frac{\dot{m}_d C_f + U_{LC}A_c}{m_e C_e}\tau\right)\right]$$

3.4

For ease of comparison with experimental data, for which hourly average values were measured, the average tank temperature during a time interval $\Delta\tau$ is also desired. This average temperature is obtained by integrating equation 3.4.

$$\overline{T}_t = \frac{\int_{\tau_{k-1}}^{\tau_k} T_t \, d\tau}{\tau_k - \tau_{k-1}} \qquad 3.5$$

This integration yields the following equation:

$$\overline{T}_t = \frac{\dot{m}_d C_f T_{in} + A_c\,(G_T\eta_o + U_{LC}T_a)}{(\dot{m}_d C_f + U_{LC}A_c)}$$

$$+ \frac{\dot{m}_d C_f\,[T_{t_o} - T_{in}] + U_{LC}A_c\,[T_{t_o} - T_a] + G_T A_c \eta_o}{[\dot{m}_d C_f + U_{LC}A_c]^2\,\Delta\tau}\,(m_c C_e)$$

$$\left\{1 - \exp\left(-\frac{[\dot{m}_d C_f + U_{LC}A_c]\,\Delta\tau}{m_e C_e}\right)\right\}$$

3.6

For an interval where there is no draw, this reduces to

$$\overline{T}_t = \frac{G_T\eta_o + U_{LC}T_a}{U_{LC}} + \left\{\frac{U_{LC}\,[T_o - T_a] + G_T\eta_o}{U_{LC}^2\,\Delta\tau\,A_c}\right\}(m_eC_e)$$

$$\left\{1 - \exp\left(-\frac{U_{LC}\,A_c\,\Delta\tau}{m_eC_e}\right)\right\}. \qquad 3.7$$

Equations 3.3 thru 3.7 all require that the value of the parameters U_{LC} and η_o be "known" for the time period under consideration. The estimation of these two parameters requires some means of estimating the radiative and convective heat transfer between collector components and each other (and the environment) and the solar flux on the tank. The determination of the loss coefficient and the optial efficiency is the topic of the next few sections.

3.4 Optical Efficiency - Shortwave Radiation Analysis

The evaluation of an optical efficiency for the collector requires that the mean solar flux on the absorber (tank) be determined. This mean solar flux is made up of beam radiation (direct and reflected) and scattered (diffuse) radiation in the collector enclosure.

$$S_m = S_{bm} + S_{dm} \qquad 3.8$$

Following a similar analysis for a concentrating collector in reference 16, the determination of an average beam flux, S_{bm}, is

accomplished using a ray-tracing approach and is described in detail in Appendix B.

The shortwave diffuse radiation is evaluated using a radiosity approach to determine the radiosities shown in Fig. 5. The equations which result are listed below for each surface.

Absorber-tank:

$$\hat{J}_t = \left(\frac{1 - \hat{\alpha}_t}{\hat{\alpha}_t}\right) S_{br} + (1 - \hat{\alpha}_t) F_{tc}\hat{J}_c + (1 - \hat{\alpha}_t) F_{tr}\hat{J}_t \qquad 3.9$$

where S_{br} is the beam radiation absorbed by the tank.

Reflector:

$$\hat{J}_r = \hat{\rho}_r (F_{rt}\hat{J}_t + F_{rc}\hat{J}_c + F_{rr}\hat{J}_r) + \text{B.R.S.} \qquad 3.10$$

where B.R.S. is the beam radiation reflected as scattered and is given by:

$$\text{B.R.S.} = G_b^T \hat{\tau}_{bc} \frac{(Z_{max} - Z_{min})\hat{\rho}_r^r}{W_r} - \frac{S_{br}A_t}{A_r} \qquad 3.11$$

Covers:

$$\hat{J}_c = \hat{\tau}_{c1}\hat{J}_2 + \hat{\rho}_{c1} (F_{ct}\hat{J}_t + F_{cr}\hat{J}_r) \qquad 3.12$$

$$\hat{J}_1 = \hat{\tau}_{c1}(F_{ct}\hat{J}_t + F_{cr}\hat{J}_r) + \hat{\rho}_{c1}\hat{J}_2 \qquad 3.13$$

$$\hat{J}_2 = \hat{\tau}_{c2}\hat{J}_4 + \hat{\rho}_{c2}\hat{J}_1 \qquad 3.14$$

$$\hat{J}_3 = \hat{\tau}_{c2}\hat{J}_1 + \hat{\rho}_{c2}\hat{J}_4 \qquad 3.15$$

$$\hat{J}_4 = \hat{\tau}_{c3} G_d^T + \hat{\rho}_{c3}\hat{J}_3 \qquad 3.16$$

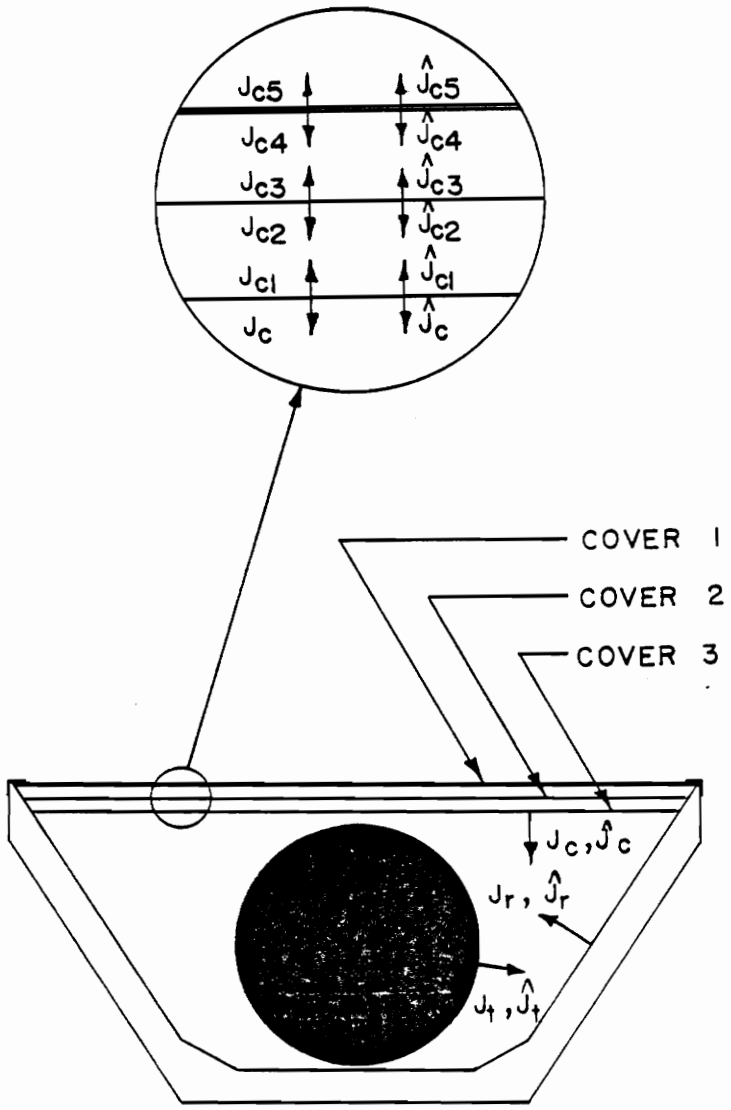

Figure 5. Radiosity Distributions in ISC B (Solar and Infrared)

These seven equations can then be solved for the seven unknowns ($\hat{J}_t$, $\hat{J}_r$, $\hat{J}_c$, $\hat{J}_1$, $\hat{J}_2$, $\hat{J}_3$, and $\hat{J}_4$) by an appropriate mathematical technique. Since the solar radiation distribution is not the same on the right and left sides for off-normal incidence, the previous seven equations are solved twice - once for each side. The left and right-side radiosities are averaged to use as inputs for the optical efficiency calculation and component energy balances in the next section. The mean diffuse radiation flux is calculated from the averaged left- and right-side radiosities

$$S_{dm} = \hat{\alpha}_t \left(F_{tc} \hat{J}_{c,avg} + F_{tr} \hat{J}_{r,avg}\right) \qquad 3.17$$

Then the energy absorbed, $Q_{absorbed}$, which is needed for the calculation of the optical efficiency (equation 3.2) is simply the product of the mean solar flux, S_m, and the tank area, A_t.

The radiation shape factors were evaluated using a result tabulated in Sparrow and Cess (17) for F_{ct}. The remainder of the shape factors were calculated using shape factor identities for enclosures, assuming that the clearance between the tank and the covers and reflector could be neglected, so that only three surfaces were considered.

Optical properties were evaluated as described in Appendix C. Note that short wave properties are denoted with a "$\hat{}$" over the symbol and beam properties are given a "b" subscript.

3.5 Component Energy Balances

Since all of the other elements of the collector are assumed to be in instantaneous thermal equilibrium with the storage tank and ambient conditions, their average hourly temperature can be found from energy balances on each element. The energy balance equations are as follows:

Reflector:

$$\frac{\varepsilon_r}{1 - \varepsilon_r}\left(\sigma T_r^4 - J_r\right) - \hat{\alpha}_{scl}\left[F_{rc}\hat{J}_c + F_{rt}\hat{J}_t + F_{rr}\hat{J}_r\right]$$

$$+ h_{rg}\left(T_r - T_g\right) + U_{ra}\left(T_r - T_a\right) - Q_{sra} = 0 \qquad 3.18$$

where Q_{sra} is the solar (shortwave) radiation absorbed by the reflector and is given by

$$Q_{sra} = G_b \tau_{bc} \cos\theta \left[Z_{max,r} + Z_{max,l} - Z_{min,r} - Z_{min,l}\right] \frac{\left(1 - \rho_r^R\right)}{2W_r} \qquad 3.19$$

Air in the Collector Enclosure:

$$h_{tg} A_t \left(T_p - T_g\right) - h_{rg} A_r \left(T_r - T_g\right) + h_{cg} A_c \left(T_c - T_g\right) = 0 \qquad 3.20$$

Cover 1 (inner):

$$\varepsilon_{c1} (2\sigma T_{c1}^{4} - J_{c2} - F_{cp}J_p - F_{cr}J_r - \hat{\alpha}_{bc1}G_b^T$$

$$- \hat{\alpha}_{sc1} (\hat{J}_{c2} + F_{cp}\hat{J}_p + F_{cr}\hat{J}_r)$$

$$+ h_{cg} (T_{c1} - T_g) + h_{21} (T_{c1} - T_{c2}) = 0 \qquad 3.21$$

Cover 2 (middle):

$$\varepsilon_{c2} (2\sigma T_{c2}^{4} - J_{c1} - J_{c4}) - \hat{\alpha}_{bc2}G_b^T - \hat{\alpha}_{sc2} (\hat{J}_{c1} + \hat{J}_{c4})$$

$$+ h_{21} (T_{c2} - T_{c1}) + h_{23} (T_{c2} - T_{c3}) = 0 \qquad 3.22$$

Cover 3 (outer):

$$\varepsilon_{c3} (2\sigma T_{c3}^{4} - J_{c3} - \sigma T_{sky}^{4}) - \hat{\alpha}_{bc3}\, G_b^T - \hat{\alpha}_{sc3} (\hat{J}_{c3} + G_d^T)$$

$$+ h_w (T_{c3} - T_a) + h_{23} (T_{c3} - T_{c2}) = 0 \qquad 3.23$$

These five equations can be solved for the five unknown temperatures in terms of calculated values for radiosities (long and short wavelength), convection coefficients, and the tank temperature. Note that the longwave radiosities and convection coefficients in equations 3.18 through 3.23 are temperature dependent, so that an iterative solution procedure using the results of the next section is required.

3.6 Infrared Radiation Analysis

Longwave radiation exchange in the collector is evaluated using analogous technique to that used for shortwave radiation. However, since the collector components are assumed to be isothermal with diffuse surface behavior, separate treatment of the right and left sides is not necessary. The equations which result from a long wave radiosity analysis are listed below for each surface.

Absorber (tank):

$$J_t = \varepsilon_t E_{bt} \rho_t (F_{tc} J_c + F_{tr} J_r) \qquad 3.24$$

Reflector:

$$J_r \varepsilon_r E_{br} + \rho_r (F_{rc} J_c + F_{rt} J_t + F_{rr} J_r) \qquad 3.25$$

Covers:

$$J_c = \varepsilon_{c1} E_{bc1} + \rho_{c1} (F_{cr} J_r + F_{ct} J_t) + \tau_{c1} J_2 \qquad 3.26$$

$$J_1 = \varepsilon_{c1} E_{bc1} + \rho_{c1} J_2 + \tau_{c1} (F_{ct} J_t + F_{cr} J_r) \qquad 3.27$$

$$J_2 = \varepsilon_{c2} E_{bc2} + \rho_{c2} J_1 + \tau_{c2} J_4 \qquad 3.28$$

$$J_3 = \varepsilon_{c2} E_{bc2} + \rho_{c2} J_4 + \tau_{c2} J_1 \qquad 3.29$$

$$J_4 = \varepsilon_{c3} E_{bc3} + \rho_{c3} J_3 + \tau_{c3} E_{bsky} \qquad 3.30$$

Equations 3.24 - 3.30 can be solved for the seven unknown radiosities (J_t, J_r, J_c, J_1, J_2, J_3, J_4) using an appropriate mathematical technique.

3.7 Convection Coefficients

The determination of free conveccion film coefficients is required for the calculation of the convective heat transfer between

the collector elements inside the collector. The geometry of the collector chosen for this analysis involves two different cases for free convection. The determination of these film coefficients is described below.

The first case is that of the free convection between the parallel flat plates (covers) and is immediately seen to be the same as that encountered for flat plate solar collectors. A recent investigation by Hollands, et al. [18] resulted in a dimensionless correlation which agrees within 5 percent of experimental data. This correlation is restricted to inclination angles from 0 to 60 degrees from the horizontal with plates heated from below. It is also limited to aspect ratios, plate width divided by air space thickness, of greater than 20 and Rayleigh numbers less than about 10^5. Since none of these restrictions limits the use of Hollands' results in the current analysis and the correlation has been experimentally verified, the following correlation by Hollands is used.

$$Nu = 1 + 1.44 \left[1 - \frac{1708}{Ra \cos \beta}\right]^+ \left(1 - \frac{(\sin 1.8\beta)^{1.6}\ 1708}{Ra \cos \beta}\right) + \left[\left(\frac{Ra \cos \beta}{5830}\right)^{1/3} - 1\right]^+ \qquad 3.31$$

where the + exponent on the brackets indicates that only positive values of the terms inside the brackets are to be used, i.e. $[X]^+ = (X + |X|)/2$. The free convection coefficient can be obtained from the Nusselt number using the definition of the Nusselt number.

$$h = Nu \frac{k}{d} \qquad 3.32$$

where d is the plate spacing.

The second case for which the free convection coefficient must be evaluated is that of the free convection heat transfer inside the collector enclosure. This involves the heat transfer from a horizontal cylinder and from several flat plates at various angles of inclination. Holman (19) presents correlations for the free convection from a horizontal cylinder and from the upper surface of cooled plates in the form

$$Nu = C\ (Gr\ Pr)^{m} \tag{3.33}$$

where $C = 0.53$ and $m = 1/4$ for a horizontal cylinder

and $C = 0.58$ and $m = 1/5$ for flat plate case.

Holman also presents several correlations for the flat plate coefficient at various inclination angles, but notes that there exists an experimental scatter of ± 20 percent. Therefore, for ease of computation, a single relation was considered adequate to represent the free convection film coefficient inside the enclosure.

$$Nu = 0.55\ (Gr\ Pr)^{1/4} \tag{3.34}$$

This relation is an approximate average of the horizontal cylinder case and the horizontal flat plate case.

The determination of the external wind coefficient, h_w, is defined so as to account for both free and forced convection heat loss. The relative importance of free and forced convection depends on the wind speed, V_w. McAdams (20) suggests a correlation for the wind coefficient of the form

$$h_w = 5.7 + 3.8\ V_w \tag{3.35}$$

which probably includes the effects of radiation. Watmuff, et al. (21) report a correlation which does not include the effects of radiation.

$$h_w = 2.8 + 3.0\ V_w \qquad 3.36$$

Since radiation heat loss has already been taken into account, equation 3.36 was used in this analysis.

3.8 Solution Technique

A flowchart of the solution procedure used to simulate the thermal performance of an ISC system is shown in Fig. 6. First, the initial temperature of the tank/fluid is set. Then, hourly average values for the sky temperature, ambient temperature, wind speed, and insulation are required as inputs. The incidence angles can be calculated from the date and time using the equations of Appendix B. From the incidence angles the optical properties of the covers can be calculated and the ray tracing procedures carried out to determine the beam solar flux on the absorber. A subsequent solution of the equations for the short wave diffuse radiosities gives a mean solar flux on the absorber, from which the optical efficiency, η_o, can be calculated.

Next, a mean tank temperature for the hour is assumed. Based on this assumed tank temperature the other component temperatures are estimated and used to calculated approximate values for the free convection coefficients. These estimated component temperatures are also used to solve for the long wave radiosities. Now, the estimated

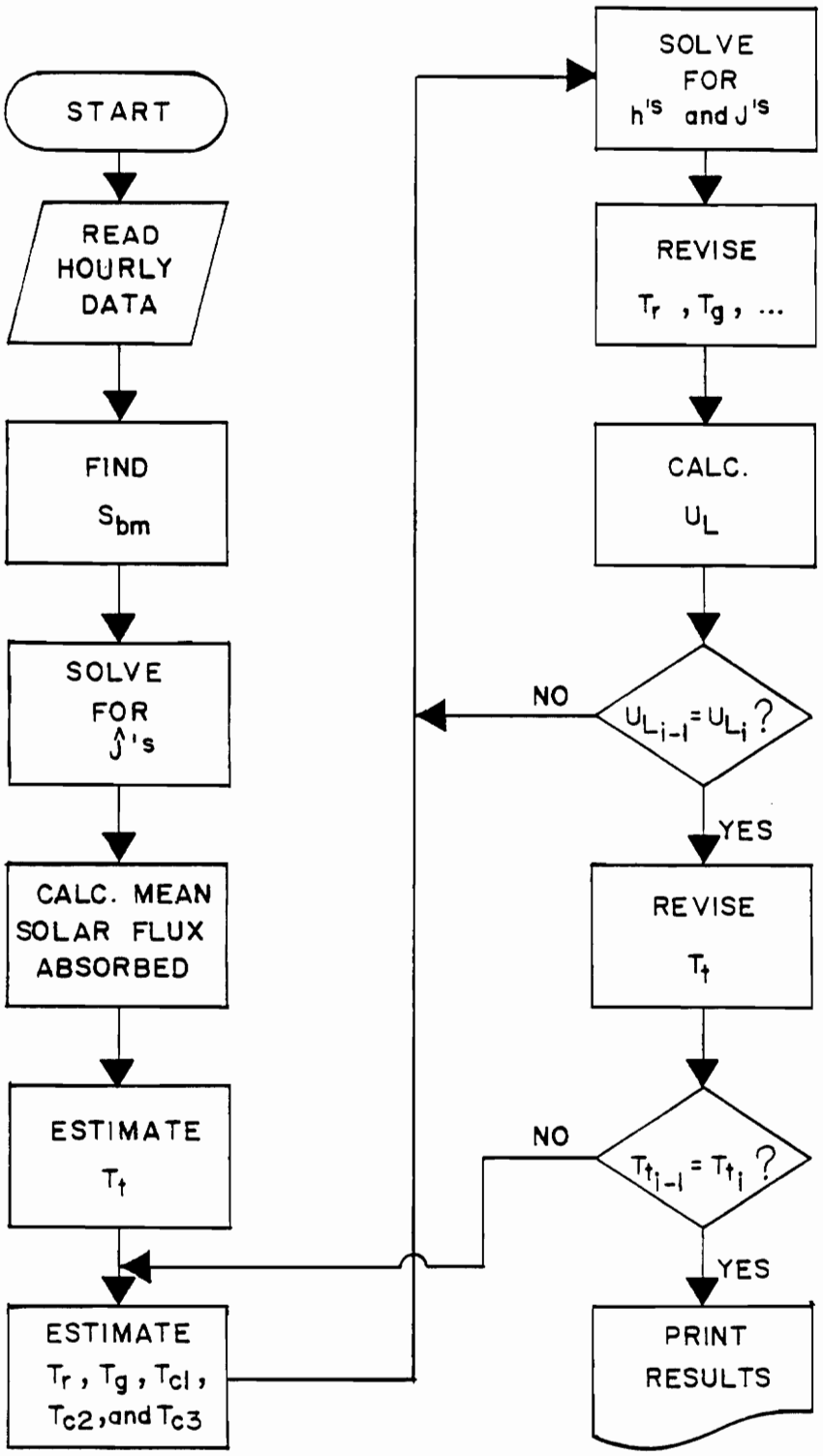

Figure 6. Flowchart for Calculation of Thermal Performance of an ISC

radiosities and convection coefficients are used to solve the component energy balances for new, revised, component temperatures. These new component temperatures are then used to obtain new values for the convection coefficients and radiosities, which in turn, are used to revise the component temperatures. This cycle is repeated until the component temperatures converge. Once the component temperatures have been determined, the loss coefficient can be evaluated.

$$U_L = \frac{h_{tg}\,(T_t - T_g) + \frac{\varepsilon_t}{1 - \varepsilon_t}\,[\sigma T_t^{\,4} - J_t]}{(T_t - T_a)} \qquad 3.37$$

Note that the loss coefficient calculated here is based on the tank area and must be multiplied by the tank-to-cover area ratio, A_t/A_c, to obtain the loss coefficient based on the cover (aperture) area as defined in the tank transient analysis. When the loss coefficient has been evaluated, the estimated mean tank temperature for the hour can be revised. Of course, for a new (revised) tank temperature the component temperature iteration must be repeated and a new U_L calculated. This procedure is repeated until the tank temperature converges. Once the mean tank temperature has been determined for one hour, the environmental conditions for the next hour are input and the procedure begun again.

IV. RESULTS AND DISCUSSION

The results of experimental tests on two ISC systems under a variety of operating, environmental, and irradiance conditions are presented in this chapter. The results are evaluated and the implications for the standard testing of ISC systems pointed out. The results of an analytical investigation of ISC B are also compared with the results of the experimental tests for the same system.

4.1 Experimental Results

The results of the all-day tests performed in this investigation are plotted in Figs. 7 through 26 and tabulated in Appendix D. Ambient conditions and irradiances are plotted against the same time scale. Recall that the designations for the types of tests were as follows:

Type I - no draw, no circulation

Type II - single draw, no circulation

Type III - no draw, circulation

The initial and final conditions, draw information, circulation flowrate, and total solar radiation incident for the test are summarized in Table 2. Calculated values for the energy withdrawn, energy stored, and daily collection efficiency are also summarized in Table 2.

The first important point which should be noted from these experimental results is the fact that the daily collection efficiency does not appear to be affected significantly by the degree of stratification, i.e. no difference between type I and III tests. Because of the

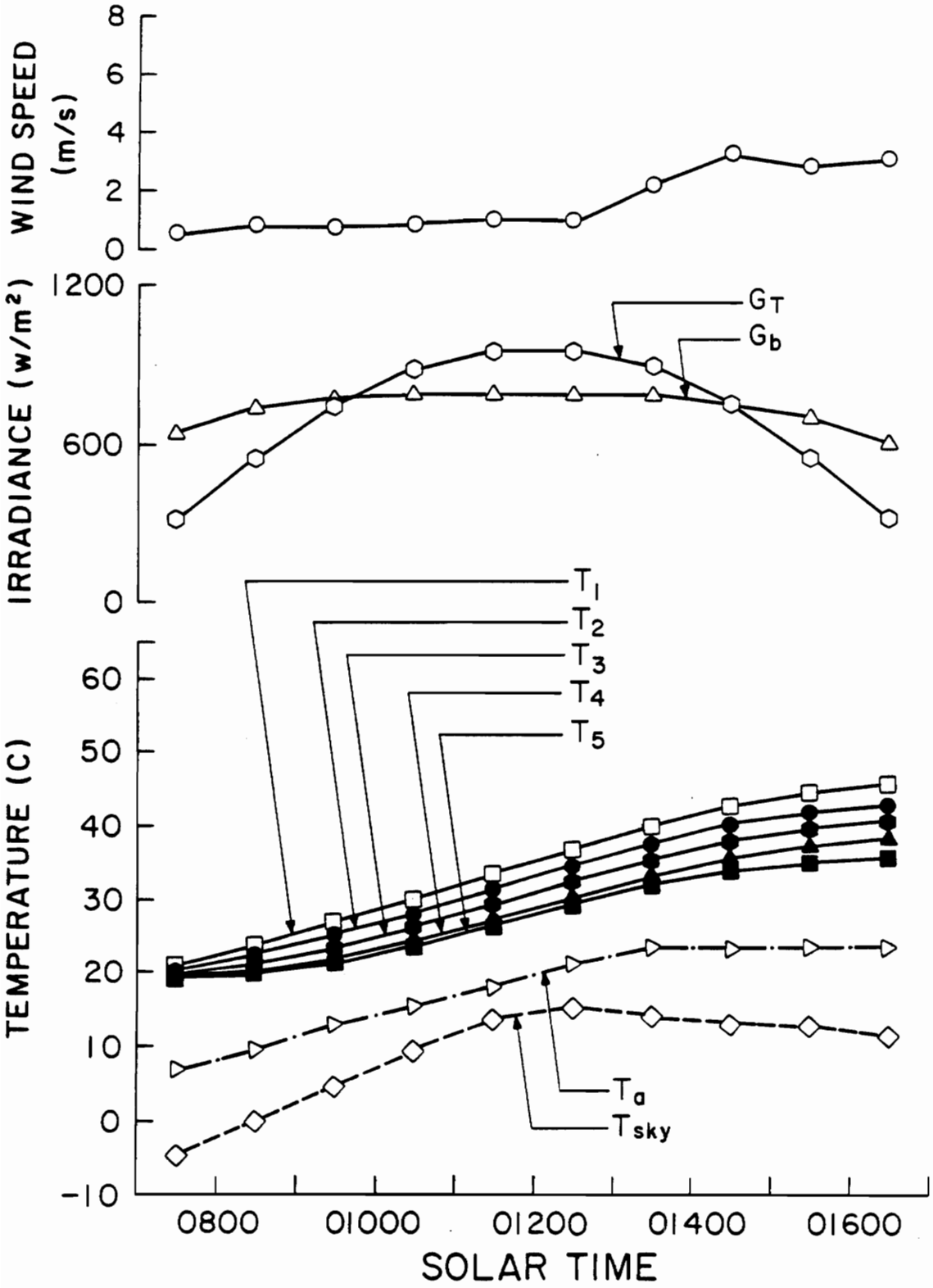

Figure 7. Performance of ISC A in a Type I Test on 5/13/83, No Circulation, No Draw

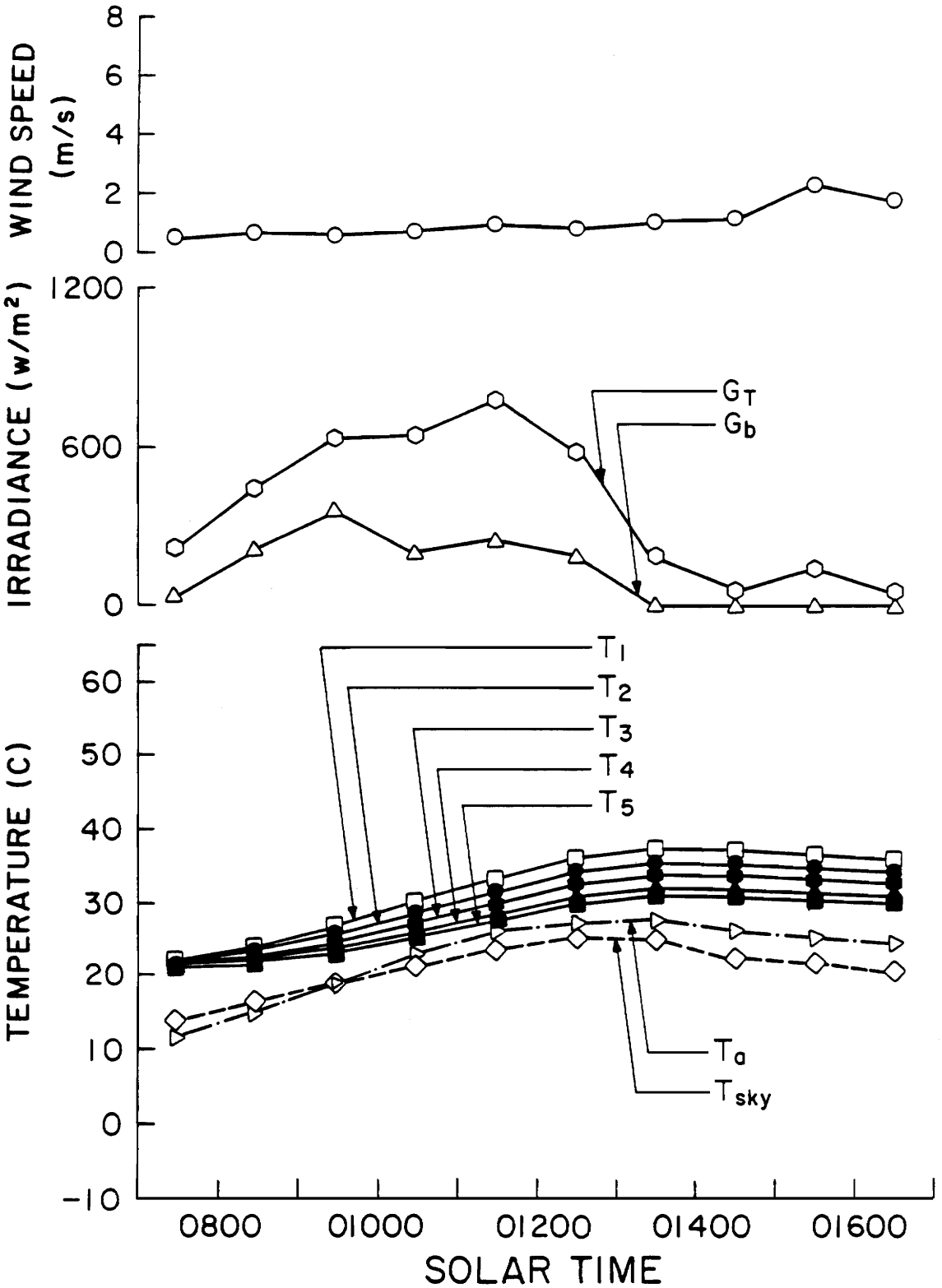

Figure 8. Performance of ISC A in a Type I Test on 5/13/83, No Circulation, No Draw

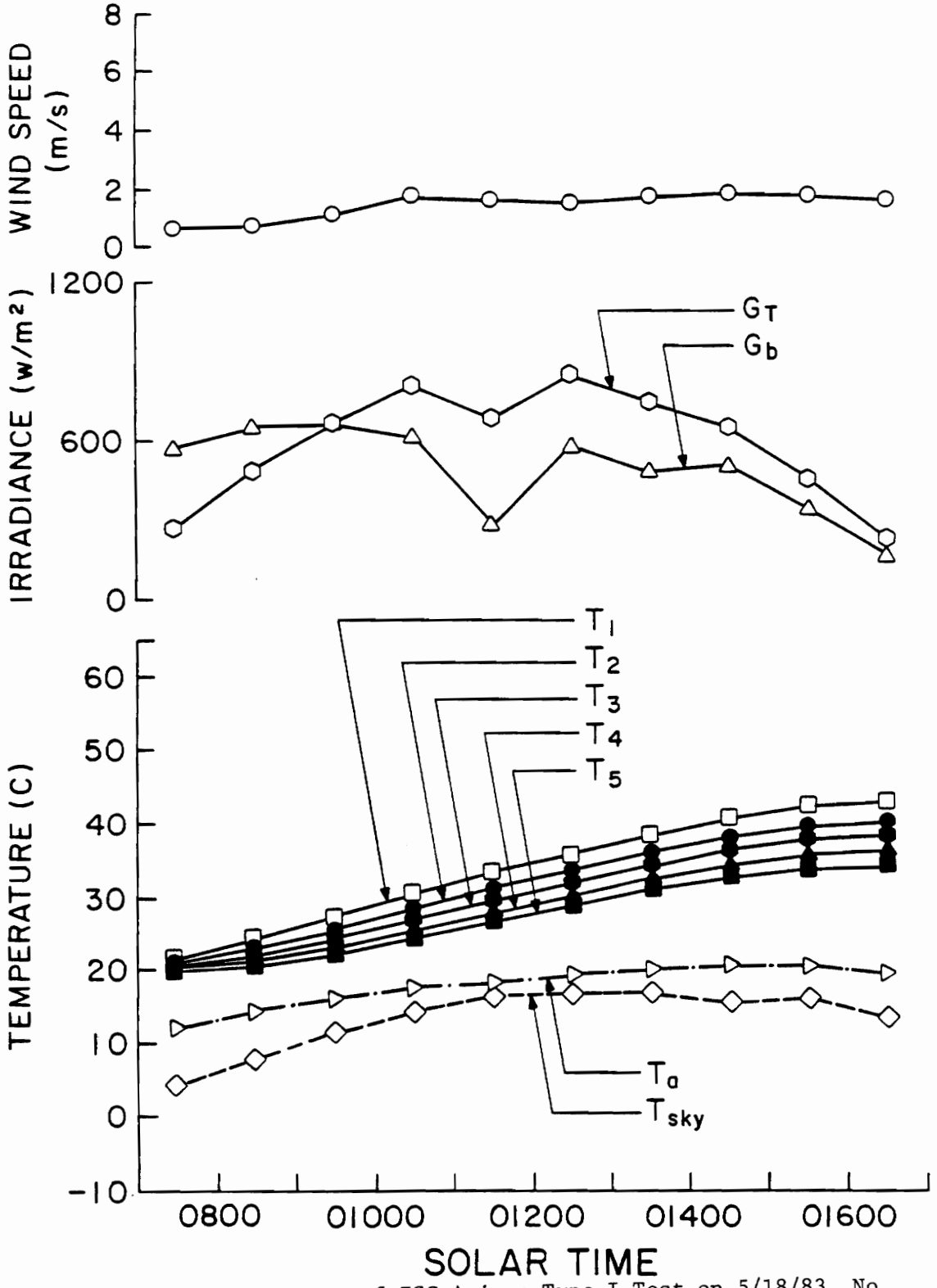

Figure 9. Performance of ISC A in a Type I Test on 5/18/83, No Circulation, No Draw

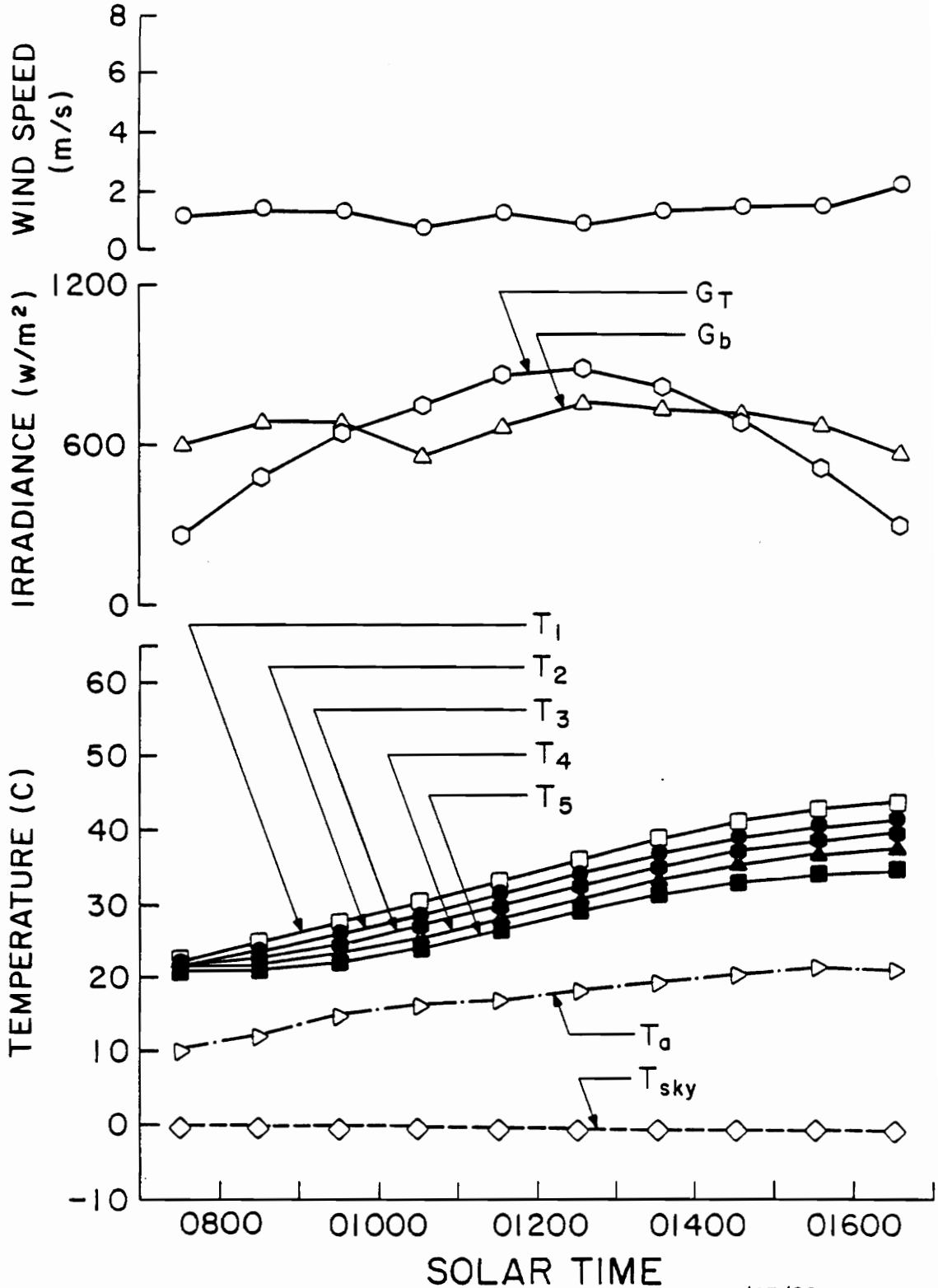

Figure 10. Performance of ISC A in a Type I Test on 5/27/83, No Circulation, No Draw

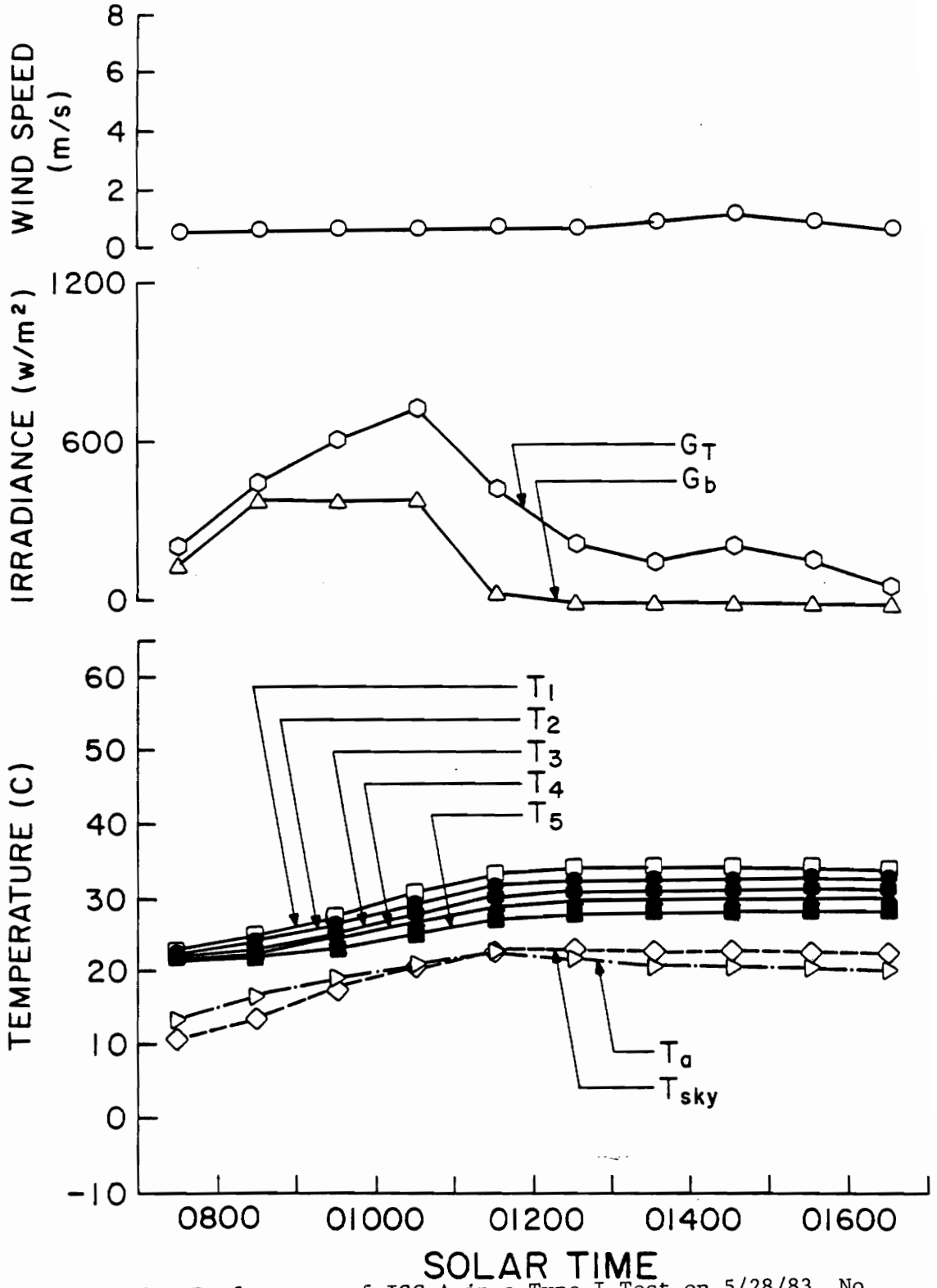

Figure 11. Performance of ISC A in a Type I Test on 5/28/83, No Circulation, No Draw

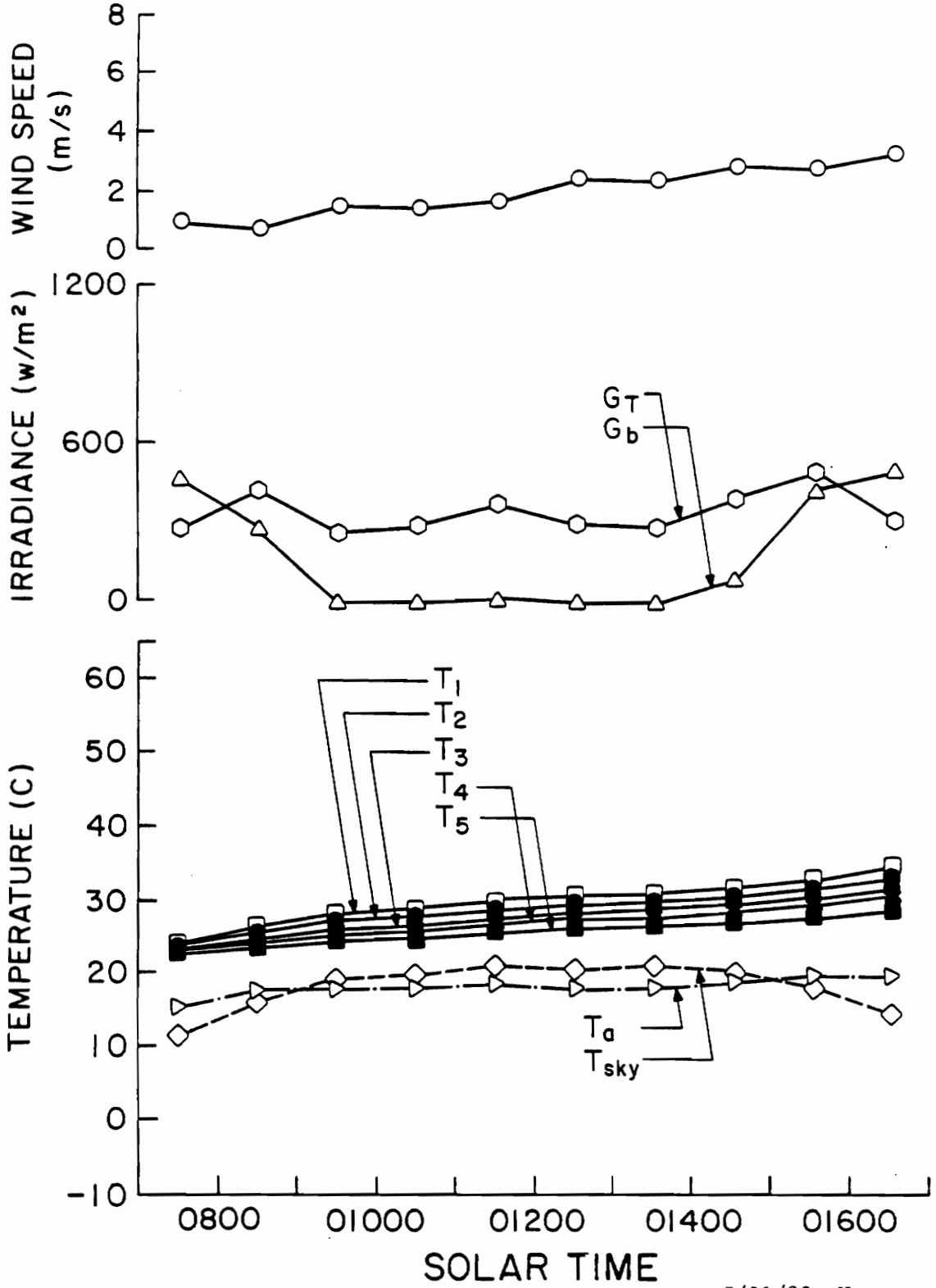

Figure 12. Performance of ISC A in a Type I Test on 5/31/83, No Circulation, No Draw

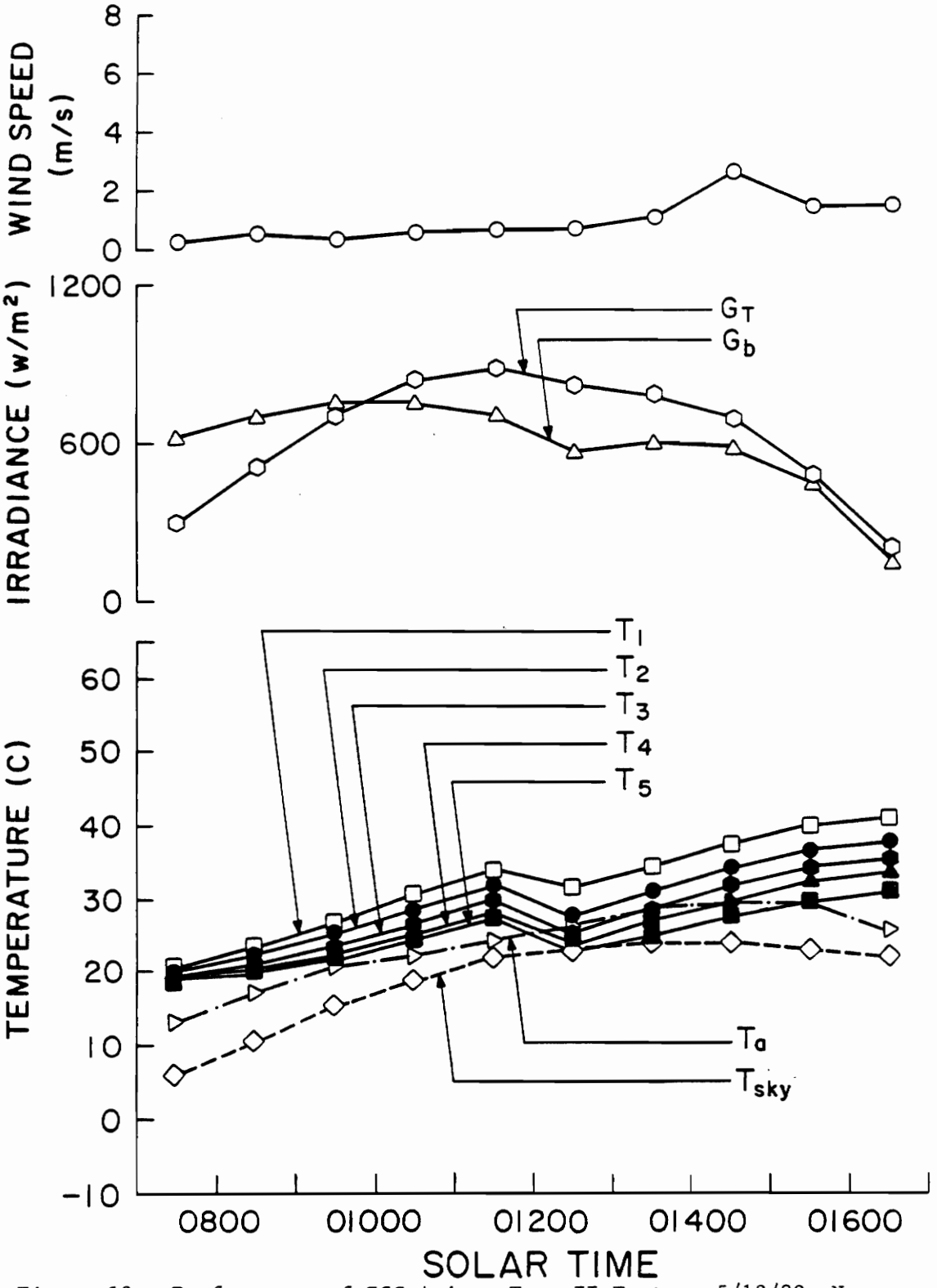

Figure 13. Performance of ISC A in a Type II Test on 5/12/83, No Circulation, Noon Draw

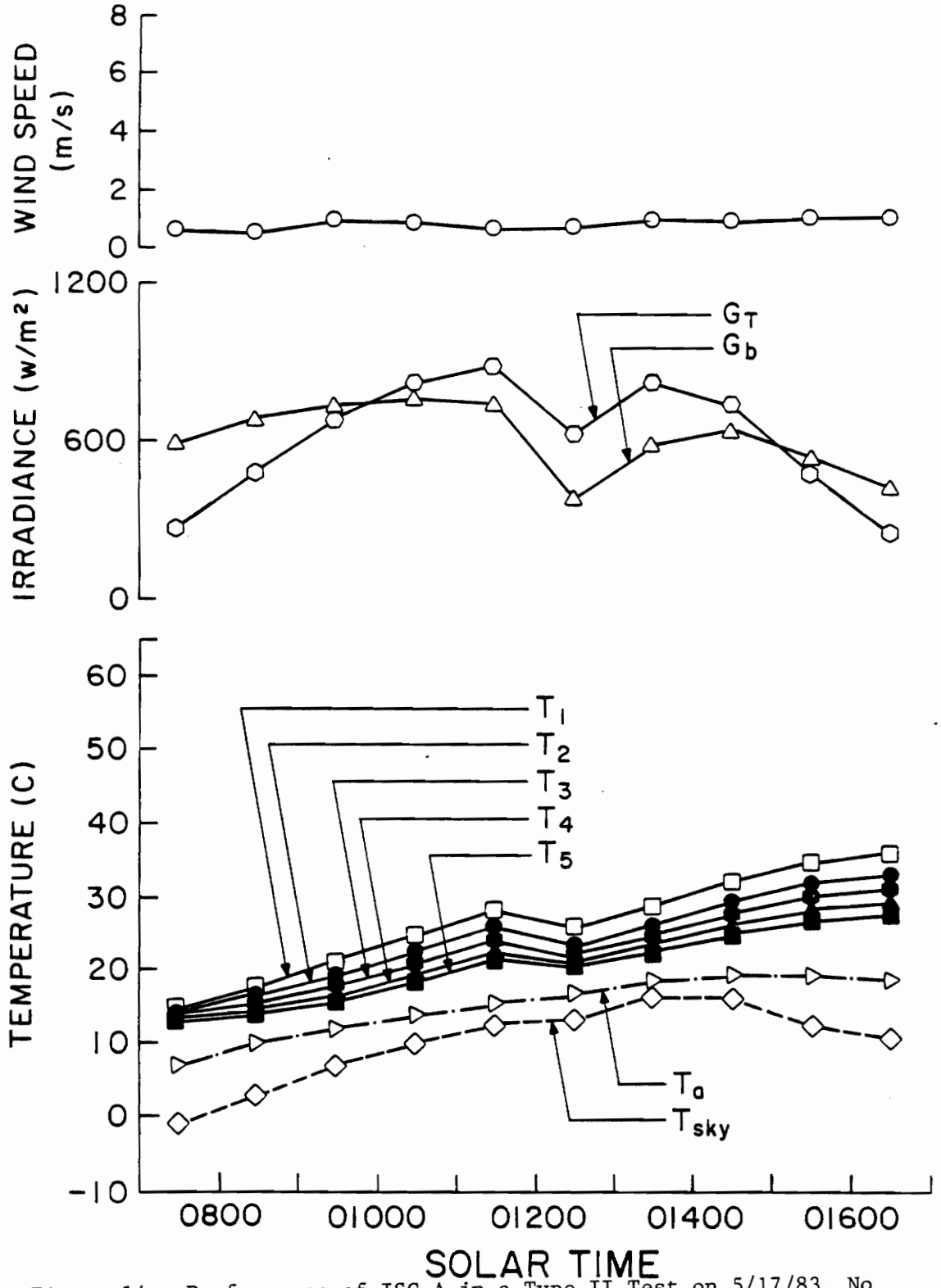

Figure 14. Performance of ISC A in a Type II Test on 5/17/83, No Circulation, Noon Draw

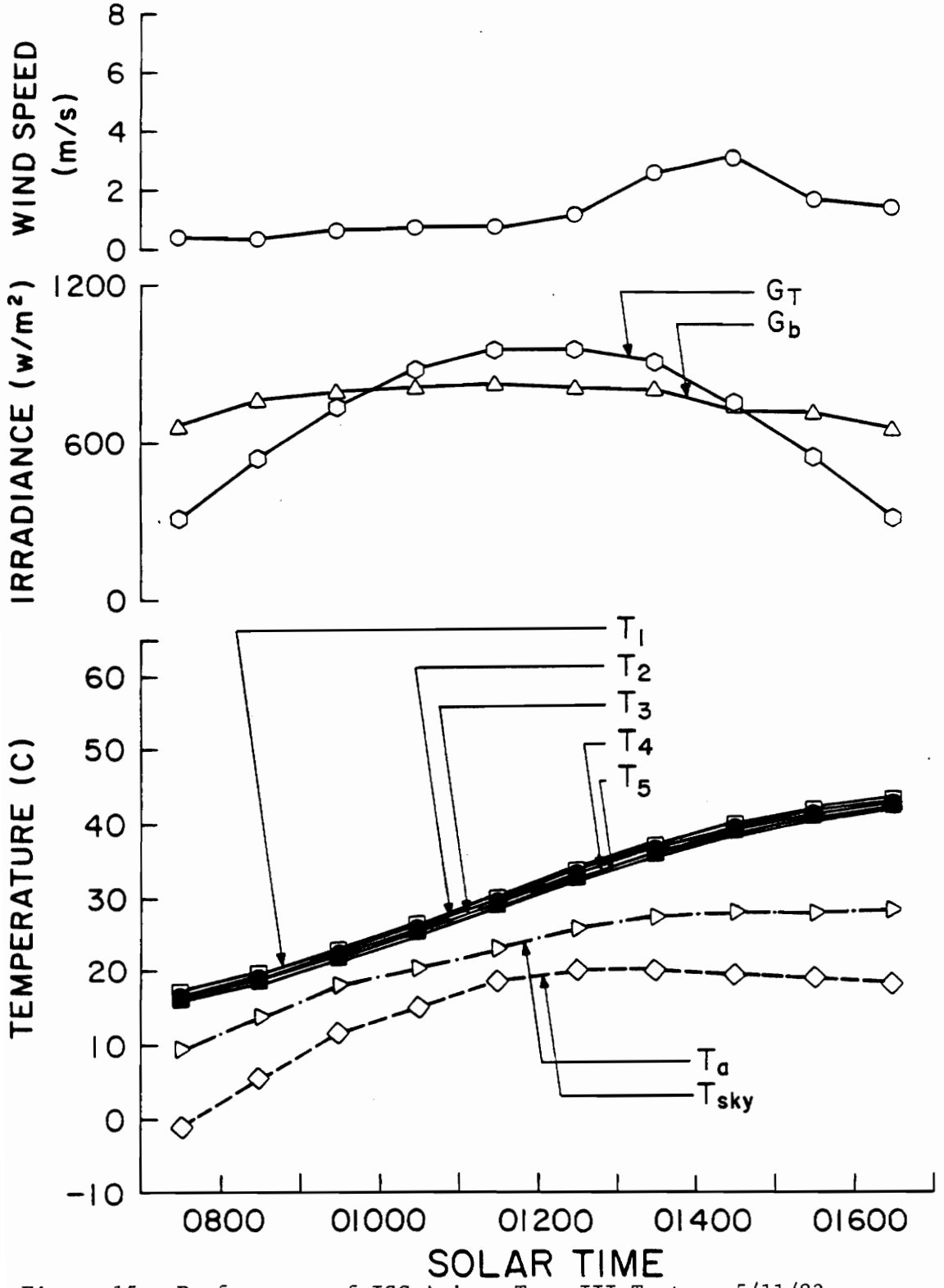

Figure 15. Performance of ISC A in a Type III Test on 5/11/83, 31.89 m^3/s Circulation, No Draw

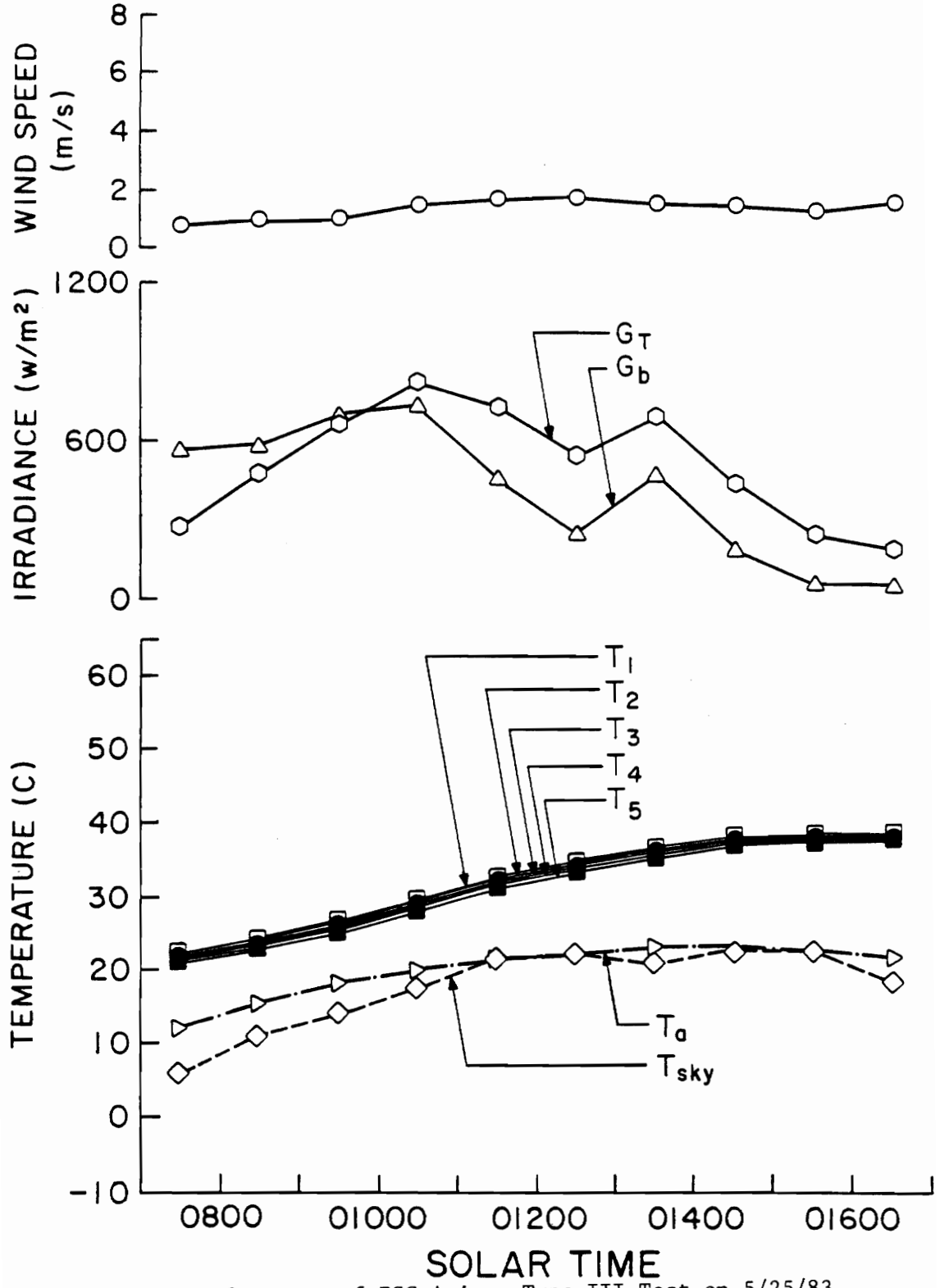

Figure 16. Performance of ISC A in a Type III Test on 5/25/83, 14.09 m^3/s Circulation, No Draw

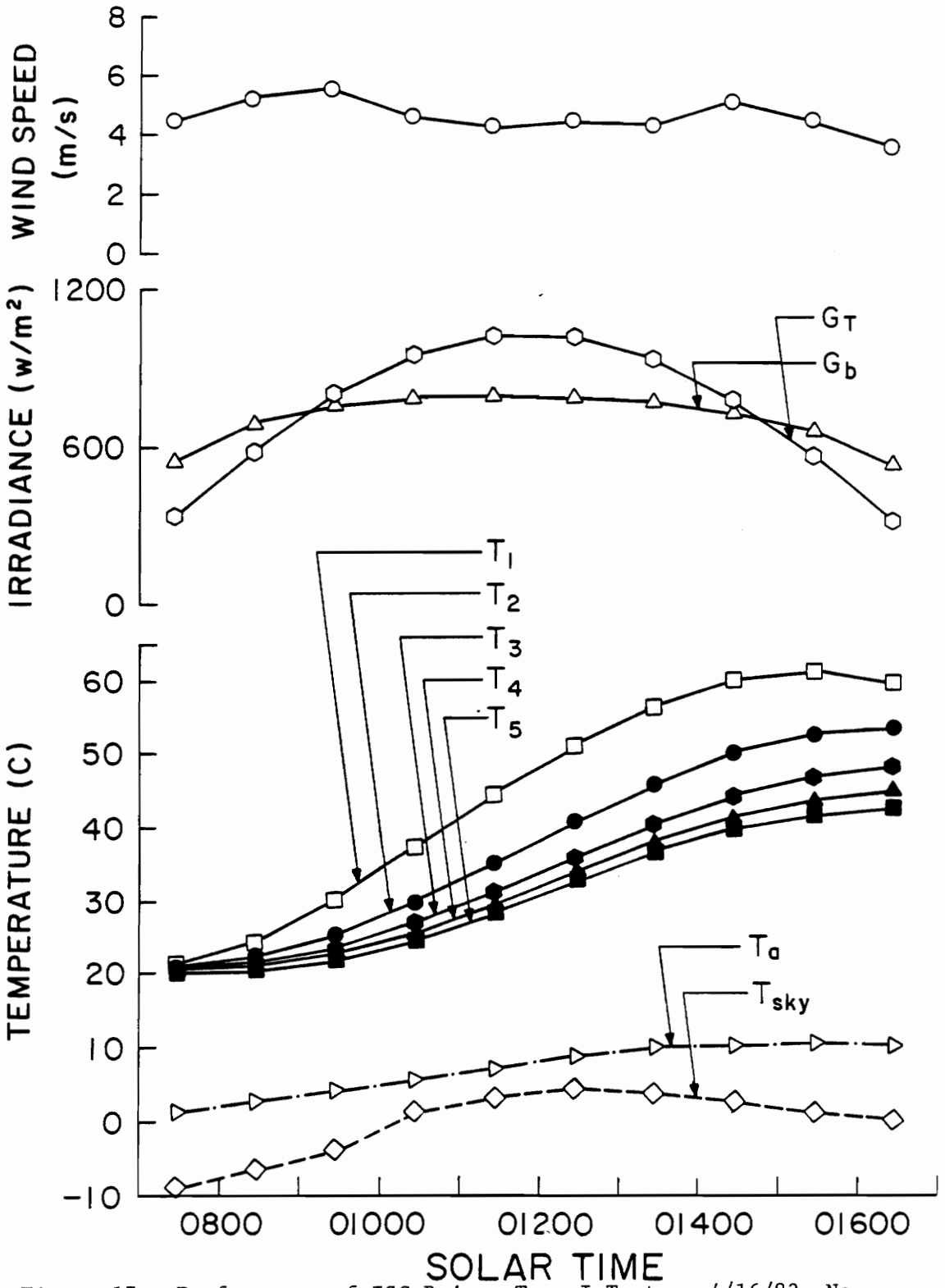

Figure 17. Performance of ISC B in a Type I Test on 4/16/83, No Circulation, No Draw

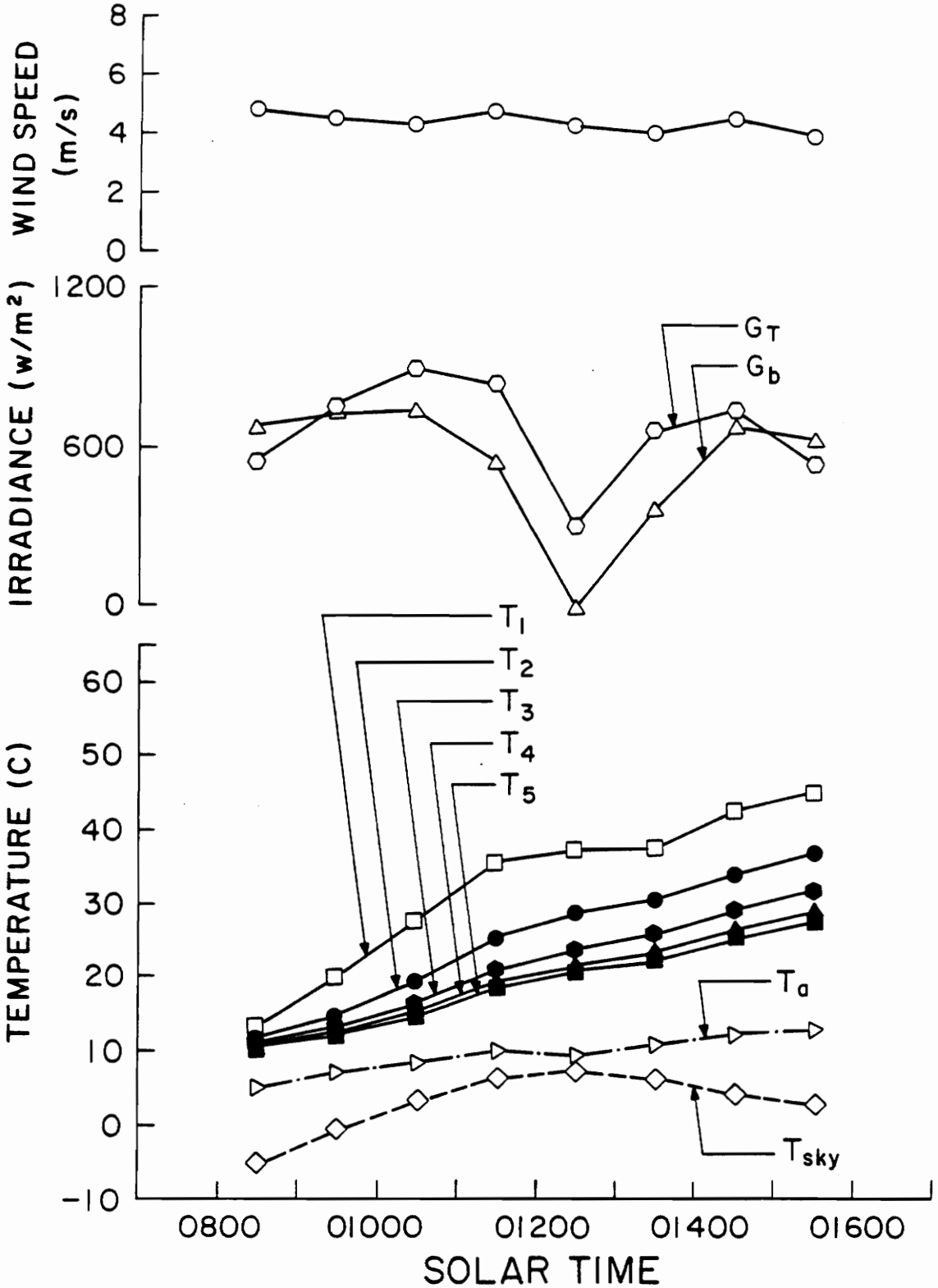

Figure 18. Performance of ISC B in a Type I Test on 4/21/83, No Circulation, No Draw

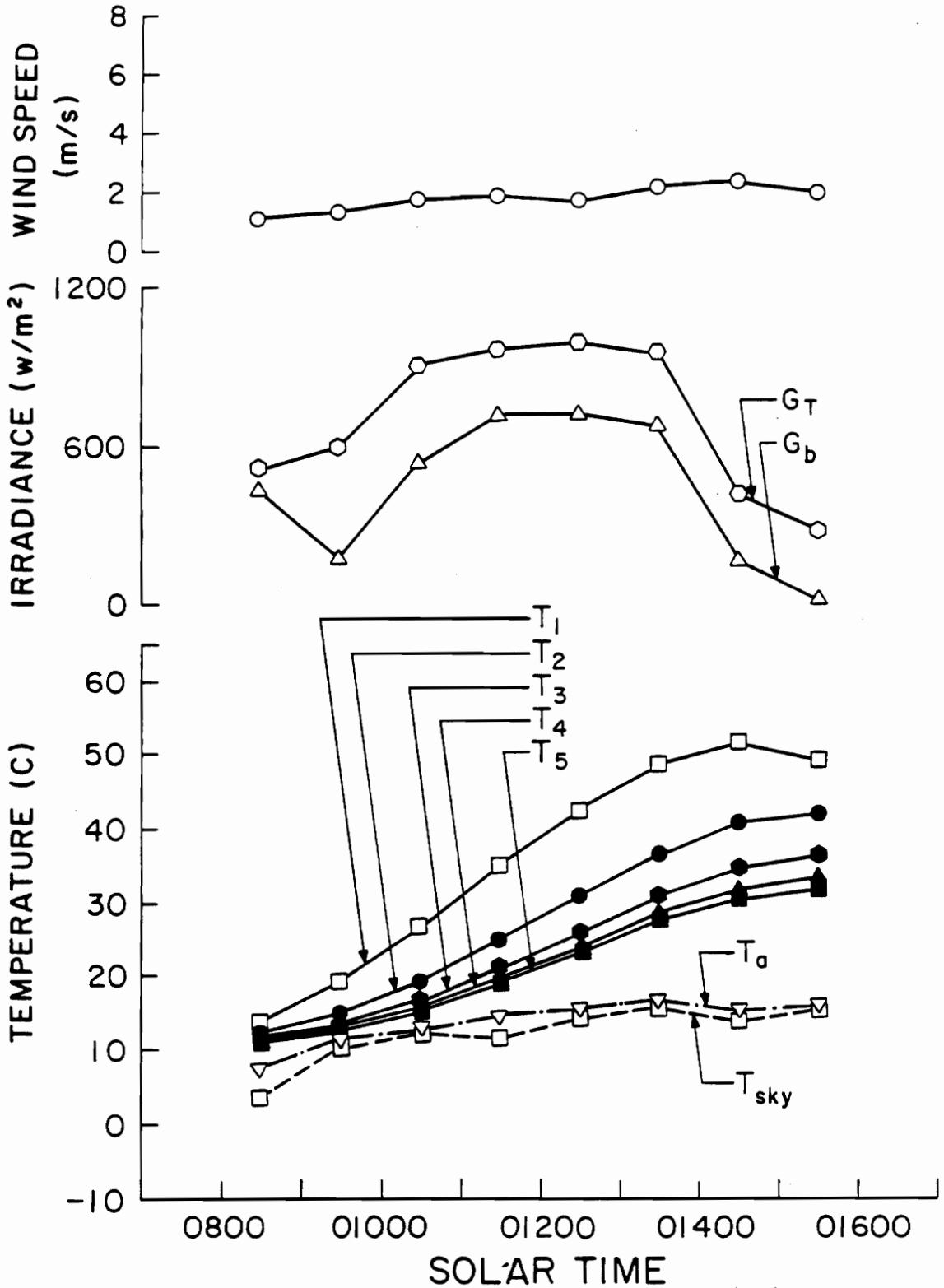

Figure 19. Performance of ISC B in a Type I Test on 4/22/83, No Circulation, No Draw

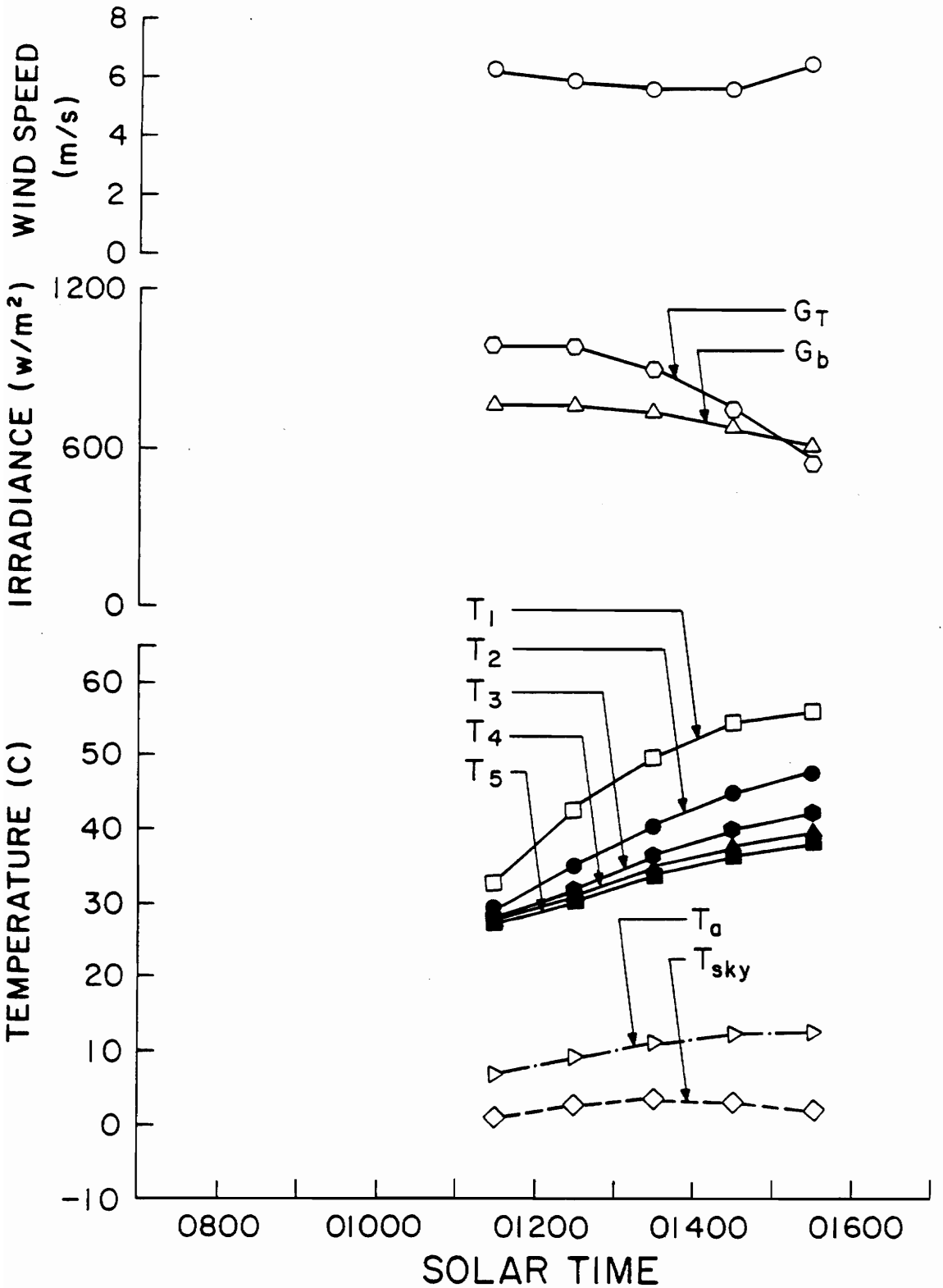

Figure 20. Performance of ISC B in a Type I Test on 4/25/83, No Circulation, No Draw

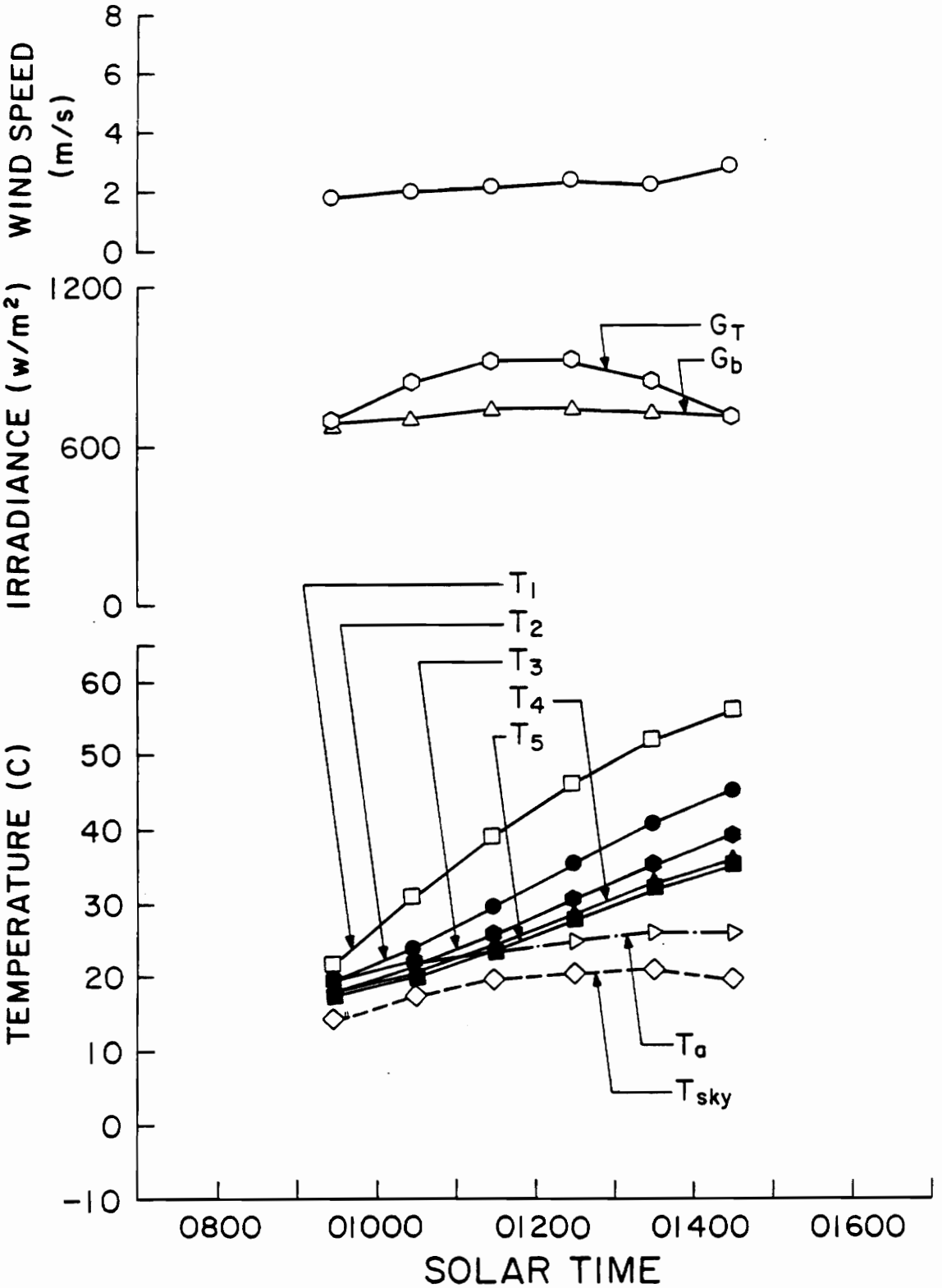

Figure 21. Performance of ISC B in a Type I Test on 4/27/83, No Circulation, No Draw

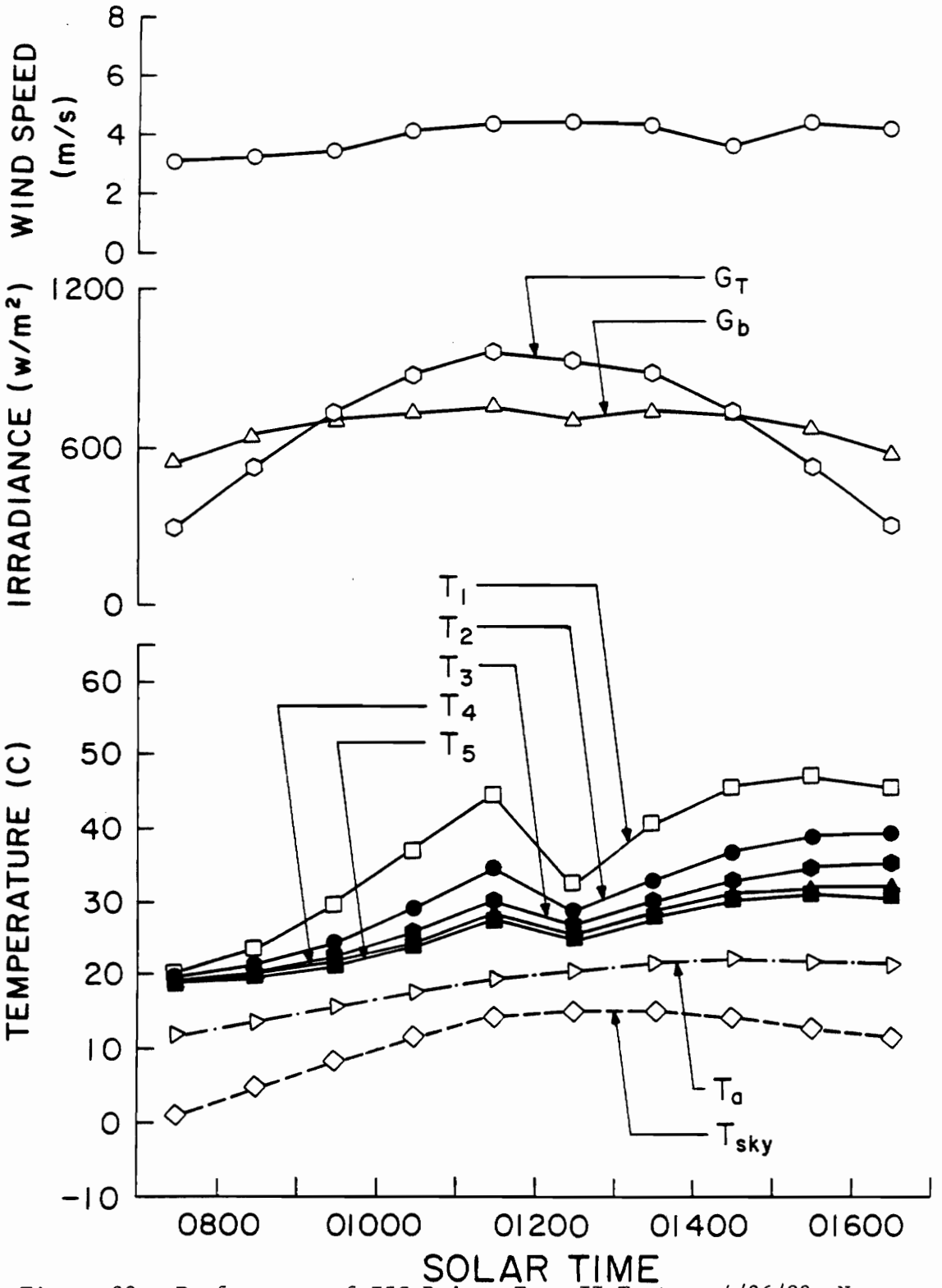

Figure 22. Performance of ISC B in a Type II Test on 4/26/83, No Circulation, Noon Draw

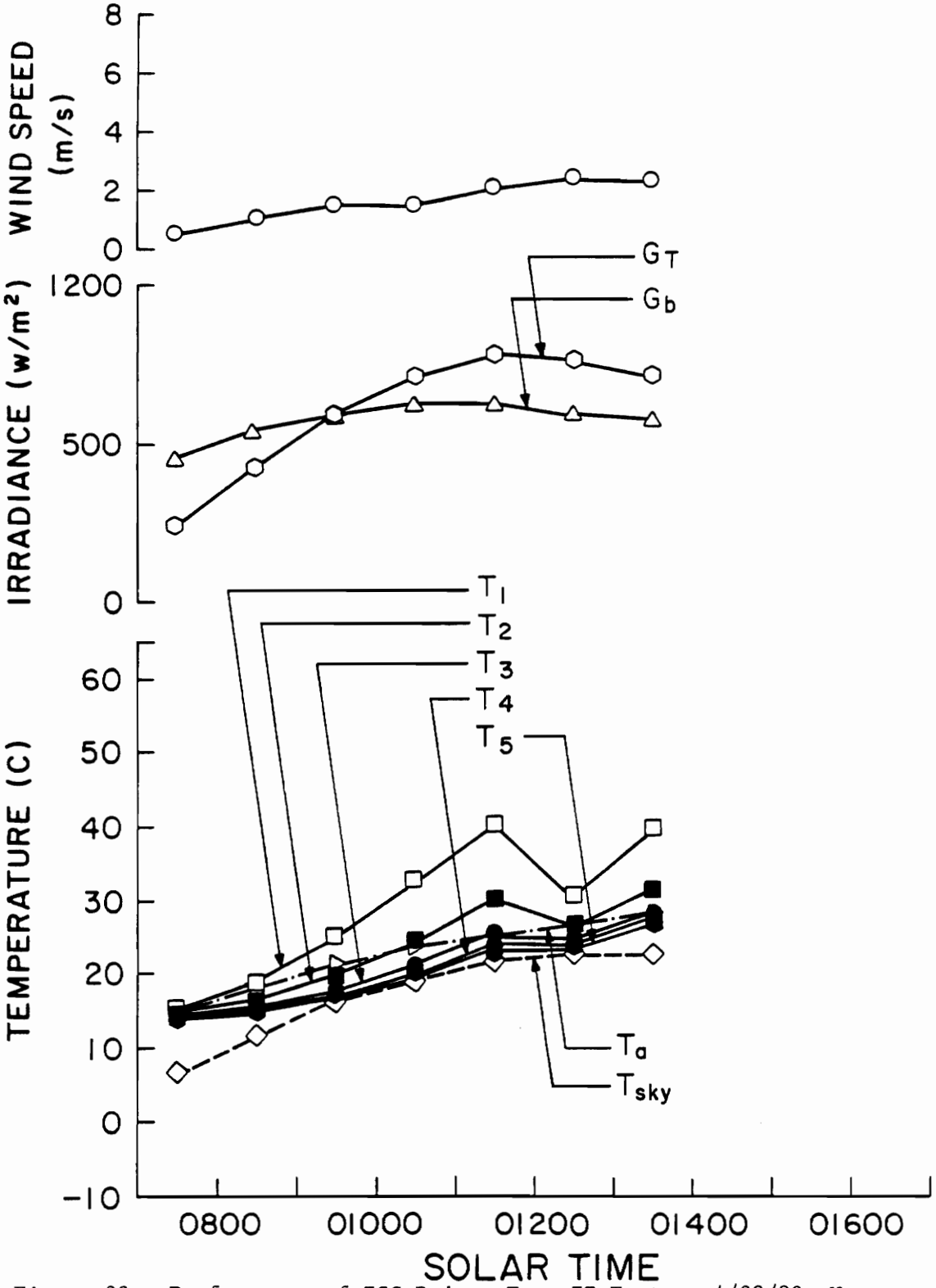

Figure 23. Performance of ISC B in a Type II Test on 4/28/83, No Circulation, Noon Draw

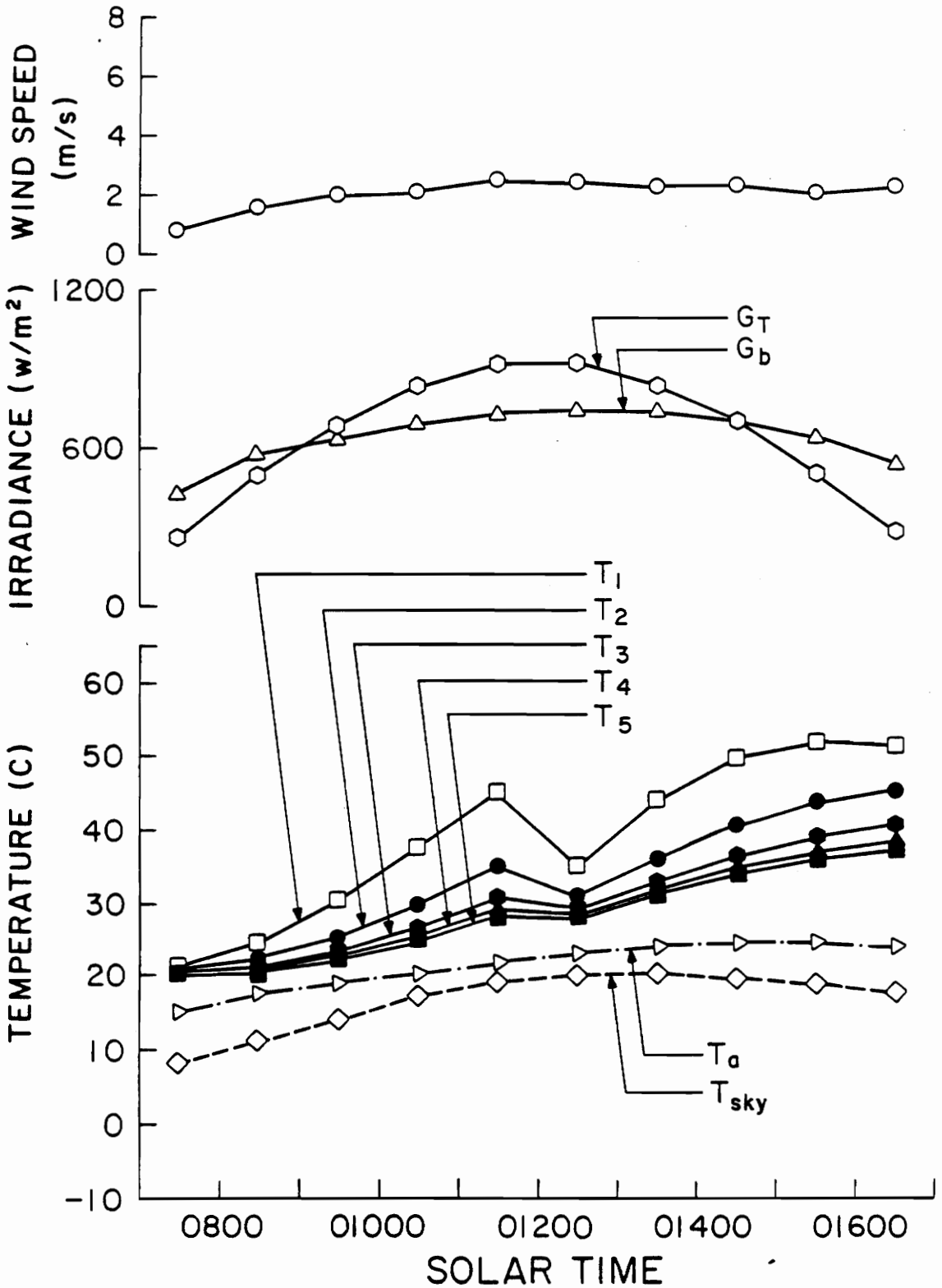

Figure 24. Performance of ISC B in a Type II Test on 5/7/83, No Circulation, Noon Draw

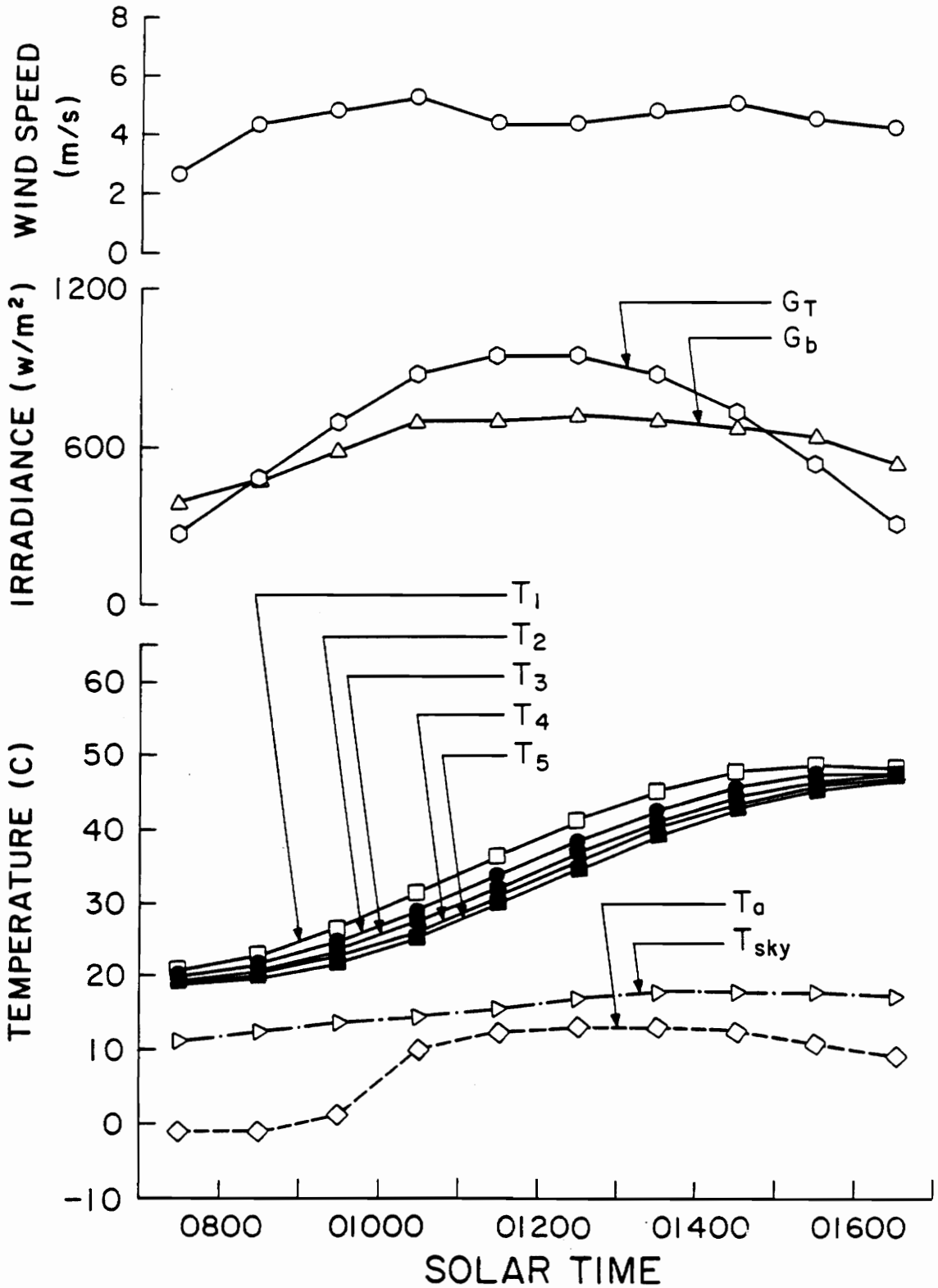

Figure 25. Performance of ISC B in a Type III Test on 5/5/83, 9.06 m^3/s Circulation, No Draw

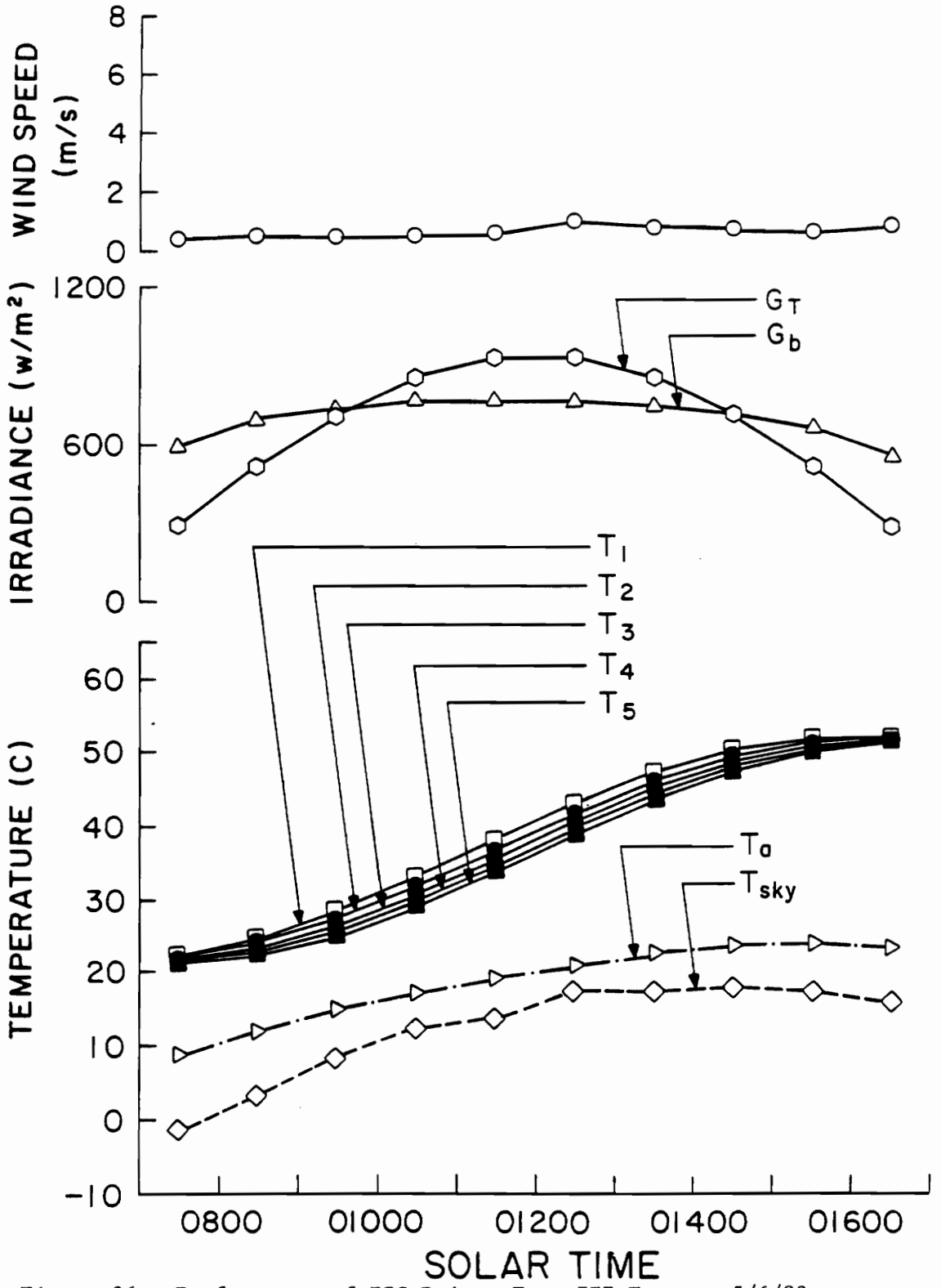

Figure 26. Performance of ISC B in a Type III Test on 5/6/83, 16.31 m^3/s Circulation, No Draw

Table 2

Test Type	Date	Duration	Draw Time	Mixing Rate (cu cm/s)	Initial Temp (C)	Final Temp (C)	Inlet Temp (C)	Draw Temp (C)	Draw Mass (kg)	Incident Energy MJ	Stored Energy MJ	Draw Energy MJ	Collection Efficiency
B I	4/16/83	7-17	--	--	21.3	49.7	--	--	--	34.71	12.61	--	0.363
B I	4/21/83	8-16	--	--	10.8	35.1	--	--	--	25.77	10.85	--	0.421
B I	4/22/83	8-16	--	--	11.2	38.8	--	--	--	27.15	12.30	--	0.453
B I	4/25/83	11-16	--	--	26.8	45.8	--	--	--	20.23	8.43	--	0.417
B II	4/26/83	7-17	1200	--	19.6	36.6	11.8	36.5	45.22	33.02	7.57	4.67	0.371
B I	4/27/83	9-15	--	--	17.6	43.9	--	--	--	24.34	11.70	--	0.481
B II	4/28/83	7-14	1200	--	14.1	33.0	13.0	32.9	45.72	24.73	8.43	3.81	0.495
B III	5/ 5/83	7-17	--	9.06	19.2	47.4	--	--	--	32.16	12.53	--	0.390
B III	5/ 6/83	7-17	--	16.31	21.4	52.3	--	--	--	32.38	13.71	--	0.424
B II	5/ 7/83	7-17	1200	--	20.8	43.2	17.5	37.1	45.95	31.59	9.96	3.77	0.435
A I	5/10/83	7-17	--	--	19.9	41.3	--	--	--	21.67	9.78	--	0.451
A III	5/11/83	7-17	--	31.89	16.0	43.4	--	--	--	21.21	12.53	--	0.591
A II	5/12/83	7-17	1200	--	19.1	36.6	17.0	35.6	46.40	19.83	8.01	3.61	0.586
A I	5/13/83	7-17	--	--	21.6	32.5	--	--	--	11.55	4.99	--	0.432
A II	5/17/83	7-17	1200	--	13.8	32.0	17.5	29.7	46.40	19.13	8.34	2.37	0.560
A I	5/18/83	7-17	--	--	20.4	38.4	--	--	--	18.35	8.23	--	0.448
A III	5/25/83	7-17	--	14.09	20.8	38.0	--	--	--	15.59	7.86	--	0.504
A I	5/27/83	7-17	--	--	21.5	40.6	--	--	--	19.96	8.73	--	0.437
A I	5/28/83	7-17	--	--	22.0	31.2	--	--	--	10.15	4.21	--	0.415
A I	5/31/83	7-17	--	--	22.5	32.0	--	--	--	10.56	4.35	--	0.412

differences in irradiance, diffuse fraction, and ambient conditions the data shows significant scatter, probably enough to mask any effects of stratification which may exist. There may in fact be an effect, but it could probably only be detected if tests were carried out under identical environmental conditions, a near impossibility for outdoor tests. A comparison of the daily collection efficiency for the different types of tests is shown in Fig. 27 for system A and Fig. 28 for system B.

The high degree of stratification which was measured for the sytems tested indicates that the energy which can be withdrawn will be significantly lower for tests with circulation than for tests without circulation. This is obvious since the outlet water for a statified system is higher than the mean tank temperature for low volume draws. Also, the results indicate that a flowrate much lower than those used for the type II tests is needed if the stratification characteristics are to be preserved. Therefore, although the degree of stratification does not seem to have a significant effect on daily collection efficiency it does appear to be important with respect to the energy withdrawn from the system. Another important point which should be noted from the experimental results is that the occurrence of a draw has an effect on the daily collection efficiency. Specifically, a draw lowers the mean temperature of the tank and increases the collection efficiency because the losses to ambient are reduced. This can be seen in Figs. 7 through 26 and by the higher temperature increase rate immediately following a draw. This can also be seen in Figs. 27 and 28 where the daily

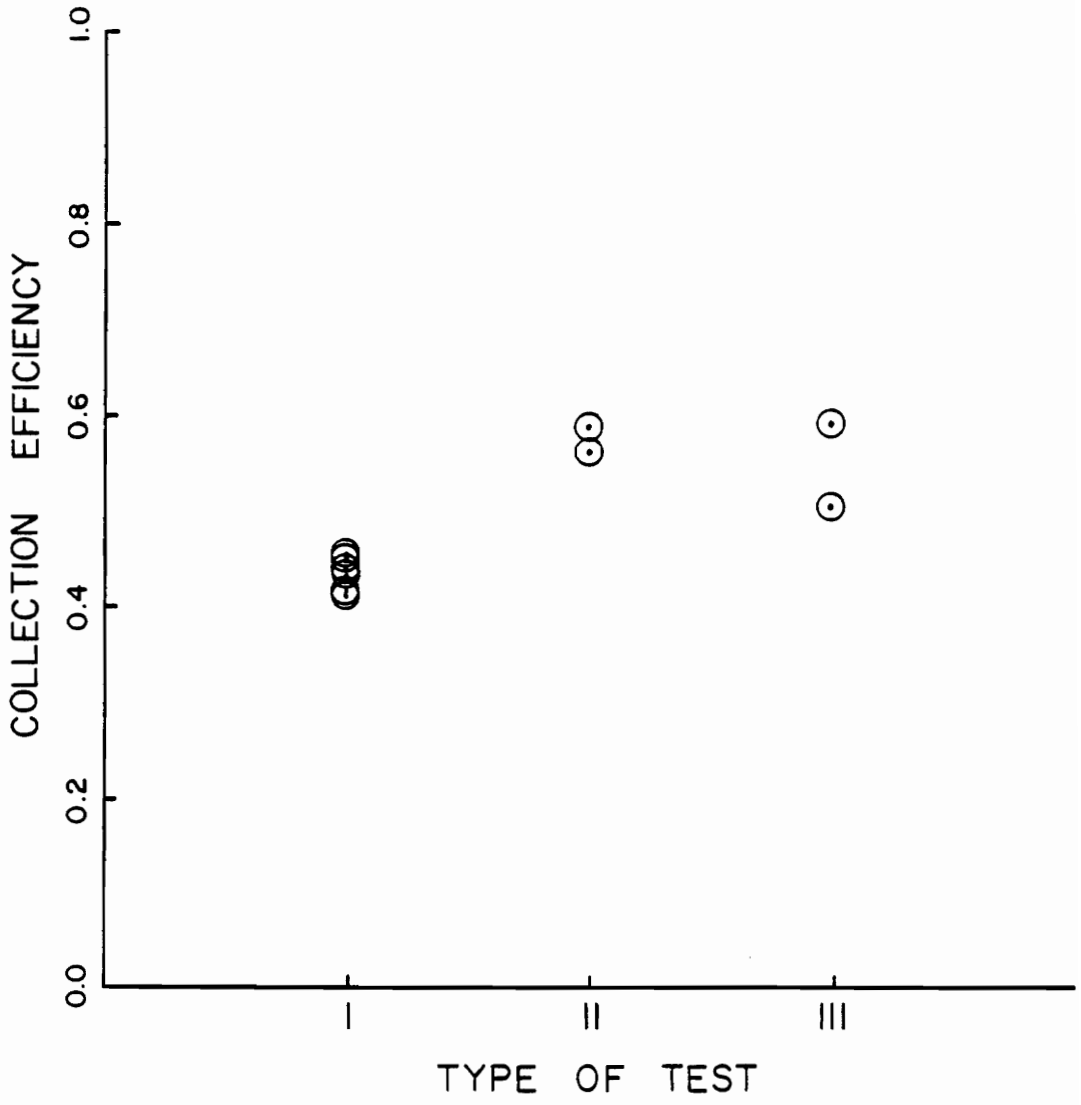

Figure 27. Comparison of the Daily Collection Efficiency of ISC A for the Three Types of Tests

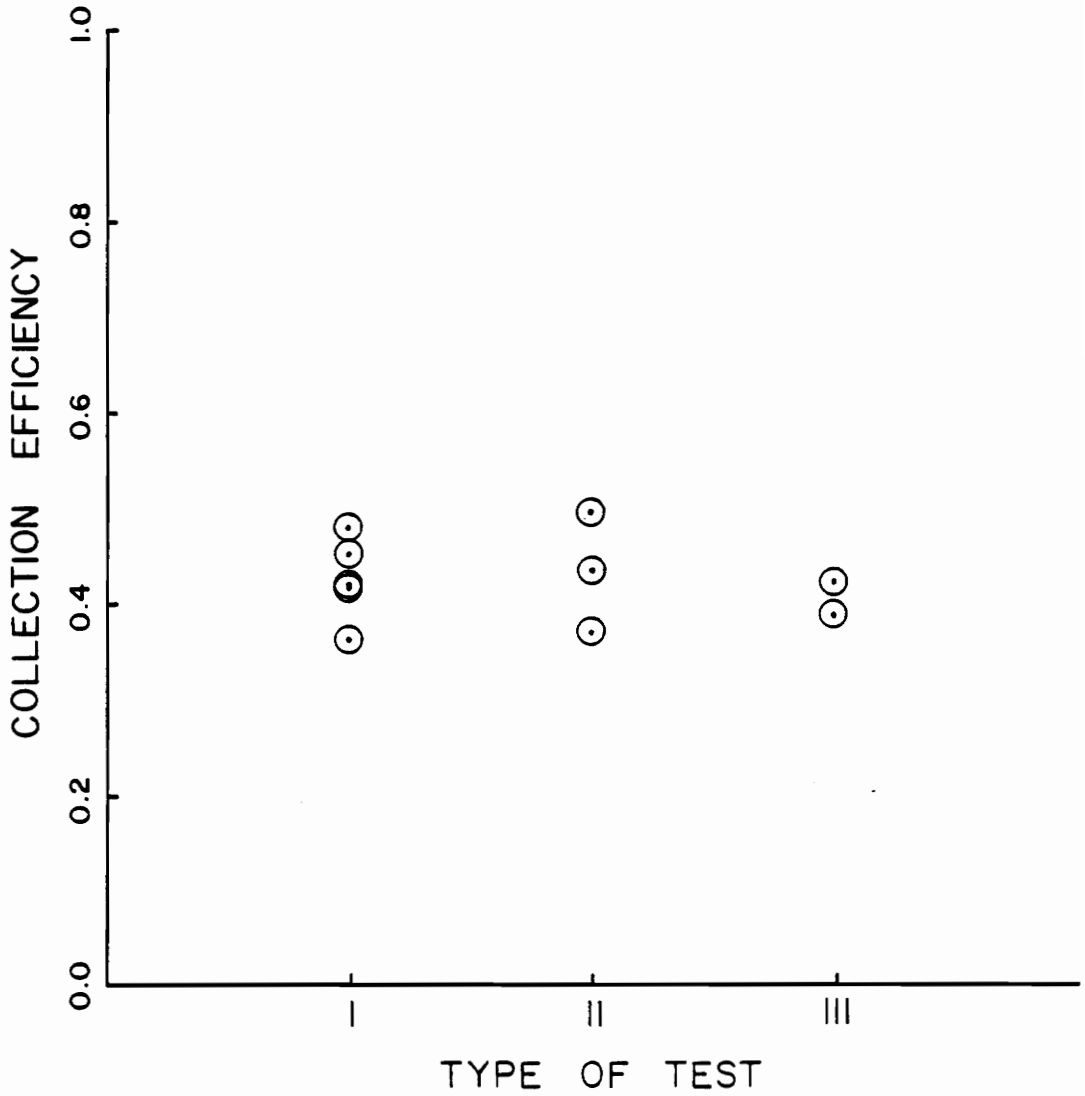

Figure 28. Comparison of the Daily Collection Efficiency of ISC B for the Three Types of Tests

collection efficiency is consistently higher for type II tests (with single noon draw).

4.2 Instantaneous Energy Technique Verification

The results presented in the previous section are based on the assumption that the energy in the tank at any instant can be approximated by the average of the measured stratified temperatures. The measurement stations for the stratified temperatures were chosen so that each measurement represents approximately one-fifth of the vertical cross-sectional area (and one-fifth of the volume) of the tank. The portion of the tank represented by each thermocouple probe is illustrated in Fig. 29. As a means of checking the assumption that the average of the stratified temperatures represents the energy in the tank the stratified temperatures were recorded at the end of several type I and II tests, when the tank was reasonably stratified. The average of these stratified temperatures is compared with the "mixed" temperatures in Fig. 30. The temperatures have been nondimensionalized by dividing by the degree of stratification, T_1-T_5. Note that the agreement is good, within three percent, but that the stratified average is consistently somewhat higher than the mixed temperature. This difference is probably caused by heating of the thermal mass of the tank, pump, piping, etc.

This technique of estimating the instantaneous energy of the tank was important for this investigation since the no draw, no circulation

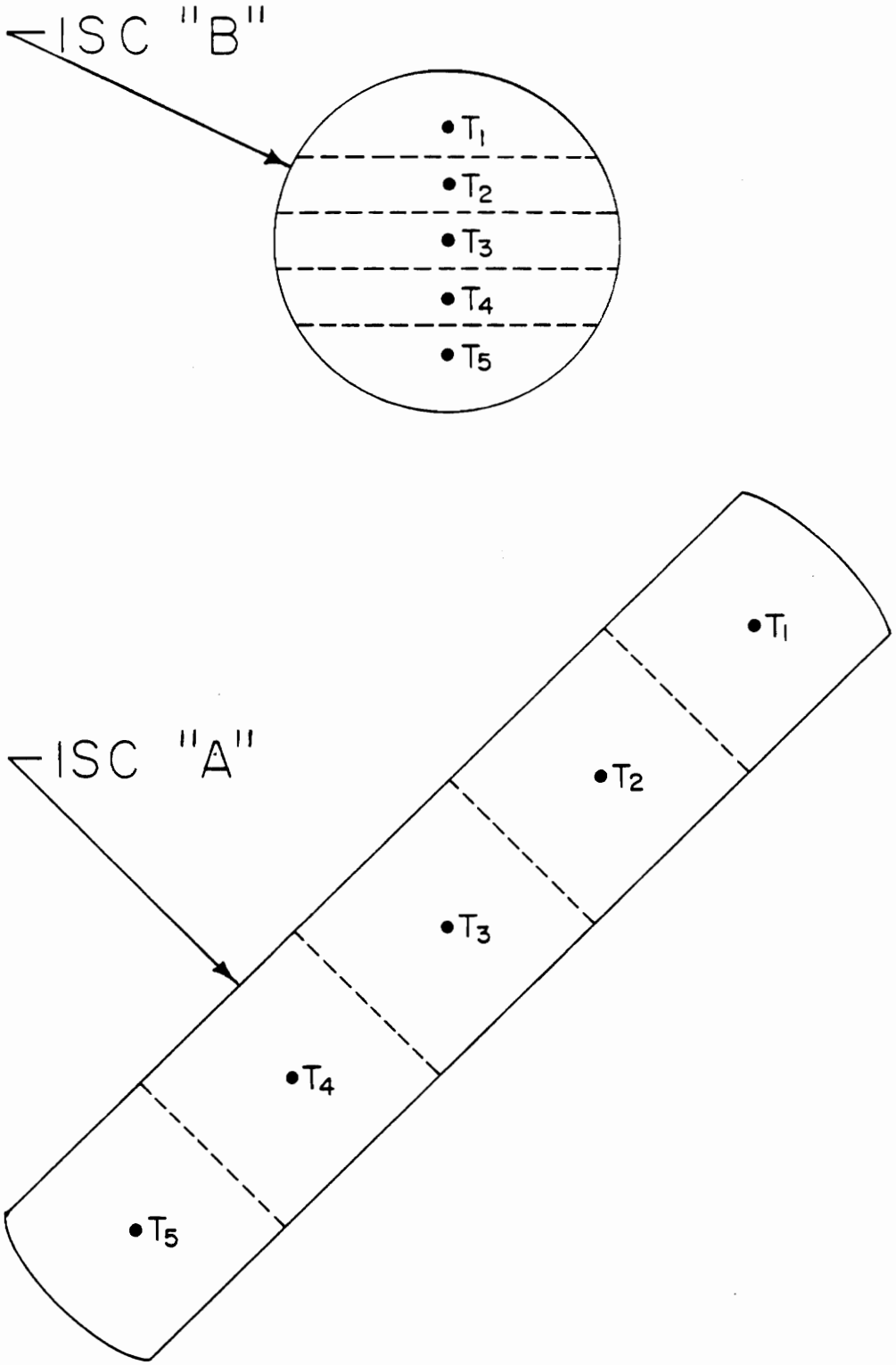

Figure 29. Thermocouple Measurement Stations for Measurement ISC Tank Stratification

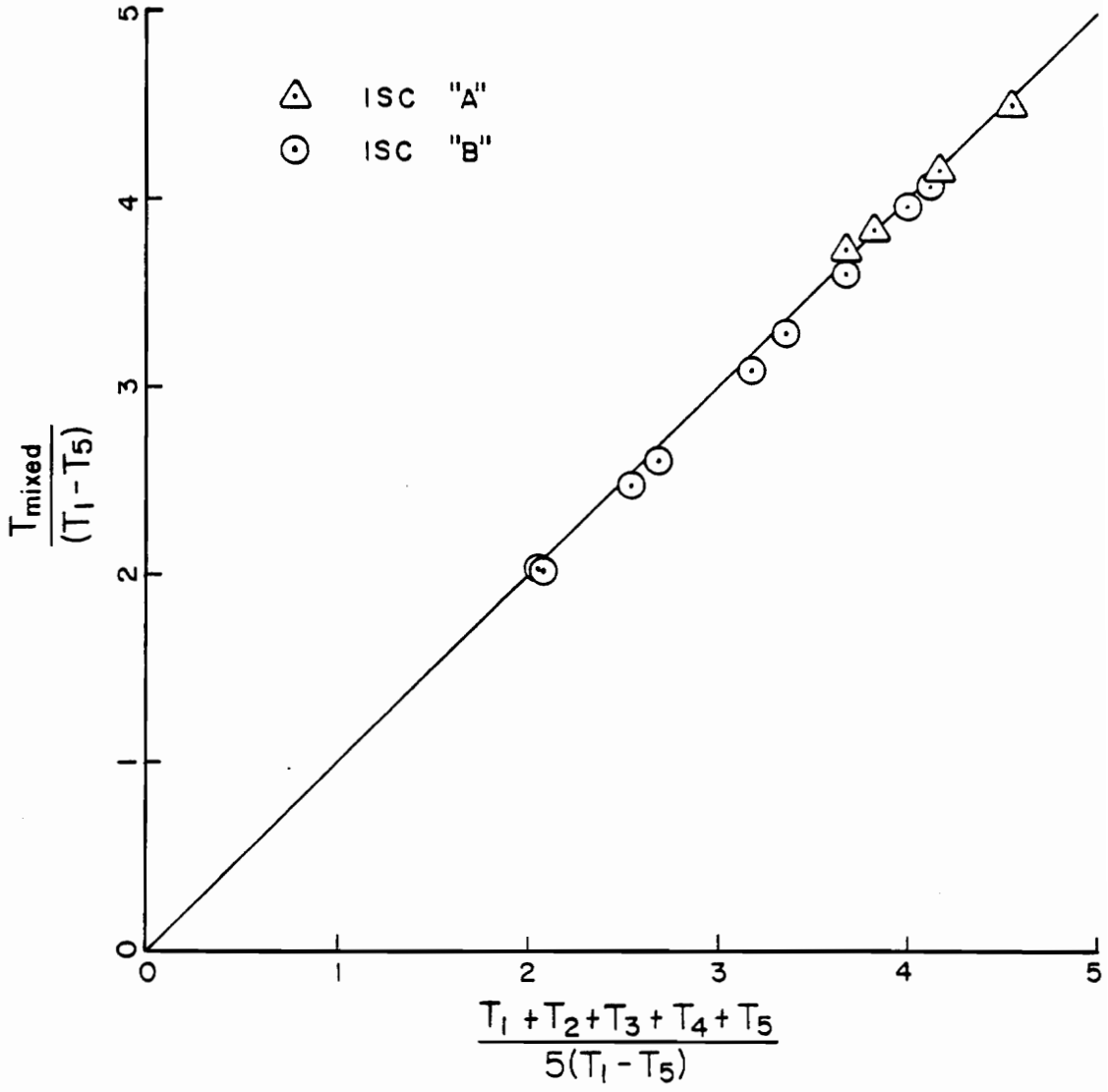

Figure 30. Comparison of Average Stratified Temperatures with "Mixed" Temperatures for ISC A & B

tests (type I) required some internal measurement of the fluid temperature (and energy). However, this technique is not a likely candidate for measuring the energy of the system in a standard test since the installation of such thermocouple probes is tedious, requiring disassembly of the ISC, and is probably not even possible for all ISC designs.

4.3 Modeling and Simulation

A mathematical model was developed to simulate the performance of system B using the techniques described in Chapter 3. This analysis was a single-node approximation for the tank temperature ignoring stratification of the fluid. This mathematical model was executed in FORTRAN code to generate predicted mean tank temperatures for the environmental conditions recorded during the all-day experimental tests. The results of these calculations are compared with the measured average tank temperature in Figs. 31 through 39 and tabulated in Appendix E. Figure 40 shows that the model is in good agreement for almost all of the experimental tests.

Several problems were encountered using this calculation procedure to predict ISC performance. Primarily, the use of the loss coefficient, U_L, presents problems not encountered with flat-plate collectors. Because of the way U_L is defined based on the temperature difference, $T_t - T_a$, the loss coefficient loses physical significance when the tank temperature is equal to the ambient temperature. This situation is encountered when the initial tank temperature is lower than the ambient

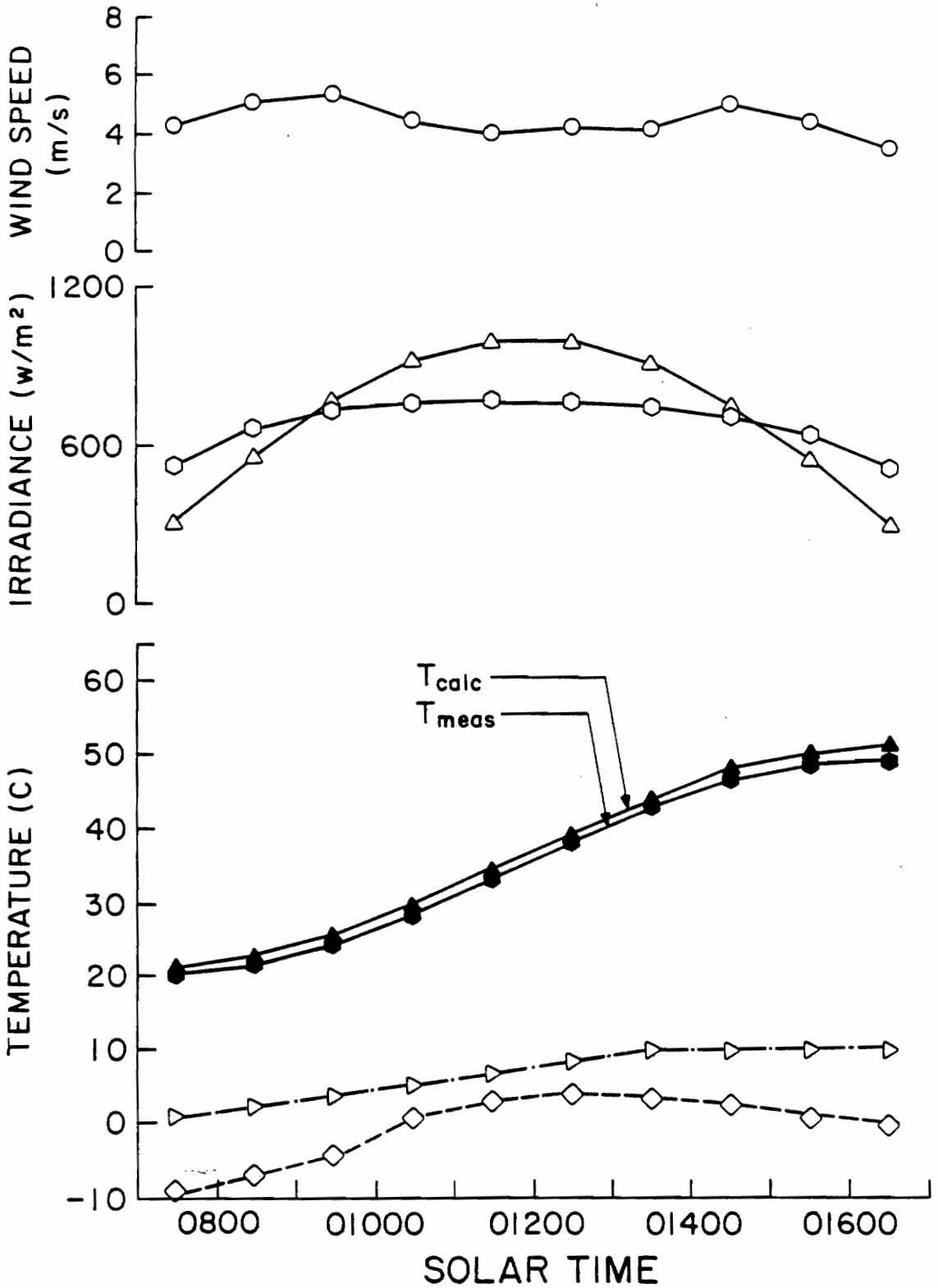

Figure 31. Comparison of Calculated and Measured Mean Tank Temperatures for a Type I Test on 4/16/83. (ISC B)

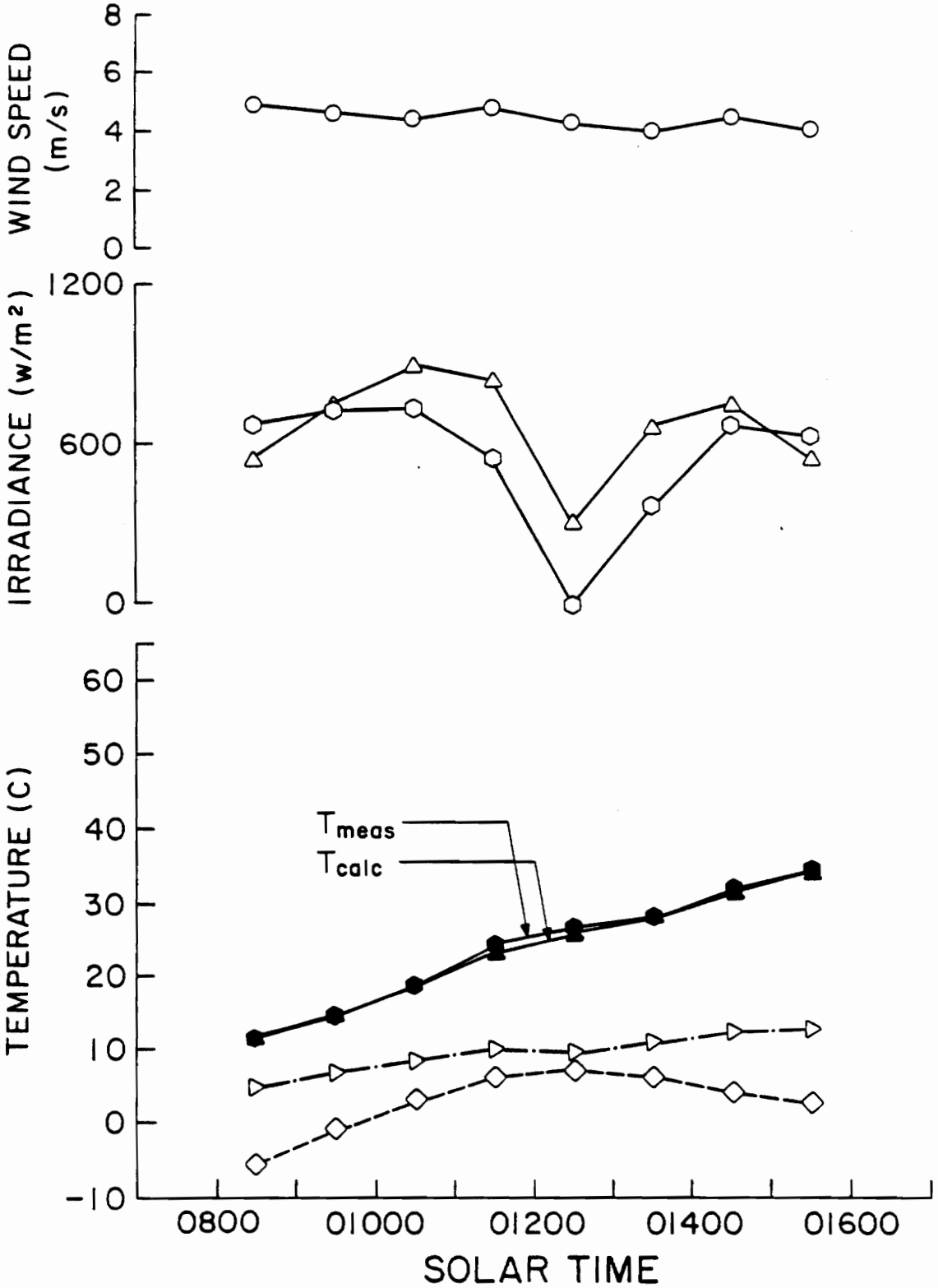

Figure 32. Comparison of Calculated and Measured Mean Tank Temperatures for a Type I Test on 4/21/83. (ISC B)

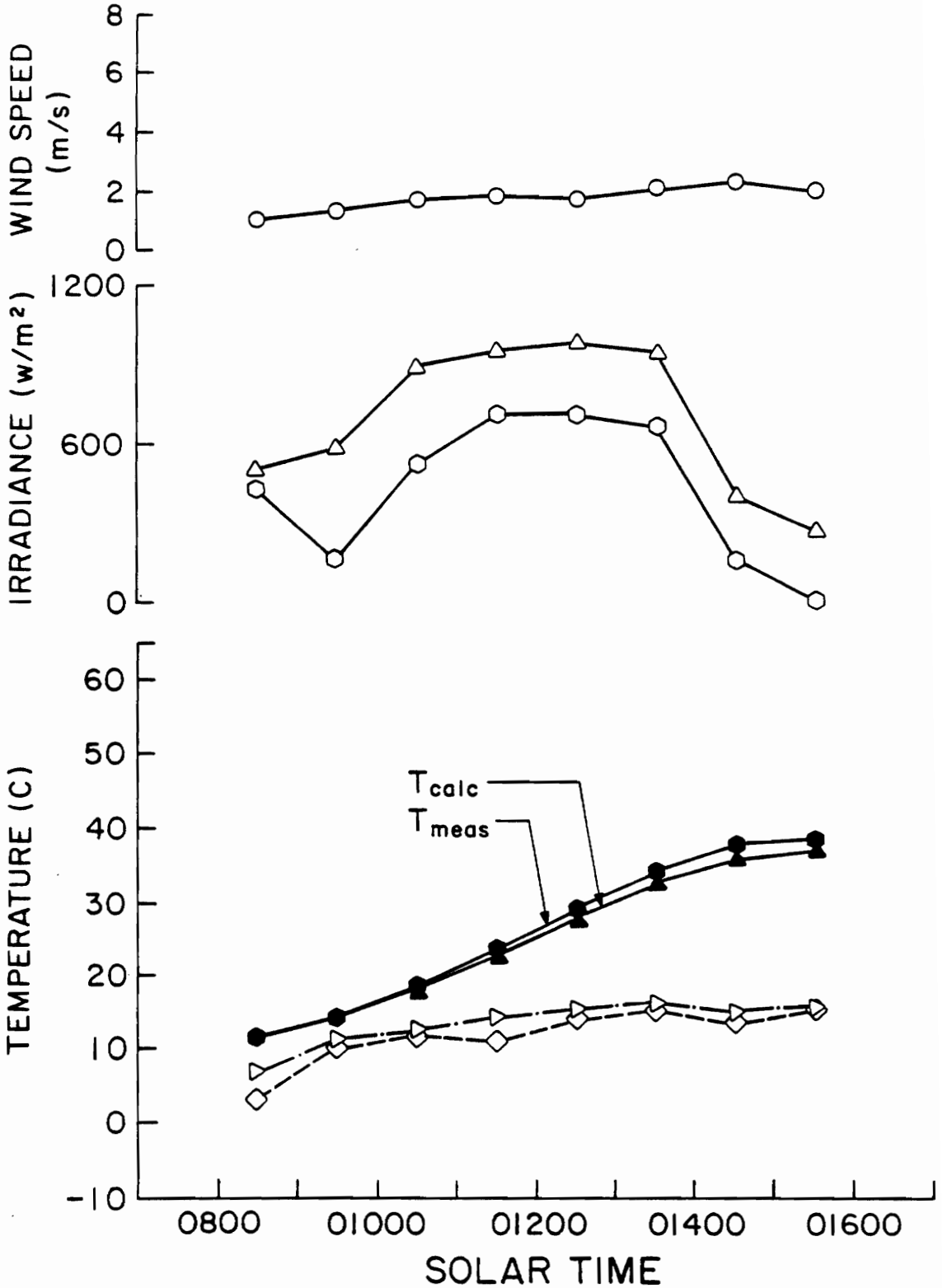

Figure 33. Comparison of Calculated and Measured Mean Tank Temperatures for a Type I Test on 4/22/83. (ISC B)

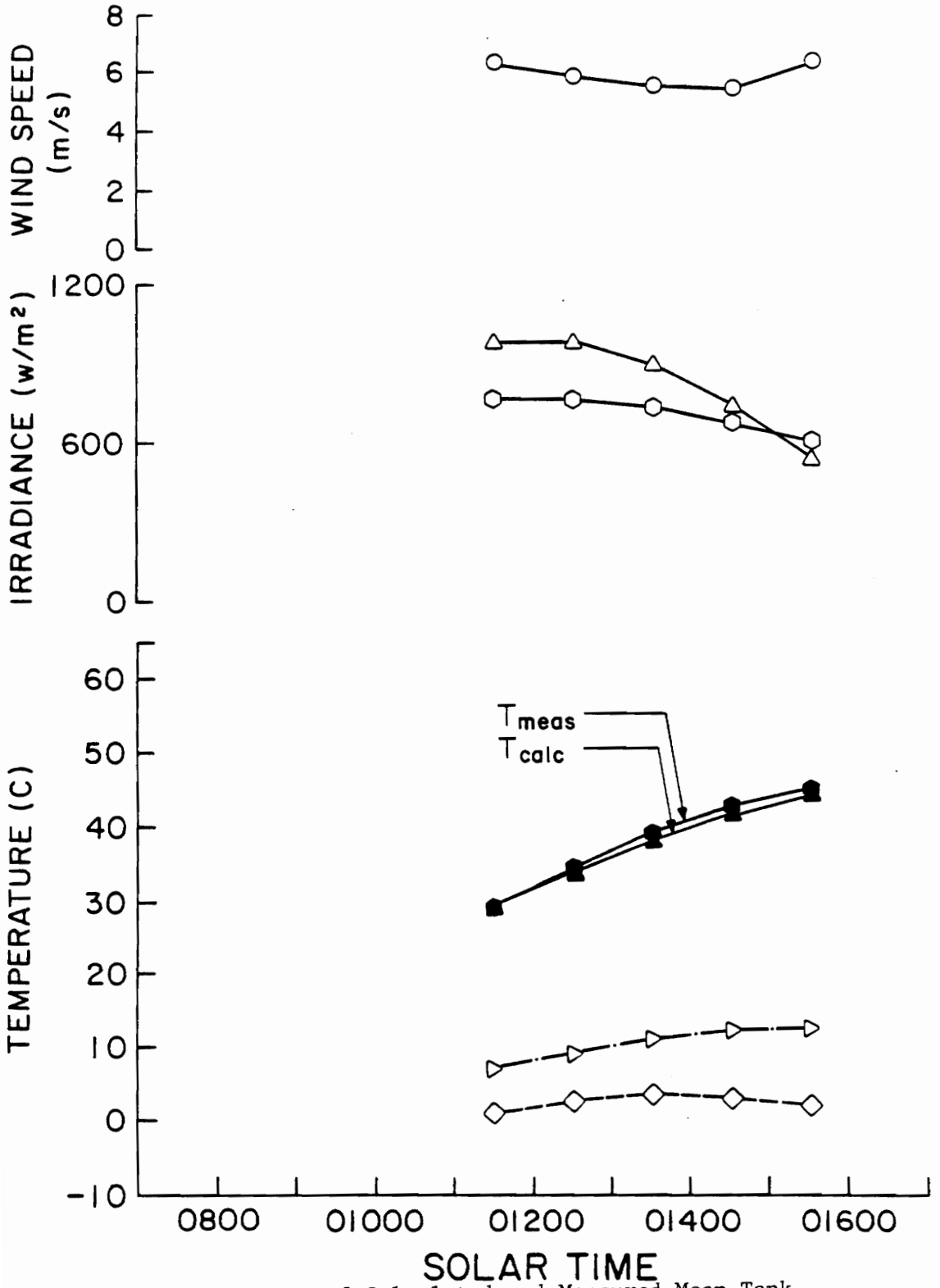

Figure 34. Comparison of Calculated and Measured Mean Tank Temperatures for a Type I Test on 4/25/83. (ISC B)

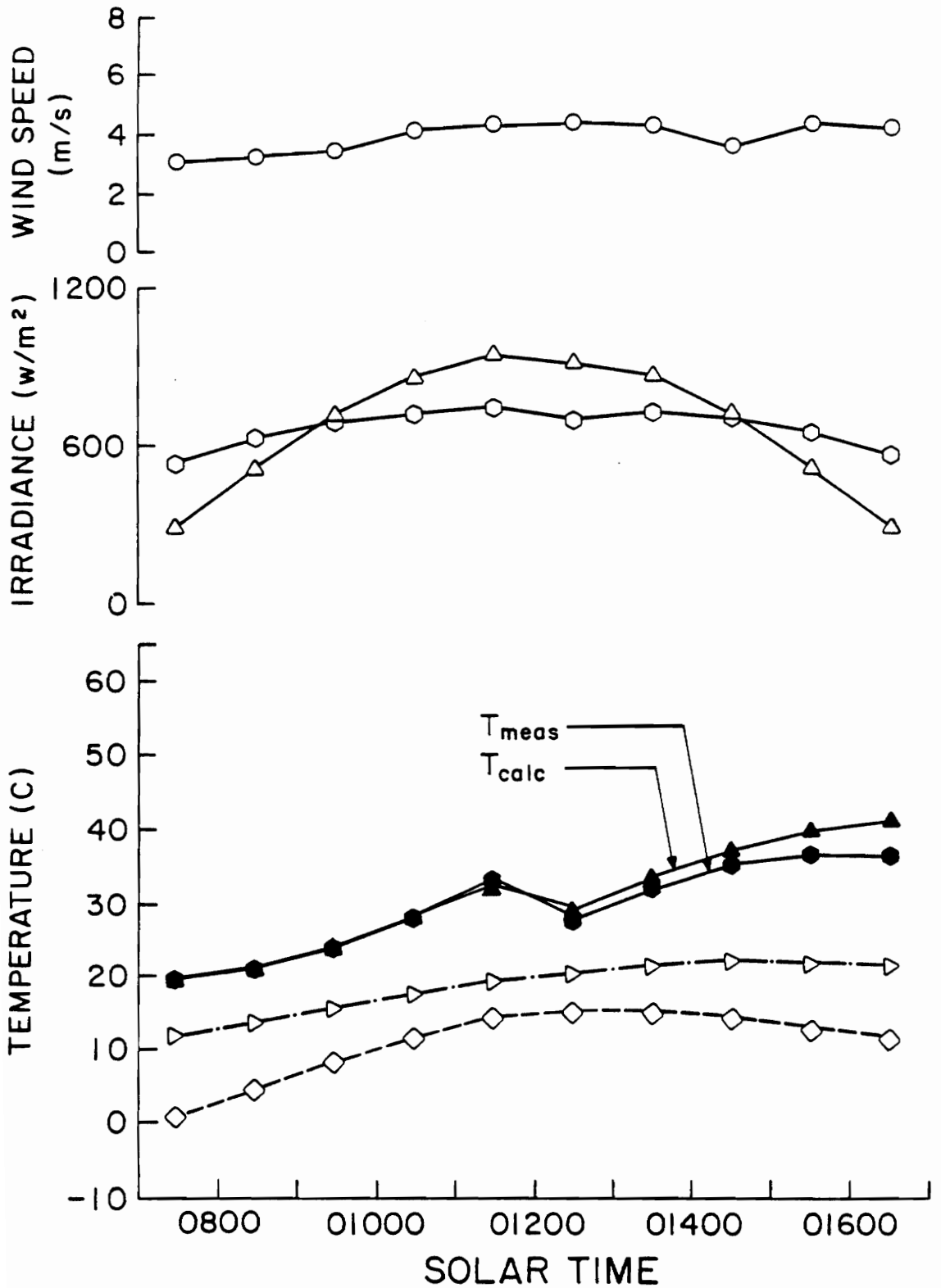

Figure 35. Comparison of Calculated and Measured Mean Tank Temperatures for a Type II Test on 4/26/83. (ISC B)

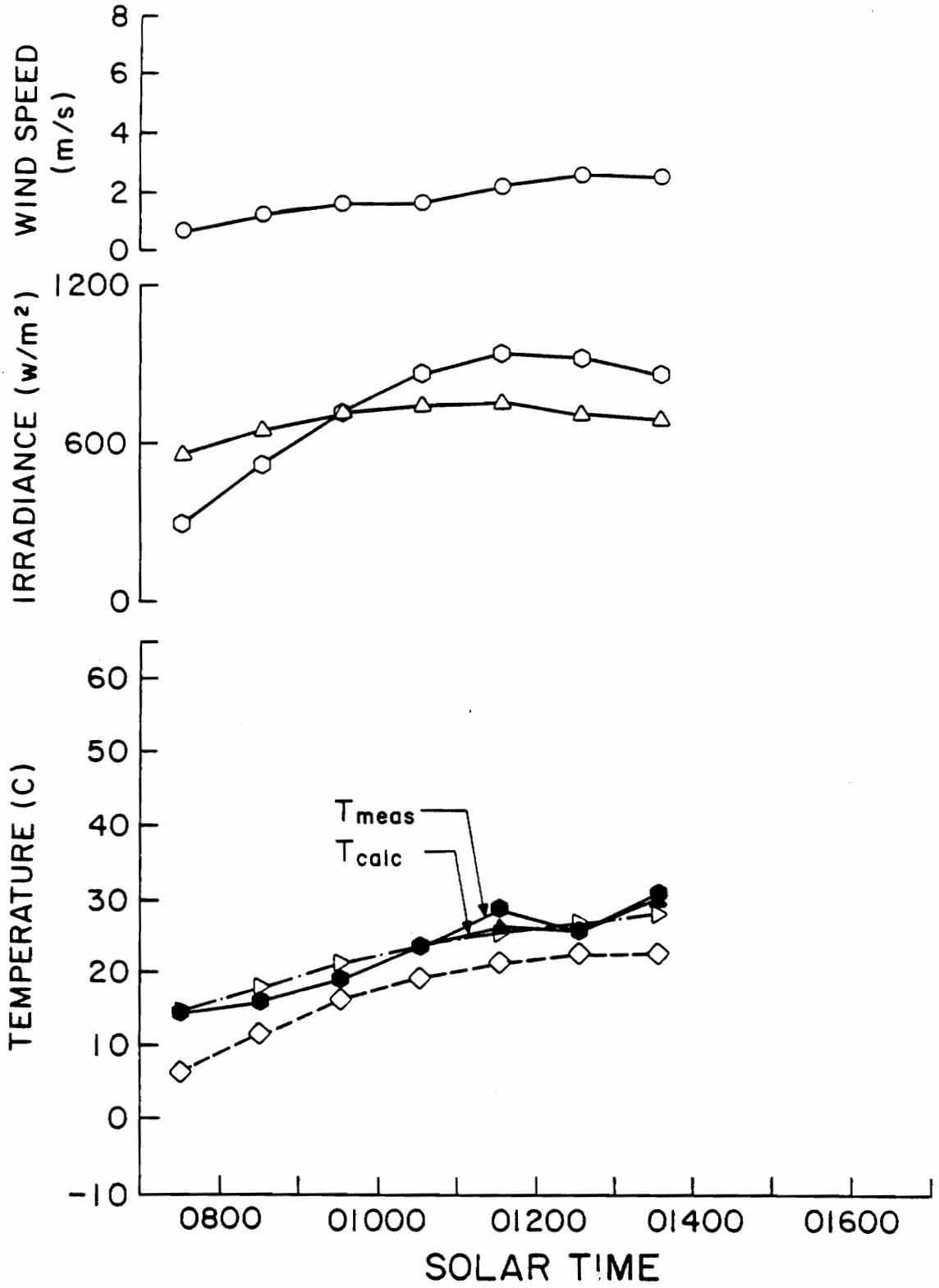

Figure 36. Comparison of Calculated and Measured Mean Tank Temperatures for a Type II Test on 4/28/83. (ISC B)

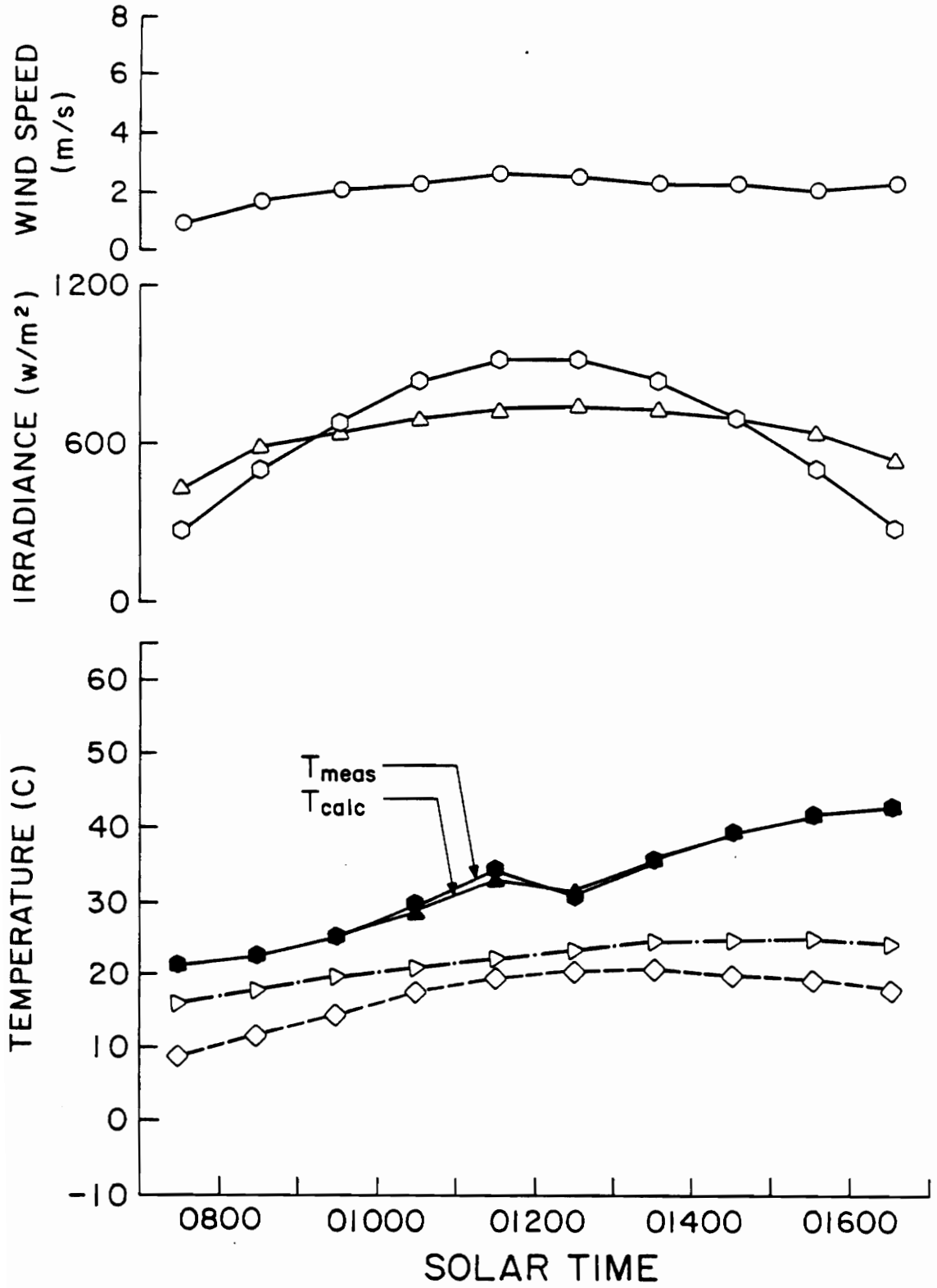

Figure 37. Comparison of Calculated and Measured Tank Temperatures for a Type II Test on 5/7/83. (ISC B)

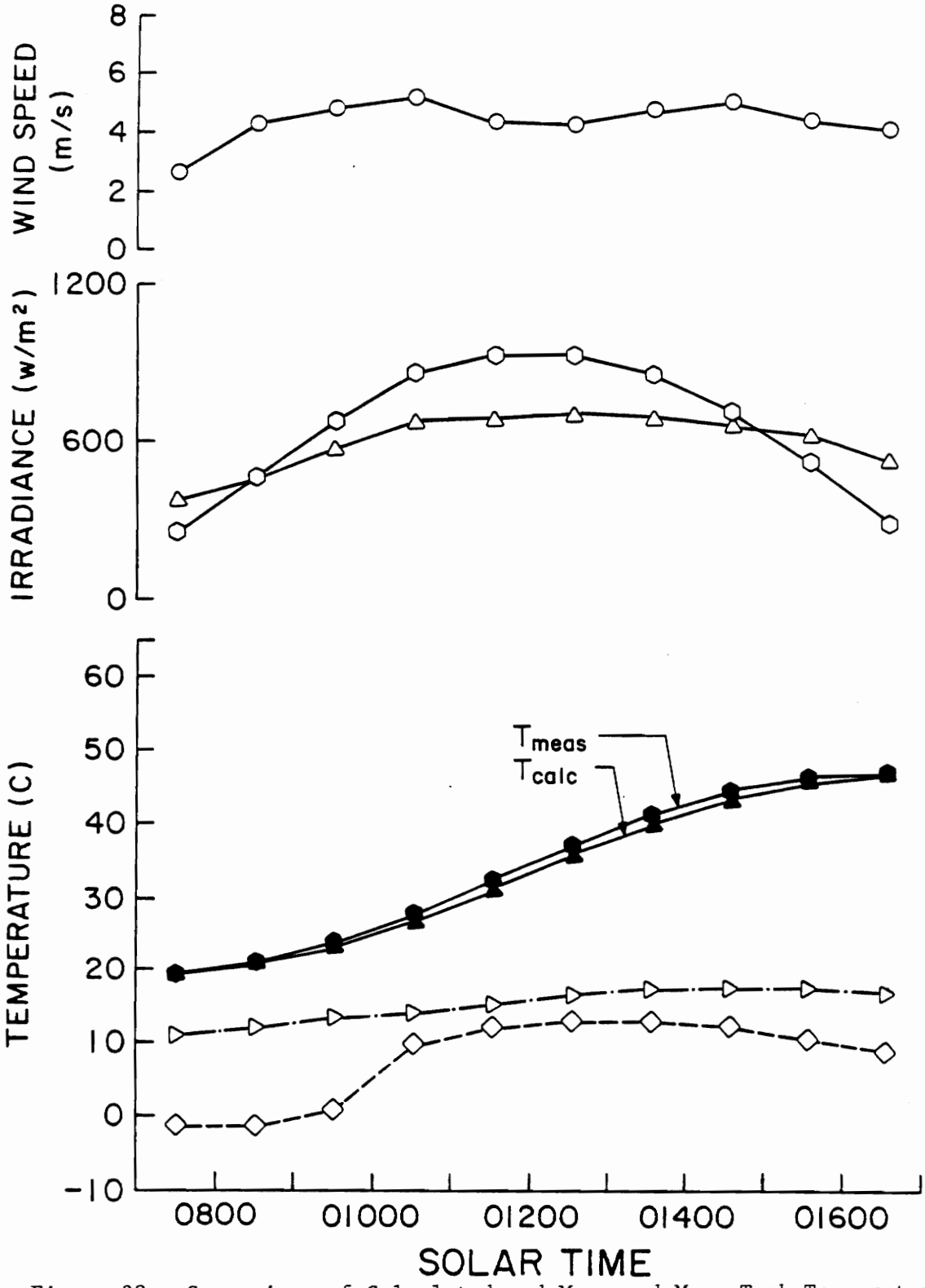

Figure 38. Comparison of Calculated and Measured Mean Tank Temperatures for a Type III Test on 5/5/83. (ISC B)

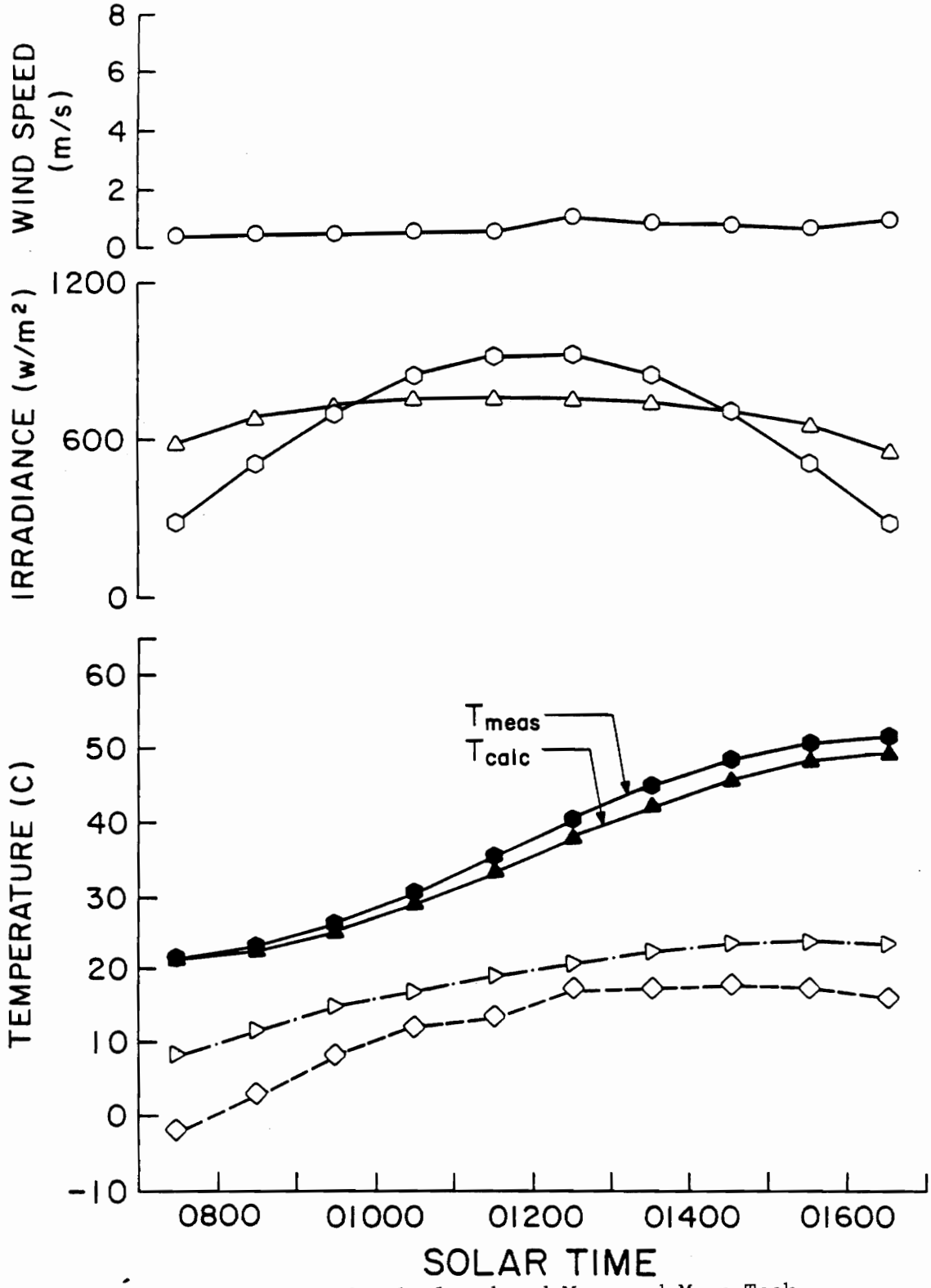

Figure 39. Comparison of Calculated and Measured Mean Tank Temperatures for a Type III Test on 5/6/83. (ISC B)

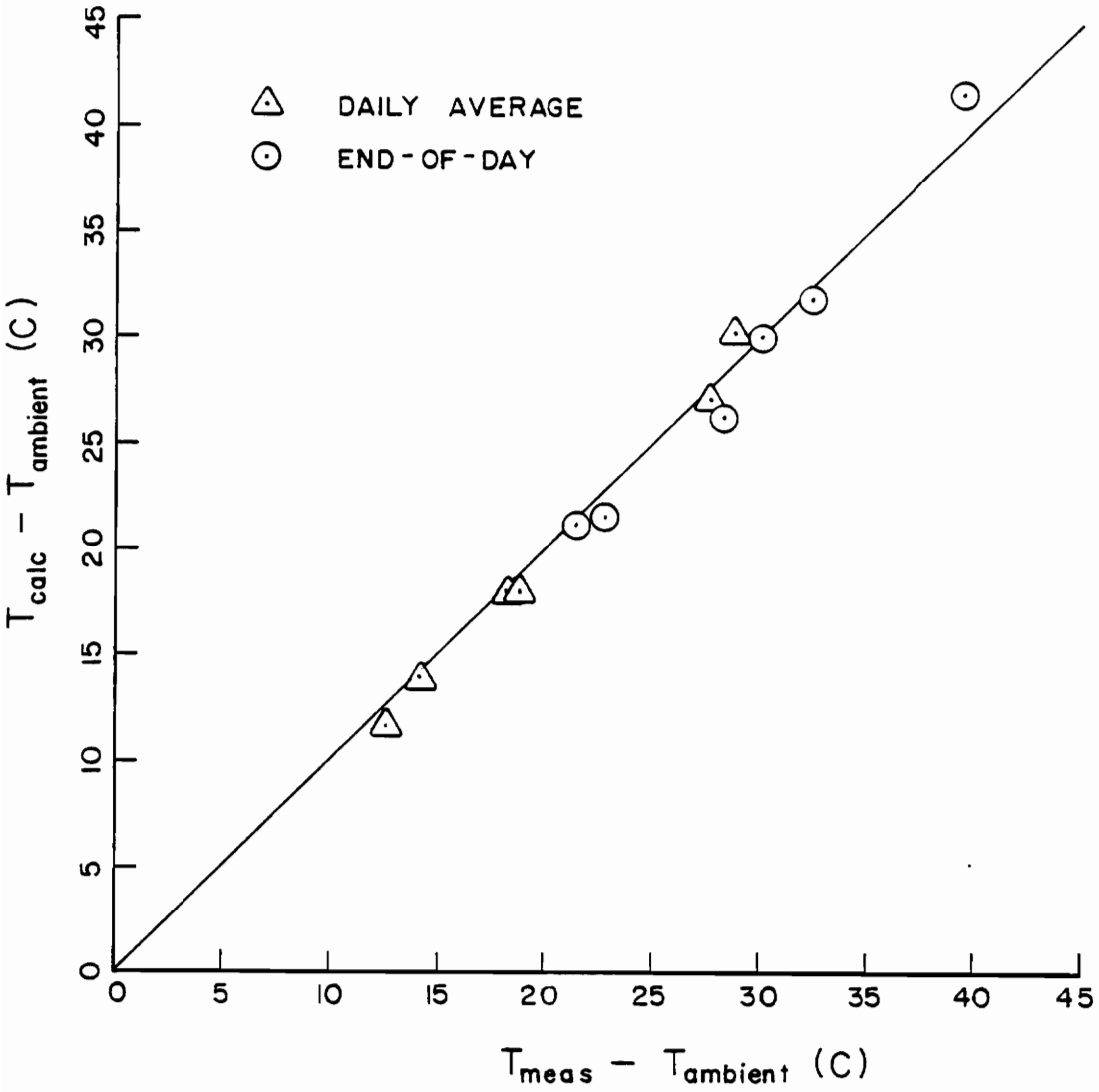

Figure 40. Comparison of End-of-Day and Daily Average Values of the Calculated Mean Tank Temperature and the Average of Measured Tank Temperatures for ISC B

temperature and the system heats up and is illustrated in Fig. 41. The scatter near $T_t = T_a$ is a result of the fact that the losses in this region are dominated by radiation losses. These radiation losses are a function of T_{sky}^4 and not T_a so that a loss coefficient based on T_a loses conventional meaning. Also, using a loss coefficient based on the mean tank temperature means that U_L, may be negative if the other components (reflector, cover 1, and air in the enclosure) have higher temperatures than the tank. This is a likely condition for the transient system since the tank has a large time constant as a result of its large thermal mass and it lags the other components in responding to incident solar radiation. The obvious solution is to use Q_{loss} directly in the transient analysis. While the Q_{loss} may still be negative when the collector is in the heating mode this will not cause computational problems when the tank and ambient temperatures are equal.

Other shortcomings of this model are primarily a result of the single-node approximation. First, this model assumes that the other components have negligible thermal mass relative to the tank/fluid. Therefore, this model may break down for systems which have a significant transient response (time constant) relative to the tank. In addition to neglecting the transient response of the other components, this model assumes no system stratification. This zero stratification model consistently underpredicts the temperature of withdrawn water since the draw temperature is not allowed to be higher than the mean tank temperature. This condition indicates problems in using this model to predict the useful energy <u>delivered</u> for an ISC system. However, the good

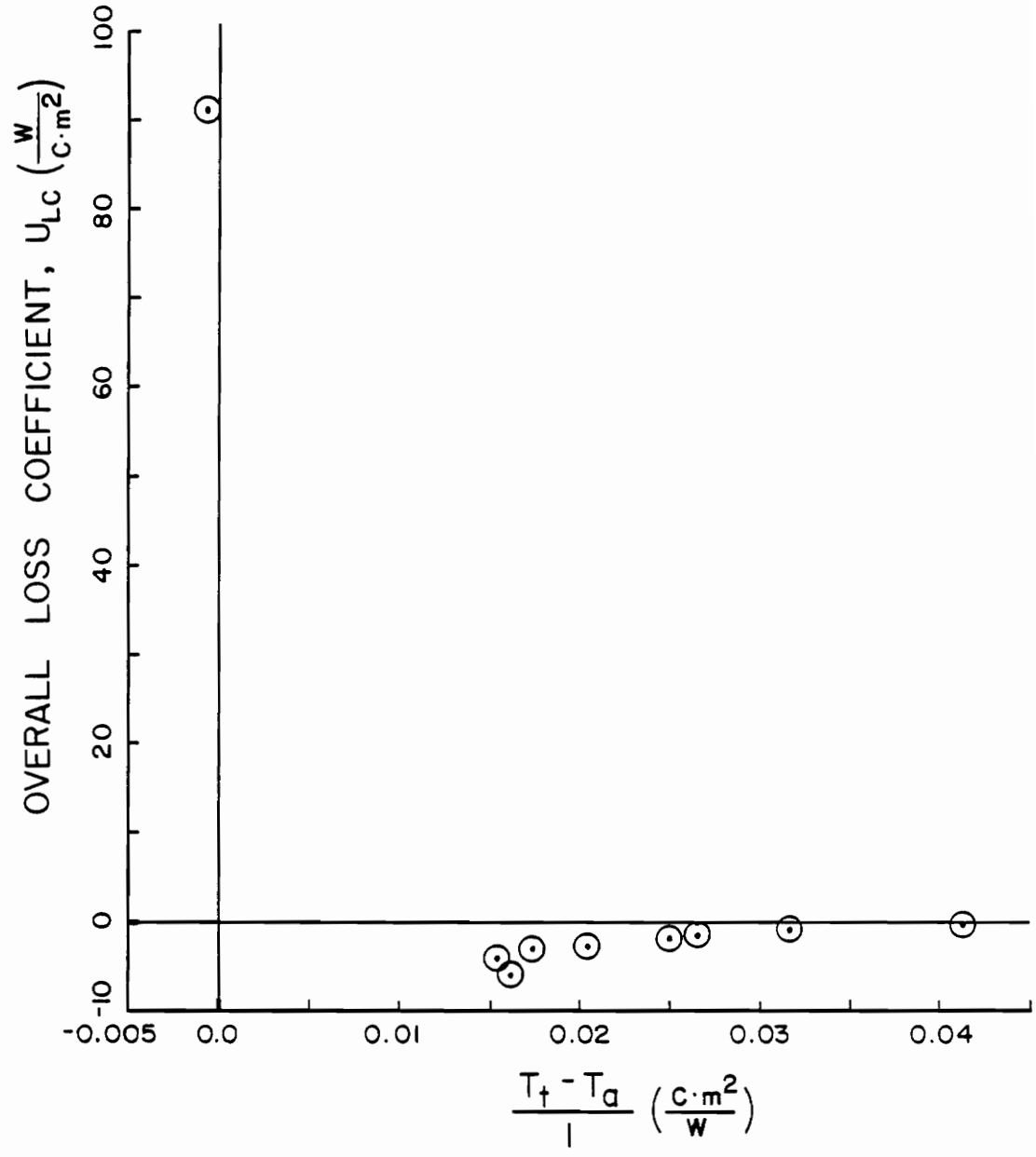

Figure 41. Comparison of Calculated Overall Loss Coefficient for ISC B for Different Tank Temperatures

agreement between calculated and measured mean tank temperatures for the "no draw" cases lends support to the assumption that the energy collected by an ISC is not greatly affected by stratification so that it may be possible to characterize the collector portion of ISC's in a test similar to those currently performed for flat-plate collectors under ASHRAE Standard 93-77.

Of primary concern in this analysis is the standard testing of ISC systems. Several implications of this modeling work are obvious with respect to the standard testing of ISC's. First, it should be noted that the use of a loss coefficient based on the tank temperature is probably not justified for ISC systems since U_L has no clear functional relationship to the quantity $T_t - T_a$ as has been established for flat-plate solar collectors. While a loss coefficient may be calculated from measured tank temperatures, it has little utility when tank and ambient temperatures are nearly equal and losses are dominated by sky temperature effects.

The results of this analysis indicate that a detailed model of an ISC system can predict with some degree of accuracy the mean tank temperatures for a given set of initial and operating conditions. However, the detailed modeling of the ray tracing, radiation shape factors, energy balances, etc. is extremely complex, even with some very sweeping simplifying assumptions, and it is not likely that a generalized model could be developed for the whole class of ISC systems which would not require a large investment of time for each individual simulation. For

this reason a model of this type is not likely to be used as the basis for any type of standard test procedure.

While the analytical model developed in this investigation is not likely to be used in any standard test procedure, the good agreement between the mean tank temperature predicted by the model and the measured mean tank temperatures from stratified tests suggests that the degree of stratification may not be an important factor in the way an ISC collects solar radiation. This comparison, coupled with the lack of significant differences between stratified and non-stratified daily collection efficiencies, implies that a test similar to ASHRAE 93-77 may be used to characterize the collector element of ISC's.

V. CONCLUSIONS

The following conclusions result from this investigation of test procedures for integral storage collectors for SDHW applications:

1. Forced flow through integral storage collectors and the resultant elimination of thermal stratification does not have a significant effect on the measured daily collection efficiency. This observation supports the hypothesis that a test similar to ASHRAE Standard 93-77 might be used to characterize the collection efficiency, incident angle modifier, and loss characteristics of ISC's.
2. It is possible to predict the thermal performance of an ISC to a reasonable accuracy. The analysis is complex and would be difficult to generalize for all ISC designs, so that such calculations are not likely to be used in generating all-day performance ratings. However, the good agreement between the analytical results (obtained assuming no thermal stratification) and the experimental results in the stratified mode supports the idea that the ISC might reasonably be tested in an ASHRAE 93-77 type test without a significant loss in accuracy attributable to stratification breakup.
3. The experimental data recorded during this investigation for a variety of initial conditions, ambient conditions, irradiance levels, and flow/draw configurations may be used to validate

any proposed test method. A valid test method should be able to duplicate the experimental results of this investigation.

Given that the collection characteristics can be obtained, a properly designed heat source may be used to input a programmed amount of energy to the tank and still preserve stratification in an ASHRAE Standard 95 type test.

REFERENCES

1. ASHRAE Standard 95-1981, "Methods of Testing to Determine the Thermal Performance of Solar Domestic Water Heating Systems," American Society of Heating, Refrigerating, and Air-Conditioning Engineers, Inc., 1791 Tullie Circle, NE, Atlanta, Georgia, 30329, December 17, 1981.

2. Hill, J. E., and A. H. Fanney, "A Proposed Procedure of Testing for Rating Solar Domestic Hot Water Systems," ASHRAE Transactions, Vol. 86, Part 1, 1980, pp. 805-822.

3. Fanney, A. H., and W. C. Thomas, "Simulation of Thermal Performance of Solar Collector Arrays, ASHRAE Transactions, Journal of Solar Energy Engineering, Vol. 103, No. 3, August 1981, pp. 258-267.

4. Cooper, R. I., and J. C. Lacey, "Evaluation of a Household Solar Water Heating System Rating Procedure Using a Reference System for Performance Comparison," Solar Energy, Vol. 26, No. 3, 1981.

5. ASHRAE Standard 93-1977, "Methods of Testing to Determine the Thermal Performance of Solar Collectors," American Society of Heating, Refrigeration, and Air-Conditioning Engineers, Inc., 1791 Tullie Circle, NE, Atlanta, Georgia 30329, revised printing 1978.

6. Fanney, A. H., W. C. Thomas, C. A. Scarbrough, and C. P. Terlizzi, "Analytical and Experimental Analysis of Procedures for Testing Solar Domestic Hot Water Systems," NBS Building Science Series 140, 1982.

7. Koldhekar, Setish M., "Temperature Stratification in Hot Water Solar Thermal Storage Tanks," AIAA Paper 81-0368, 1981.

8. Stickney, B. L., and C. Nagy, "Performance Comparisons of Several Passive Solar Water Heaters," Proceedings of the Fifth National Passive Solar Conference, ASISES, 1980.

9. Stickney, B. L., "Comparative Performance Indices for Batch Water Heaters," Proceedings of the Sixth National Passive Solar Conference, ASISES, Sept. 8-12, 1981.

10. Burton, J. W., and P. R. Zweig, "Side by Side Comparison Study of Integral Passive Solar Water Heaters," Proceedings of the Sixth National Passive Solar Conference, ASISES, Sept. 8-12, 1981.

11. Sodha, M. S., P. K. Bansal, and N. D. Kaushik, "Performance of Collector/Storage Solar Water Heaters: Arbitrary Demand Pattern," Energy Conversion and Management, Vol. 21, No. 4, pp. 229-238, 1981.

12. Sodha, M. S., P. K. Bansal, and S. C. Kaushik, "Simple Transient Thermal Model for Collector/Storage Solar Water Heater," International Journal of Energy Research, Vol. 5, No. 95, 1981.

13. Garg, H. P., and U. Rani, "Theoretical and Experimental Studies on Collector/Storage Type Solar Water Heater," Solar Energy, Vol. 29, No. 6, pp. 1981, 467-478.

14. "TRNSYS, A Transient System Simulation Program," User's Manual, Report 38, Solar Energy Laboratory, Engineering Experiment Station, University of Wisconsin-Madison, April 1981.

15. Reichmuth, H., and D. Robison, "An Analytical Model and Associated Test Procedure for Predicting the Performance of Batch Type Solar DHW Systems," Progress in Passive Solar Energy Systems, American Solar Energy Society, Inc., 1982.

16. Thomas, W. C., "Solar Collector Evaluation," VPI&SU Report No. ENG 79.20, Mechanical Engineering Department, VPI&SU, Blacksburg, Va., 1979.

17. Sparrow, E. M., and R. D. Cess, Radiation Heat Transfer, Brooks/Cole Publishing Company, Belmont, California, 1967, p. 301.

18. Hollands, K. G. T., T. E. Unny, G. D. Raithby, and L. Konicek, "Free Convection Heat Transfer Across Inclined Air Layers," Journal of Heat Transfer, Vol. 98, 1976, pp. 189-193.

19. Holman, J. P., Heat Transfer, 5th ed., McGraw-Hill, New York, 1981, p. 275.

20. McAdams, W. H., Heat Transmission, 3rd ed., McGraw-Hill, New York, 1954.

21. Watmuff, J. H., W. W. S. Charters, and D. Procter, "Solar and Wind Induced External Coefficients for Solar Collectors," Comples, Vol. 2, 1977.

22. Duffie, J. A., and W. A. Beckman, Solar Engineering of Thermal Processes, Wiley, 1980.

23. Thomas, W. C., "Thermal Efficiency Test Procedures for a Cylindrical Concentrating Collector," Solar Concentrating Collectors, Proceedings of the ERDA Conference on Concentrating Solar Collectors, Session 6, Georgia Institute of Technology, September 26-28, 1977.

24. Johnson, L. W. and R. D. Riess, Numerical Analysis, 2nd ed., Addison-Wesley, Reading, Massachusetts, 1982, p. 146.

25. Ramsey, J. W., J. T. Borzoni, and T. H. Holland, "Development of Flat-Plate Solar Collectors for the Heating and Cooling of Buildings," NTIS # N75-264951, June 1975, pp. 123-144.

APPENDIX A

Automatic Data Acquisition System

Introduction

The very nature of solar energy research requires that meteorological instrumentation, temperatures, and other data be continuously monitored over relatively long periods ot time. Therefore, this automatic data acquisition system has been built for the Solar Collector Research Laboratory at VPI&SU to facilitate research requiring long term, continuous tests up to one week unattended after initialization.

Previous research efforts at VPI&SU made use of chart recorders to continuously monitor test conditions. Average or accumulative data then had to be obtained by manual integration of the chart trace using a planimeter or some other graphical technique. This tedious method was replaced with ten channels of electronic integrators to obtain a true average over the five-minute reset cycle of the integrators, avoiding the limitations of digital sampling techniques for rapidly changing variables. Recording these five-minute averages manually still required many manhours for a test of any significant length. Also, these techniques have many opportunities for human error in data entry to the mainframe computer or manual recording of data.

An automatic data acquisition system, currently in use in the Solar Lab, was developed to accomplish several goals. First, the

collection of the signals from the electronic integrators using a microcomputer allows for continuous data collection, 24 hours/day, for periods up to one week without human intervention. Also, this system virtually eliminates the possibility of introducing human error into the data, since the parity checks in digital transmission do not allow any errors in the transfer of the data from the data acqusition system to the mainframe computer. And finally, this system allows for the introduction of the calibration characteristics of the transducers directly into the software so that real data (in meaningful units) can be displayed continuously by the microcomputer. Thus, if a transducer is producing inconsistent results or if a parameter drifts out of its allowable range then the test can be aborted before a whole day (or week) is wasted. A schematic of the system is shown in Fig. A.1 and described in more detail on subsequent pages.

Principles of Operation

1) Transducer signals are input to electronic integrators built by AGM Electronics, Inc. These integrators consist of an input amplifier (single ended), a voltage controlled oscillator (VCO), a counter, and a dual-slope integrating A/D converter. The counter produces a "ramp" output proportional to the accumulated number of pulses from the VCO since the last reset. When a clock pulse is received from an external clock (every five minutes) the peak value of the ramp is measured by the A/D converter, the ramp is reset to zero, and another integration cycle is begun.

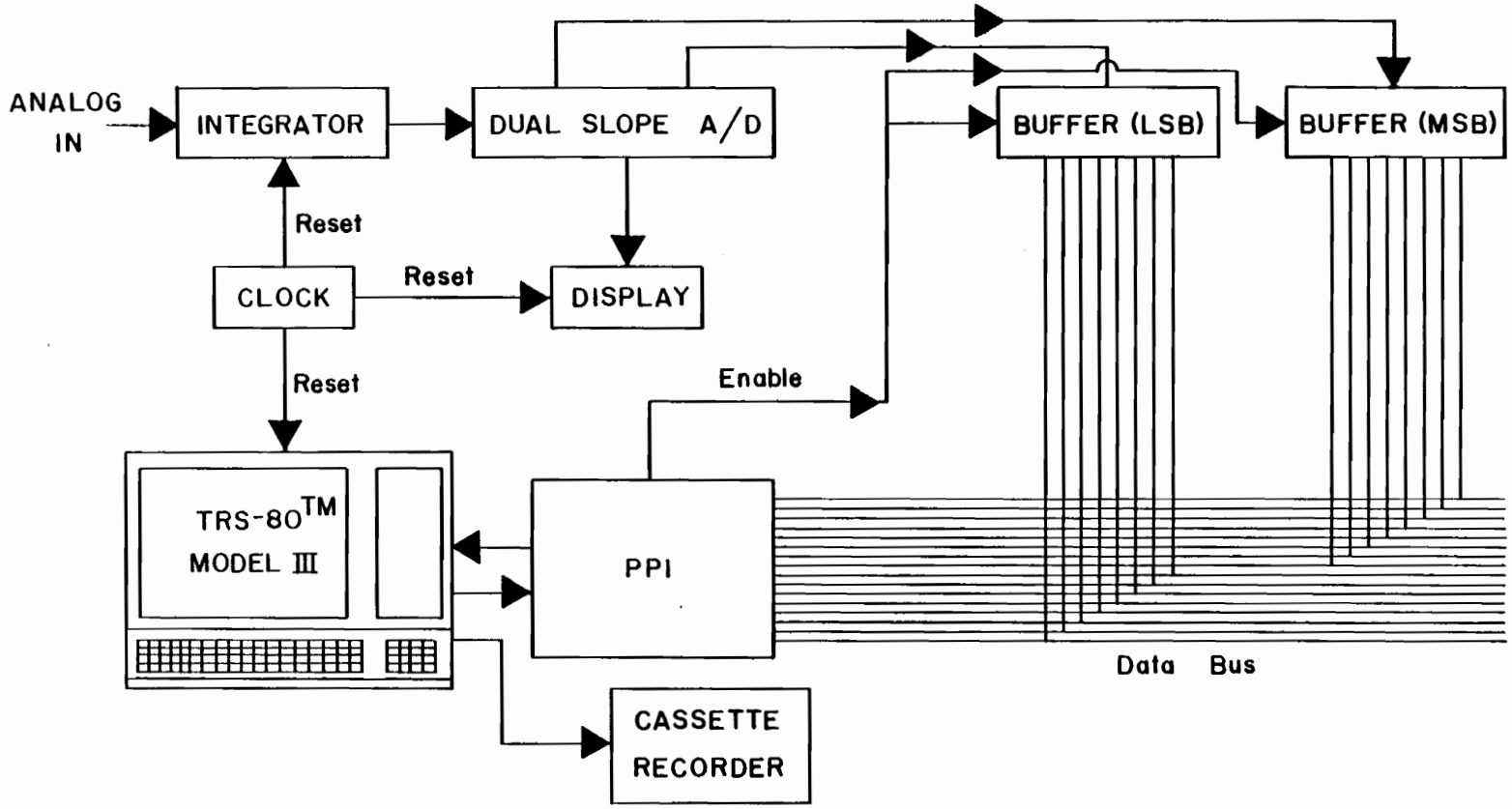

Figure A.1. Schematic of the Automatic Data Acquisition System for the VPI&SU Solar Collector Research Laboratory

2) The A/D converter, Analogic AN2570, provides a 3 1/2 digit LED display and a parallel BCD (binary-coded decimal) output. The output of the AN2570 is, by design, proportional to the true average value of the transducer signal over the five-minute integration period. The AN2570 also latches the average value so that it is displayed continuously until an updated average is available.

3) The 14-bit BCD signal from the AN2570 is split into two signals, one consisting of the six Most Significant Bits (MSB) and the other consisting of the eight Least Significant Bits (LSB). These two numbers are stored in two 8-bit buffers until "enabled" by the control circuitry. When "enabled" the buffers transmit their information to a 14-bit data bus and eventually to the TRS-80™.

4) The same reset signal (from the clock) which controls the electronic integrators also is received by the microcomputer telling it that a new set of data is ready to be collected from the buffers. The microcomputer then sequentially addresses each 8-bit buffer through a Tychon Programmable Peripheral Interface Adapter (PPIA). The PPIA interprets a binary code for the device address of each buffer and "enables" only that buffer requested by the microcomputer. The PPIA then relays the bits on the data bus to

the microcomputer according to a control register code provided by the microcomputer.

5) Once the BCD data has been collected from each channel and stored in an array in decimal form (after conversion from BCD), an equation for the transducer calibration curve is used to obtain "real" data in terms of W/m^2 insolation, degrees Celsius, or m/s wind velocity, for instance. Then the microcomputer goes into a wait mode until the next reset pulse is received from the clock.

6) After twelve five-minute cycles an hourly average, or cumulative, value can be obtained using the software. Likewise daily, weekly, monthly, or even yearly values could be obtained if enough memory space was available in the microcomputer. The current configuration saves hourly and daily values and stores them on cassette tape for subsequent transfer to the mainframe computer for analysis. This eliminates any opportunity for human error in data collection or computer data entry.

APPENDIX B

Optical Ray-Tracing for Beam Radiation

The beam radiation angles of importance to this study are shown in Fig. B.1. The equations for the incident angle and zenith angle are summarized below for a south-facing collector, making use of the "artificial latitude" simplifications as in Duffie and Beckman (22):

$$\cos\theta = \cos(\phi - \beta)\cos\delta\cos\omega + \sin(\phi - \beta)\sin\delta \qquad \text{B.1}$$

$$\cos\theta_Z = \sin\delta\sin\phi + \cos\delta\cos\phi\cos\omega \qquad \text{B.2}$$

Equations for ψ and ζ are from Thomas (23) and are listed below.

$$\psi = \beta - \arctan(\tan\theta_Z \cos\gamma_{sun}) \qquad \text{B.3}$$

$$\tan\zeta = \tan\theta_Z \sin\gamma_{sun}\cos\psi \qquad \text{B.4}$$

where

$$\sin\gamma_{sun} = \cos\delta\sin\omega/\sin\theta_Z \qquad \text{B.5}$$

The beam radiation incident on the tank is composed of direct (nonreflected) and reflected beam radiation. The approach used to calculate the mean flux on the tank from beam radiation was taken from Thomas (16) with several modifications and extensions. A two-dimensional ray-tracing scheme is used which follows the path of each "ray" which is incident on the collector and determines when the ray either intercepts the tank-absorber, exits through the covers, or (after 11 or more reflections) is taken to be completely diffuse radiation and added to the scattered (diffuse) radiosity of the reflector.

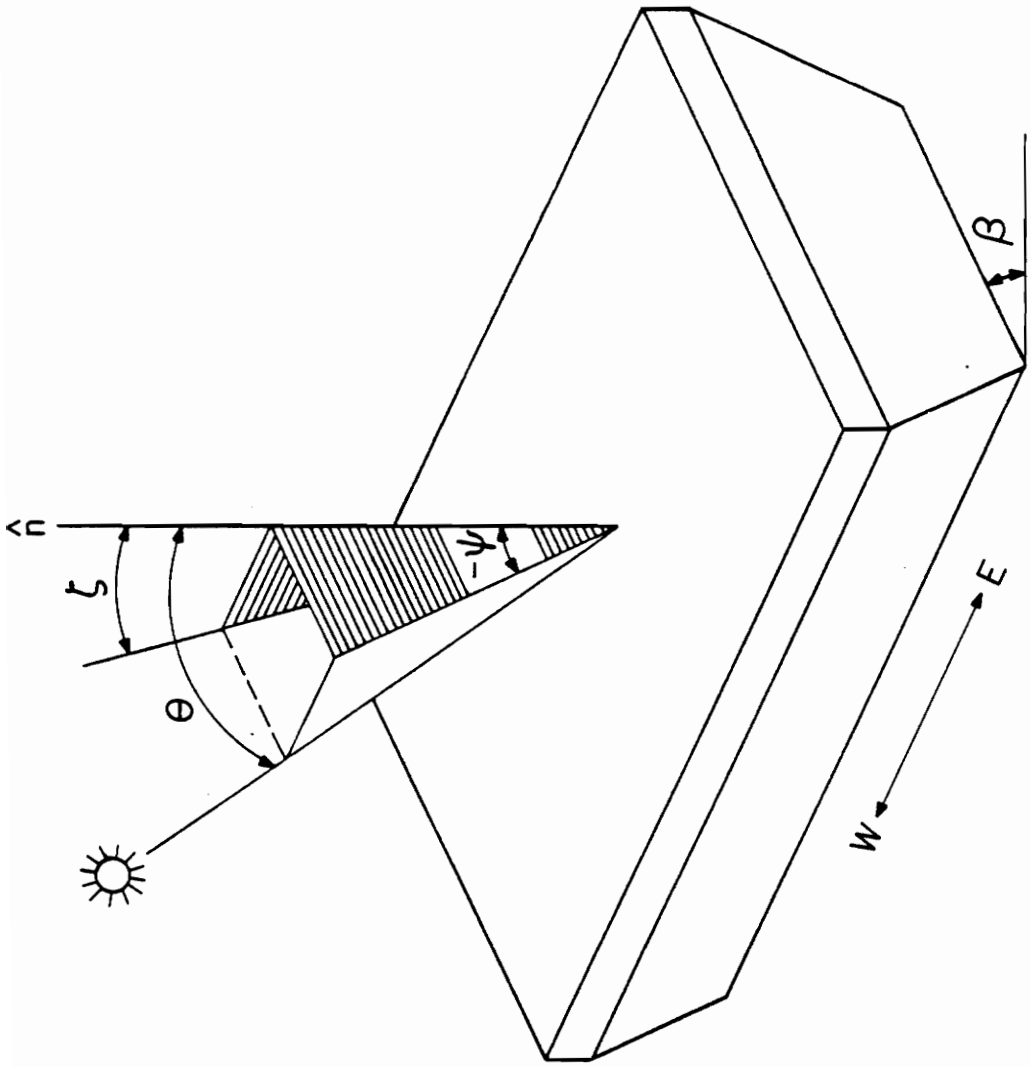

Figure B.1. Beam Radiation Geometry for ISC B

Figure B.2 shows a representative ray incident on the reflector. For any given incident angle, ψ, the limits of the reflector area which receive beam radiation, i.e. are not shaded by the tank or reflector itself, can be easily determined. The procedure involves finding an equation for the incident ray of the form

$$X = A + B(Z) \tag{B.6}$$

and determining where this ray intersects the reflector profile curve defined by $C = C(Z)$. If a function $F(Z)$ is defined such that

$$F(Z) = X - C = A + B(Z) - C(Z) \tag{B.7}$$

then the intersection of the ray and the reflector is simply the root of $F(Z)$. The bisection method (24) is used to find the root of $F(Z)$ since it is absolutely convergent if two bounding values for Z are known. Other methods for finding the root of $F(Z)$ were considered and discarded because of convergence problems when the reflector profile $C(Z)$ has a discontinuous derivative (slope) as in system B of this investigation. In this manner the limiting shading points of the reflector are calculated for the right and left sides of the reflector. To simplify the analysis the equations were developed only for positive values of ψ since a negative ψ corresponds to interchanging right and left sides. For the determination of each shading point different values of the constants A and B are needed.

For Z_{min},r:

$$B = -1/\tan \psi \tag{B.8}$$

$$A = b_c + R_t\ (1 + 1/\sin \psi) \tag{B.9}$$

For Z_{max},r:

$$Z_{max},r = W_a/2 \tag{B.10}$$

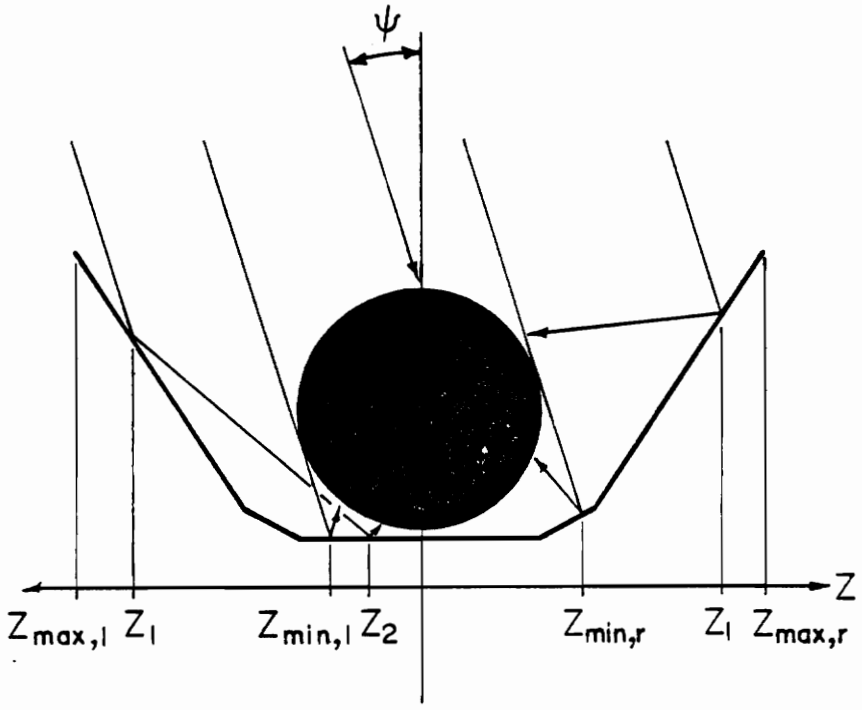

Figure B.2. Ray-Trace Diagram for the Geometry of ISC B

For $Z_{min,1}$: $B = 1/\tan \psi$ B.11

$A = b_c + R_t (1 - 1/\sin \psi)$ B.12

For $Z_{max,1}$: $B = 1/\tan \psi$ B.13

$A = C (W_a/2) - B W_a/2$ B.14

For a ray which strikes the reflector at a point Z, C(Z) the x-axis intercept of the reflected ray is

$$\xi(Z) = \frac{\left[1 - \left(\frac{dC}{dZ}\right)^2\right] (Z - X\tan \psi) + 2 \left(\frac{dC}{dZ}\right) (X + Z\tan \psi)}{Z \left(\frac{dC}{dZ}\right) - \left[1 - \left(\frac{dC}{dZ}\right)^2\right] \tan \psi} \qquad \text{B.15}$$

Multiple reflections occur if $\xi < 0$, and the ray "hits" the tank if it passes within a distance less than R_t from the center. If the ray neither intersects the tank nor reflects again it becomes diffuse. For multiple reflections, the equation of the once-reflected ray is

$$X(Z) = \left[C(Z_1) - \xi_1\right] Z/Z_1 + \xi_1 \qquad \text{B.16}$$

and a second reflection occurs at Z_2, where Z_2 is the root of

$$C(Z_2) = \left[C(Z_1) - \xi_1\right] \frac{Z_2}{Z_1} + \xi_1 \qquad \text{B.17}$$

This procedure is repeated to find if more reflections occur. If ξ is still less than zero after 11 reflections the radiation associated with the ray is taken to be diffuse and is added to the diffuse component. For less than 11 reflections the increment of beam radiation reaching the absorber, for an increment ΔZ of the reflector, is

$$\gamma_i = \hat{\tau}_{bc} \hat{\rho}_{br}^{\,j} \Delta Z \, G_b^{\,T}/\pi R_t \qquad \text{B.18}$$

where j is the number of reflections. The total flux reaching the tank by reflection is then

$$S_r = \sum_{i=1}^{n} \gamma_i \qquad \text{B.19}$$

where $n = (Z_{max} - Z_{min})/\Delta Z$

The right side of the collector is evaluated using a positive ψ and the left side using a negative ψ. The process is repeated for ΔZ of decreasing size and tested to see if γ changes by more than five percent. If so, ΔZ is divided by 10 repeatedly until the change is less than five percent.

The direct (non-reflected) radiation on the tank is determined simply by calculating the portion of the tank which is not shaded by the reflector side walls, if any, and dividing by the total projected area of the tank to get the fraction of direct radiation incident on the tank.

Finally, the average beam flux on the tank is

$$S_{bm} = \frac{1}{2}\left(S_{r,R} + S_{r,L}\right) + S_{b,D} \qquad \text{B.20}$$

where $S_{r,R}$, $S_{r,L}$, and $S_{b,D}$ are the right- and left-side reflected and direct components, respectively.

APPENDIX C

Optical Properties of a 3-Cover System

Since ISC systems are non-tracking, they receive solar radiation over a wide range of incidence angles during the course of a day. In order to accurately model this type of collector the determination of the optical properties of the covers must be established at any given incidence angle.

The reflection of unpolarized radiation passing from medium 1 with a refractive index, n_1, to medium 2 with a refractive index, n_2, can be found from Fresnel's expressions.

$$r_m = \frac{\sin^2 (\theta_2 - \theta_1)}{\sin^2 (\theta_2 + \theta_1)} \qquad C.1$$

$$r_n = \frac{\tan^2 (\theta_2 - \theta_1)}{\tan^2 (\theta_2 + \theta_1)} \qquad C.2$$

$$r = \frac{1}{2} (r_m + r_n) \qquad C.3$$

Subscripts m and n refer to the components of the incident radiation perpendicular and parallel to the plane of incidence, respectively. For unpolarized radiation the total reflection is taken to be the average of these two components. The angles θ_1 and θ_2 are the angles of incidence and refraction, respectively, and are related to the indices of refraction by Snell's law.

$$n_1 \sin \theta_1 = n_2 \sin \theta_2 \qquad C.4$$

For radiation where medium 1 is air ($n_1 \sim 1$) this reduces to

$$\sin \theta_2 = \sin \theta_1 / n_2 \qquad \text{C.5}$$

In the case of a solar collector cover there are two interfaces which contribute to the reflection losses. Therefore the reflection at each interface is combined to give an expression for the reflective losses in a single cover.

$$\rho = r \left[1 + \frac{(1 - r)^2 \tau_a^2}{1 - r^2 \tau_a^2}\right] \qquad \text{C.6}$$

This equation includes the effect of radiation absorbed in the cover through the term τ_a. This absorption of radiation in a partially transparent medium is described by Bouger's law.

$$\tau_a = \exp \left[\frac{-\kappa L}{\cos \theta_2}\right] \qquad \text{C.7}$$

The extinction coefficient, K, is assumed constant in the solar spectrum and the cover thickness, L, divided by the cosine of the refracted angle gives the actual path length for the radiation inside the cover. Now the transmittance of the cover, including absorption and reflection losses, can be calculated.

$$\tau = \frac{(1 - r)^2 \tau_a}{1 - r^2 \tau_a^2} \qquad \text{C.8}$$

The reflectance and transmittance calculated from equations C.6 and C.8 apply in general for any single cover of a multiple cover system. For the purposes of this investigation it is desired,

however, to determine an effective transmittance for the whole cover system and the fraction of the radiation incident upon the top cover which is absorbed in each cover. Ramsey, et al. have derived expressions for the absorptance, transmittance, and reflectance of multiple cover systems (25). The pertinent results are summarized below for a 3-cover system. The following nomenclature is used.

ρ_n = reflectance of a single cover with the properties of cover n (n_n, r_n, K_n, L_n).

τ_n = transmittance of a single cover with the properties of cover n.

$\rho^{(m)}$ = effective reflectance of an m cover system.

$\tau^{(m)}$ = effective transmittance of an m cover system.

$\alpha_n^{(m)}$ = absorption of cover n in an m cover system (referenced to the radiation incident on the top cover - cover m).

$$\rho_1^{(1)} = \rho_1$$

$$\rho^{(2)} = \rho_2 + \frac{\rho_1 \tau_2^2}{1 - \rho_1 \rho_2}$$

$$\rho^{(3)} = \rho_3 + \frac{(\tau_3)^2 \rho^{(2)}}{1-\rho^{(2)}\rho_3}$$

$$\alpha_1^{(3)} = (1 - \rho_1 - \tau_1) \left(\frac{\tau_2}{1-\rho^{(1)}\rho_2}\right) \left(\frac{\tau_3}{1-\rho^{(2)}\rho_3}\right) = \hat{\alpha}_{bc1}$$

$$\alpha_2^{(3)} = \left[1 - \rho_2 - \left(\frac{\tau_2}{1-\rho_1^{(1)}\rho_2}\right)\left(\rho^1\tau_2 - \rho^1 + 1\right)\right]\left(\frac{\tau_3}{1-\rho^{(2)}\rho_3}\right) = \hat{\alpha}_{bc2}$$

$$\alpha_3^{(3)} = 1 - \rho_3 - \frac{\tau_3}{1-\rho^{(2)}\rho_3}\left(\rho^2\tau_3 - \rho^2 + 1\right) = \hat{\alpha}_{bc3}$$

$$\tau^{(3)} = \frac{\tau_1\tau_2\tau_3}{(1-\rho^{(1)}\rho_2)(1-\rho^{(2)}\rho_3)} = \hat{\tau}_{bc}$$

The short wave diffuse cover properties, $\hat{\tau}_c$, $\hat{\rho}_c$, and $\hat{\alpha}_c$ are obtained for each cover individually by evaluating the expressions for the single-cover properties ρ and τ above at an effective incidence angle of 60 degrees as suggested in reference 22 (p. 182). Then, $\hat{\alpha}_c$ can be evaluated for each cover from the identity $\alpha = 1 - \tau - \rho$.

COLLECTOR B, 4/16/83, NO MIXING, NO DRAW

TEST STARTING AT 7:00
TEST DURATION = 10 HOURS
INITIAL TEMP = 21.3 C
FINAL TEMP = 49.7 C

HOUR ENDING	MEASURED TANK TEMPERATURES T5 (C)	T4 (C)	T3 (C)	T2 (C)	T1 (C)	WIND VEL (M/S)	SKY TEMP (C)	AMB TEMP (C)	IRRAD BEAM (W/SQ M)	IRRAD TOTL (W/SQ M)
800	20.18	20.74	20.71	21.04	21.25	4.41	-9.41	1.29	546	333
900	20.31	21.15	21.46	22.38	24.30	5.20	-6.71	2.60	690	583
1000	21.73	22.62	23.42	25.31	29.99	5.49	-4.10	4.05	761	800
1100	24.44	25.46	26.75	29.78	37.22	4.57	1.14	5.52	790	951
1200	28.23	29.35	31.08	35.13	44.44	4.21	3.32	7.01	798	1026
1300	32.43	33.67	35.77	40.66	50.94	4.41	4.40	8.70	793	1023
1400	36.46	37.86	40.32	45.84	56.32	4.26	3.76	10.07	775	938
1500	39.67	41.30	44.16	50.06	60.03	5.08	2.67	10.11	734	781
1600	41.69	43.67	46.76	52.63	61.10	4.46	1.14	10.34	662	566
1700	42.65	44.99	48.15	53.50	59.60	3.58	0.03	10.25	535	319

INCIDENT ENERGY = 0.34711E+08 JOULES
STORED ENERGY = 0.12611E+08 JOULES
WITHDRAWN ENERGY = 0.0 JOULES
COLLECTION EFF. = 0.363
AVG FLOWRATE = 0.0 CU M/SEC

COLLECTOR B, 4/21/83, NO MIXING, NO DRAW

TEST STARTING AT 8:00
TEST DURATION = 8 HOURS
INITIAL TEMP = 10.8 C
FINAL TEMP = 35.1 C

HOUR ENDING	MEASURED TANK TEMPERATURES T5 (C)	T4 (C)	T3 (C)	T2 (C)	T1 (C)	WIND VEL (M/S)	SKY TEMP (C)	AMB TEMP (C)	IRRAD BEAM (W/SQ M)	IRRAD TOTL (W/SQ M)
900	10.79	11.13	11.19	11.65	13.35	4.97	-5.28	5.22	693	561
1000	12.25	12.78	13.31	14.98	20.23	4.68	-0.65	7.13	746	770
1100	14.90	15.52	16.66	19.64	27.91	4.47	3.32	8.63	759	919
1200	18.80	19.64	21.29	25.54	35.95	4.90	6.51	10.30	560	860
1300	21.07	21.83	24.06	29.06	37.55	4.42	7.55	9.70	5	318
1400	22.73	23.66	26.20	30.94	37.90	4.15	6.51	11.10	383	684
1500	25.73	26.86	29.50	34.31	43.01	4.63	4.40	12.65	694	766
1600	28.00	29.39	32.09	37.22	45.53	4.09	2.89	13.04	648	557

INCIDENT ENERGY = 0.25772E+08 JOULES
STORED ENERGY = 0.10845E+08 JOULES
WITHDRAWN ENERGY = 0.0 JOULES
COLLECTION EFF. = 0.421
AVG FLOWRATE = 0.0 CU M/SEC

COLLECTOR B, 4/22/83, NO MIXING, NO DRAW

TEST STARTING AT 8:00
TEST DURATION = 8 HOURS
INITIAL TEMP = 11.2 C
FINAL TEMP = 38.8 C

HOUR ENDING	MEASURED TANK TEMPERATURES T5 (C)	T4 (C)	T3 (C)	T2 (C)	T1 (C)	WIND VEL (M/S)	SKY TEMP (C)	AMB TEMP (C)	IRRAD BEAM (W/SQ M)	IRRAD TOTL (W/SQ M)
900	11.25	11.74	11.68	12.33	14.05	1.12	3.76	7.45	450	525
1000	12.69	13.17	13.51	15.18	19.45	1.37	10.59	11.70	185	609
1100	15.43	16.00	16.84	19.59	26.92	1.81	12.57	12.78	550	915
1200	19.28	19.97	21.32	25.26	35.27	1.95	11.78	14.73	734	977
1300	23.63	24.07	26.25	31.15	42.57	1.77	14.51	15.76	736	1008
1400	27.85	28.85	31.13	36.87	48.91	2.24	16.03	16.90	688	968
1500	30.84	32.09	34.85	41.19	51.98	2.40	14.12	15.49	182	430
1600	32.10	33.85	36.72	42.39	49.55	2.09	15.84	15.99	28	294

INCIDENT ENERGY = 0.27152E+08 JOULES
STORED ENERGY = 0.12307E+08 JOULES
WITHDRAWN ENERGY = 0.0 JOULES
COLLECTION EFF. = 0.453
AVG FLOWRATE = 0.0 CU M/SEC

COLLECTOR B, 4/25/83, NO MIXING, NO DRAW

TEST STARTING AT 11:00
TEST DURATION = 5 HOURS
INITIAL TEMP = 26.8 C
FINAL TEMP = 45.8 C

HOUR ENDING	MEASURED TANK TEMPERATURES T5 (C)	T4 (C)	T3 (C)	T2 (C)	T1 (C)	WIND VEL (M/S)	SKY TEMP (C)	AMB TEMP (C)	IRRAD BEAM (W/SQ M)	IRRAD TOTL (W/SQ M)
1200	27.36	27.80	28.39	29.74	33.06	6.37	1.14	7.06	785	1006
1300	30.69	31.35	32.14	35.38	43.00	5.97	2.89	9.28	784	1005
1400	34.13	35.03	36.78	40.94	50.21	5.67	3.76	11.33	758	922
1500	36.89	38.26	40.34	45.48	54.92	5.62	3.32	12.51	698	769
1600	38.66	40.26	42.94	48.31	56.43	6.52	2.24	12.83	632	565

INCIDENT ENERGY = 0.20234E+08 JOULES
STORED ENERGY = 0.84344E+07 JOULES
WITHDRAWN ENERGY = 0.0 JOULES
COLLECTION EFF. = 0.417
AVG FLOWRATE = 0.0 CU M/SEC

COLLECTOR B, 4/26/83, NO MIXING, NOON DRAW

TEST STARTING AT 7:00
TEST DURATION = 10 HOURS
INITIAL TEMP = 19.6 C
FINAL TEMP = 36.6 C

DRAW STARTING AT 1200 AND LASTING 2. MINUTES
DRAW MASS = 45.2 KG
DRAW TEMP = 36.5 C
MAIN TEMP = 11.8 C

HOUR ENDING	MEASURED TANK TEMPERATURES T5 (C)	T4 (C)	T3 (C)	T2 (C)	T1 (C)	WIND VEL (M/S)	SKY TEMP (C)	AMB TEMP (C)	IRRAD BEAM (W/SQ M)	IRRAD TOTL (W/SQ M)
800	19.30	19.66	19.60	20.09	20.57	3.21	1.14	12.30	558	313
900	19.99	20.42	20.60	21.70	23.95	3.36	5.04	13.86	656	541
1000	21.60	22.12	22.74	24.82	29.88	3.61	8.57	15.92	719	746
1100	24.35	24.87	26.19	29.46	37.41	4.33	11.98	17.97	753	895
1200	28.13	28.86	30.63	35.01	44.95	4.53	14.70	19.76	778	981
1300	25.28	26.05	27.17	29.01	32.86	4.55	15.46	20.72	725	949
1400	28.37	29.09	30.39	33.22	40.88	4.46	15.46	21.87	758	904
1500	30.64	31.69	33.32	37.11	46.06	3.77	14.70	22.59	743	757
1600	31.45	32.37	35.16	39.37	47.55	4.55	13.16	22.16	686	553
1700	30.96	32.52	35.79	39.81	45.92	4.37	11.98	21.91	598	324

INCIDENT ENERGY = 0.33018E+08 JOULES
STORED ENERGY = 0.75713E+07 JOULES
WITHDRAWN ENERGY = 0.46745E+07 JOULES
COLLECTION EFF. = 0.371
AVG FLOWRATE = 0.0 CU M/SEC

COLLECTOR B, 4/27/83, NO MIXING, NO DRAW

TEST STARTING AT 9:00
TEST DURATION = 6 HOURS
INITIAL TEMP = 17.6 C
FINAL TEMP = 43.9 C

HOUR ENDING	MEASURED TANK TEMPERATURES T5 (C)	T4 (C)	T3 (C)	T2 (C)	T1 (C)	WIND VEL (M/S)	SKY TEMP (C)	AMB TEMP (C)	IRRAD BEAM (W/SQ M)	IRRAD TOTL (W/SQ M)
1000	17.85	18.31	18.45	19.48	22.26	2.02	14.51	19.97	710	726
1100	20.39	21.00	21.78	24.33	31.32	2.25	17.90	22.59	728	873
1200	24.03	24.81	26.19	30.02	39.56	2.38	20.10	23.87	762	953
1300	28.30	28.89	31.02	35.86	46.76	2.62	21.00	25.29	770	959
1400	32.38	33.29	35.70	41.30	52.65	2.47	21.53	26.37	753	880
1500	35.75	36.44	39.69	45.68	56.68	3.13	20.10	26.43	735	742

INCIDENT ENERGY = 0.24340E+08 JOULES
STORED ENERGY = 0.11701E+08 JOULES
WITHDRAWN ENERGY = 0.0 JOULES
COLLECTION EFF. = 0.481
AVG FLOWRATE = 0.0 CU M/SEC

COLLECTOR B, 4/28/83, NO MIXING NOON DRAW

TEST STARTING AT 7:00
TEST DURATION = 7 HOURS
INITIAL TEMP = 14.1 C
FINAL TEMP = 33.0 C

DRAW STARTING AT 1200 AND LASTING 2. MINUTES
DRAW MASS = 45.7 KG
DRAW TEMP = 32.9 C
MAIN TEMP = 13.0 C

HOUR ENDING	MEASURED TANK TEMPERATURES T5 (C)	T4 (C)	T3 (C)	T2 (C)	T1 (C)	WIND VEL (M/S)	SKY TEMP (C)	AMB TEMP (C)	IRRAD BEAM (W/SQ M)	TOTL
800	13.88	14.23	14.19	14.72	15.22	0.63	6.51	14.82	565	304
900	14.60	15.00	15.28	16.47	18.96	1.21	11.59	18.02	663	527
1000	16.38	16.82	17.59	19.79	25.06	1.65	16.41	21.37	719	728
1100	19.31	19.91	21.20	24.61	32.83	1.62	19.19	23.69	756	878
1200	23.19	24.14	25.80	30.30	40.60	2.21	21.53	25.49	767	957
1300	23.34	24.08	24.91	26.48	30.56	2.56	22.77	26.90	729	943
1400	26.88	27.34	28.75	31.59	39.92	2.47	22.77	28.22	709	878

INCIDENT ENERGY = 0.24729E+08 JOULES
STORED ENERGY = 0.84327E+07 JOULES
WITHDRAWN ENERGY = 0.38076E+07 JOULES
COLLECTION EFF. = 0.495
AVG FLOWRATE = 0.0 CU M/SEC

COLLECTOR B, 5/5/83, MIXING, NO DRAW

TEST STARTING AT 7:00
TEST DURATION = 10 HOURS
INITIAL TEMP = 19.2 C
FINAL TEMP = 47.4 C

HOUR ENDING	MEASURED TANK TEMPERATURES T5 (C)	T4 (C)	T3 (C)	T2 (C)	T1 (C)	WIND VEL (M/S)	SKY TEMP (C)	AMB TEMP (C)	IRRAD BEAM (W/SQ M)	IRRAD TOTL (W/SQ M)
800	18.92	19.27	19.35	19.87	20.61	2.66	-1.10	11.26	395	278
900	19.92	20.37	20.77	21.59	22.82	4.39	-1.10	12.35	474	489
1000	21.94	22.63	23.32	24.63	26.48	4.87	1.14	13.68	593	705
1100	25.27	26.15	27.20	28.75	31.30	5.33	9.99	14.39	706	887
1200	29.70	30.66	31.85	33.59	36.39	4.49	12.37	15.55	714	958
1300	34.47	35.43	36.63	38.24	41.08	4.45	13.16	16.99	731	961
1400	39.00	39.91	40.97	42.46	45.16	4.86	13.16	17.83	717	888
1500	42.61	43.50	44.42	45.65	47.89	5.17	12.57	17.97	694	745
1600	45.25	45.95	46.58	47.42	48.74	4.64	10.79	17.88	653	549
1700	46.71	47.10	47.32	47.62	48.21	4.33	9.18	17.24	555	321

INCIDENT ENERGY = 0.32155E+08 JOULES
STORED ENERGY = 0.12533E+08 JOULES
WITHDRAWN ENERGY = 0.0 JOULES
COLLECTION EFF. = 0.390
AVG FLOWRATE = 0.90584E-05 CU M/SEC

COLLECTOR B, 5/6/83, MIXING, NO DRAW

TEST STARTING AT 7:00
TEST DURATION = 10 HOURS
INITIAL TEMP = 21.4 C
FINAL TEMP = 52.3 C

HOUR ENDING	MEASURED TANK TEMPERATURES T5 (C)	T4 (C)	T3 (C)	T2 (C)	T1 (C)	WIND VEL (M/S)	SKY TEMP (C)	AMB TEMP (C)	IRRAD BEAM (W/SQ M)	IRRAD TOTL (W/SQ M)
800	21.15	21.60	21.76	22.35	22.32	0.54	-1.56	8.72	609	311
900	22.31	22.93	23.40	24.18	24.60	0.65	3.32	12.12	712	536
1000	24.86	25.68	26.40	27.46	28.42	0.65	8.57	15.33	757	729
1100	28.83	29.85	30.70	31.84	33.14	0.67	12.57	17.33	786	878
1200	33.78	34.76	35.64	36.75	38.20	0.72	13.93	19.56	786	951
1300	38.99	39.83	40.71	41.75	43.11	1.16	17.71	21.17	785	956
1400	43.82	44.52	45.35	46.23	47.49	0.97	17.71	22.88	772	881
1500	47.70	48.34	49.01	49.77	50.65	0.94	18.27	23.96	743	736
1600	50.39	50.82	51.27	51.77	52.27	0.82	17.71	24.30	688	539
1700	51.82	51.95	52.14	52.44	52.62	1.06	16.41	23.78	585	312

INCIDENT ENERGY = 0.32383E+08 JOULES
STORED ENERGY = 0.13714E+08 JOULES
WITHDRAWN ENERGY = 0.0 JOULES
COLLECTION EFF. = 0.424
AVG FLOWRATE = 0.16314E-04 CU M/SEC

COLLECTOR B, 5/7/83, NO MIXING, NOON DRAW

TEST STARTING AT 7:00
TEST DURATION = 10 HOURS
INITIAL TEMP = 20.8 C
FINAL TEMP = 43.2 C

DRAW STARTING AT 1200 AND LASTING 2. MINUTES
DRAW MASS = 45.9 KG
DRAW TEMP = 37.1 C
MAIN TEMP = 17.5 C

HOUR ENDING	MEASURED TANK TEMPERATURES T5 (C)	T4 (C)	T3 (C)	T2 (C)	T1 (C)	WIND VEL (M/S)	SKY TEMP (C)	AMB TEMP (C)	IRRAD BEAM (W/SQ M)	IRRAD TOTL (W/SQ M)
800	20.70	21.06	20.97	21.38	21.82	0.90	8.57	15.94	445	283
900	21.20	21.70	21.87	22.84	25.08	1.67	11.59	17.92	599	517
1000	22.64	23.29	23.89	25.81	30.81	2.14	14.51	19.72	654	700
1100	25.11	25.93	27.11	30.22	37.97	2.25	17.71	20.99	715	858
1200	28.67	29.61	31.30	35.54	45.45	2.66	19.55	22.32	750	942
1300	28.38	29.01	29.79	31.35	35.39	2.57	20.64	23.42	764	941
1400	31.78	32.37	33.54	36.46	44.40	2.43	21.00	24.57	755	865
1500	34.57	35.43	36.96	41.16	50.18	2.45	20.10	24.91	723	722
1600	36.55	37.62	39.54	44.32	52.38	2.21	19.55	25.11	665	527
1700	37.78	38.93	41.21	45.75	51.77	2.44	18.27	24.50	565	307

INCIDENT ENERGY = 0.31591E+08 JOULES
STORED ENERGY = 0.99608E+07 JOULES
WITHDRAWN ENERGY = 0.37668E+07 JOULES
COLLECTION EFF. = 0.435
AVG FLOWRATE = 0.57283E-09 CU M/SEC

COLLECTOR A, 5/10/83, NO MIXING, NO DRAW

TEST STARTING AT 7:00
TEST DURATION = 10 HOURS
INITIAL TEMP = 19.9 C
FINAL TEMP = 41.3 C

HOUR ENDING	MEASURED TANK TEMPERATURES T5 (C)	T4 (C)	T3 (C)	T2 (C)	T1 (C)	WIND VEL (M/S)	SKY TEMP (C)	AMB TEMP (C)	IRRAD BEAM (W/SQ M)	TOTL
800	19.60	19.86	20.06	20.79	21.25	0.63	-4.80	6.99	658	326
900	20.18	20.64	21.50	22.82	24.00	0.94	0.03	9.67	752	561
1000	21.62	22.27	23.67	25.42	27.09	0.85	4.82	13.10	797	761
1100	23.96	24.67	26.50	28.35	30.42	0.95	9.59	15.76	814	904
1200	26.75	27.56	29.65	31.71	33.85	1.12	13.74	18.29	813	975
1300	29.70	30.58	32.79	35.03	37.15	1.09	15.65	21.55	814	977
1400	32.34	33.72	35.87	38.05	40.39	2.36	14.51	23.90	814	920
1500	34.29	35.93	38.40	40.63	43.08	3.41	13.35	23.69	767	775
1600	35.45	37.71	40.09	42.33	45.01	2.99	13.16	23.87	725	572
1700	36.10	38.79	41.11	43.38	46.16	3.25	11.59	23.92	630	340

INCIDENT ENERGY = 0.21669E+08 JOULES
STORED ENERGY = 0.97795E+07 JOULES
WITHDRAWN ENERGY = 0.0 JOULES
COLLECTION EFF. = 0.451
AVG FLOWRATE = 0.0 CU M/SEC

COLLECTOR A, 5/11/83, MIXING, NO DRAW

TEST STARTING AT 7:00
TEST DURATION = 10 HOURS
INITIAL TEMP = 16.0 C
FINAL TEMP = 43.4 C

HOUR ENDING	MEASURED TANK TEMPERATURES T5 (C)	T4 (C)	T3 (C)	T2 (C)	T1 (C)	WIND VEL (M/S)	SKY TEMP (C)	AMB TEMP (C)	IRRAD BEAM (W/SQ M)	IRRAD TOTL (W/SQ M)
800	16.14	16.56	16.71	17.40	17.16	0.39	-1.10	9.30	672	317
900	18.44	18.94	19.11	19.80	19.69	0.33	5.46	13.88	767	548
1000	21.45	22.10	22.24	22.90	22.82	0.60	11.59	18.17	800	739
1100	24.97	25.60	25.78	26.30	26.37	0.72	15.08	20.56	818	887
1200	28.78	29.44	29.56	30.06	30.13	0.74	18.82	23.13	830	960
1300	32.60	33.16	33.27	33.84	33.82	1.13	20.10	25.85	814	962
1400	35.99	36.62	36.73	37.18	37.19	2.55	20.10	27.48	810	915
1500	38.78	39.31	39.41	39.82	39.91	3.10	19.55	28.02	734	753
1600	40.88	41.27	41.43	41.82	41.90	1.65	19.19	27.95	721	552
1700	42.44	42.89	42.54	43.26	43.29	1.40	18.27	28.31	660	328

INCIDENT ENERGY = 0.21212E+08 JOULES
STORED ENERGY = 0.12526E+08 JOULES
WITHDRAWN ENERGY = 0.0 JOULES
COLLECTION EFF. = 0.591
AVG FLOWRATE = 0.0 CU M/SEC

COLLECTOR A, 5/12/83, NO MIXING, NOON DRAW

TEST STARTING AT 7:00
TEST DURATION = 10 HOURS
INITIAL TEMP = 19.1 C
FINAL TEMP = 36.6 C

DRAW STARTING AT 1200 AND LASTING 2. MINUTES
DRAW MASS = 46.4 KG
DRAW TEMP = 35.6 C
MAIN TEMP = 17.0 C

HOUR ENDING	MEASURED TANK TEMPERATURES T5 (C)	T4 (C)	T3 (C)	T2 (C)	T1 (C)	WIND VEL (M/S)	SKY TEMP (C)	AMB TEMP (C)	IRRAD BEAM (W/SQ M)	IRRAD TOTL (W/SQ M)
800	19.05	19.31	19.36	20.24	20.62	0.39	5.88	13.22	641	312
900	19.97	20.51	21.19	22.59	23.67	0.68	10.59	17.38	720	531
1000	21.97	22.61	23.77	25.52	27.11	0.52	15.46	21.03	776	729
1100	24.59	25.51	26.95	28.80	30.78	0.76	19.19	22.52	781	864
1200	27.71	28.68	30.34	32.34	34.39	0.88	22.42	24.57	734	915
1300	23.00	24.24	25.63	27.97	31.97	0.89	23.65	26.72	597	854
1400	25.55	27.42	29.03	31.49	34.89	1.31	24.52	29.02	633	821
1500	28.26	30.55	32.34	34.74	38.00	2.90	24.52	30.03	619	727
1600	30.36	33.00	34.87	37.23	40.57	1.71	23.65	30.05	481	513
1700	31.62	34.39	36.22	38.50	41.84	1.78	22.77	26.19	180	241

INCIDENT ENERGY = 0.19828E+08 JOULES
STORED ENERGY = 0.80060E+07 JOULES
WITHDRAWN ENERGY = 0.36102E+07 JOULES
COLLECTION EFF. = 0.586
AVG FLOWRATE = 0.0 CU M/SEC

COLLECTOR A, 5/13/83, NO MIXING, NO DRAW

TEST STARTING AT 7:00
TEST DURATION = 10 HOURS
INITIAL TEMP = 21.6 C
FINAL TEMP = 32.5 C

HOUR ENDING	MEASURED TANK TEMPERATURES T5 (C)	T4 (C)	T3 (C)	T2 (C)	T1 (C)	WIND VEL (M/S)	SKY TEMP (C)	AMB TEMP (C)	IRRAD BEAM (W/SQ M)	IRRAD TOTL (W/SQ M)
800	21.41	21.77	21.73	22.15	22.17	0.51	11.98	14.00	44	226
900	21.88	22.38	22.67	23.54	24.12	0.67	15.46	16.56	221	450
1000	23.25	23.92	24.63	25.92	26.98	0.59	19.19	19.15	369	638
1100	25.34	26.13	27.24	28.73	30.28	0.71	23.13	21.60	203	650
1200	27.64	28.49	29.82	31.49	33.24	0.93	26.24	23.69	249	786
1300	29.94	30.98	32.46	34.24	36.14	0.79	27.08	25.18	192	591
1400	31.08	32.04	33.69	35.39	37.39	1.04	27.59	24.82	2	194
1500	30.95	31.72	33.50	35.17	37.12	1.16	26.24	22.50	0	61
1600	30.49	31.44	33.19	34.80	36.57	2.29	25.38	21.85	2	142
1700	29.93	31.12	32.77	34.30	35.83	1.77	24.52	20.42	0	53

INCIDENT ENERGY = 0.11552E+08 JOULES
STORED ENERGY = 0.49882E+07 JOULES
WITHDRAWN ENERGY = 0.0 JOULES
COLLECTION EFF. = 0.432
AVG FLOWRATE = 0.0 CU M/SEC

COLLECTOR A, 5/17/83, NO MIXING, NOON DRAW

TEST STARTING AT 7:00
TEST DURATION = 10 HOURS
INITIAL TEMP = 13.8 C
FINAL   TEMP = 32.0 C

DRAW STARTING AT 1200 AND LASTING 2. MINUTES
DRAW MASS = 46.4 KG
DRAW TEMP = 29.7 C
MAIN TEMP = 17.5 C

HOUR ENDING	MEASURED TANK TEMPERATURES T5 (C)	T4 (C)	T3 (C)	T2 (C)	T1 (C)	WIND VEL (M/S)	SKY TEMP (C)	AMB TEMP (C)	IRRAD BEAM (W/SQ M)	IRRAD TOTL (W/SQ M)
800	13.52	13.84	14.21	14.81	15.31	0.73	-0.42	7.43	620	290
900	14.49	14.99	15.86	17.08	18.30	0.64	3.54	10.48	711	508
1000	16.29	17.05	18.34	19.81	21.58	0.99	7.34	12.41	762	705
1100	18.95	19.84	21.28	23.02	25.14	0.96	10.39	14.23	784	847
1200	21.94	22.83	24.49	26.40	28.60	0.78	12.96	15.67	766	906
1300	20.96	21.53	22.24	23.86	26.28	0.85	13.54	16.99	405	651
1400	22.75	23.73	24.89	26.50	28.95	1.09	16.59	18.77	607	849
1500	25.10	26.46	27.96	29.73	32.32	1.00	16.59	19.63	665	761
1600	26.91	28.60	30.34	32.22	35.04	1.10	12.77	19.61	559	495
1700	27.67	29.69	31.40	33.32	36.18	1.13	10.99	18.95	443	267

INCIDENT ENERGY = 0.19133E+08 JOULES
STORED ENERGY   = 0.83426E+07 JOULES
WITHDRAWN ENERGY = 0.23684E+07 JOULES
COLLECTION EFF. = 0.560
AVG FLOWRATE   = 0.0 CU M/SEC

COLLECTOR A, 5/18/83, NO MIXING, NO DRAW

TEST STARTING AT 7:00
TEST DURATION = 10 HOURS
INITIAL TEMP = 20.4 C
FINAL TEMP = 38.4 C

HOUR ENDING	MEASURED TANK TEMPERATURES T5 (C)	T4 (C)	T3 (C)	T2 (C)	T1 (C)	WIND VEL (M/S)	SKY TEMP (C)	AMB TEMP (C)	IRRAD BEAM (W/SQ M)	IRRAD TOTL (W/SQ M)
800	20.21	20.61	20.69	21.22	21.81	0.71	4.61	12.53	587	283
900	20.91	21.53	22.19	23.23	24.48	0.81	8.16	14.64	672	501
1000	22.46	23.30	24.42	25.73	27.45	1.17	11.78	16.35	681	685
1100	24.68	25.64	27.08	28.60	30.57	1.81	14.51	17.70	636	828
1200	27.00	27.95	29.70	31.38	33.45	1.72	16.59	18.52	301	704
1300	29.08	30.24	32.07	33.81	35.90	1.61	16.97	19.61	596	872
1400	31.24	32.60	34.53	36.27	38.49	1.85	17.16	20.26	502	768
1500	32.91	34.57	36.63	38.37	40.77	1.89	15.84	20.78	526	668
1600	33.84	35.91	38.02	39.78	42.35	1.84	16.41	20.74	359	473
1700	34.10	36.55	38.59	40.36	42.93	1.69	13.54	19.58	182	240

INCIDENT ENERGY = 0.18350E+08 JOULES
STORED ENERGY = 0.82297E+07 JOULES
WITHDRAWN ENERGY = 0.0 JOULES
COLLECTION EFF. = 0.448
AVG FLOWRATE = 0.0 CU M/SEC

COLLECTOR A, 5/25/83, MIXING, NO DRAW

TEST STARTING AT 7:00
TEST DURATION = 10 HOURS
INITIAL TEMP = 20.8 C
FINAL TEMP = 38.0 C

HOUR ENDING	MEASURED TANK TEMPERATURES T5 (C)	T4 (C)	T3 (C)	T2 (C)	T1 (C)	WIND VEL (M/S)	SKY TEMP (C)	AMB TEMP (C)	IRRAD BEAM (W/SQ M)	IRRAD TOTL (W/SQ M)
800	20.53	21.13	21.39	21.97	22.01	0.63	5.67	11.70	563	273
900	22.25	22.99	23.37	24.04	24.10	0.86	10.79	15.21	588	476
1000	24.68	25.47	25.91	26.55	26.61	0.91	13.74	17.97	709	669
1100	27.64	28.43	28.90	29.48	29.55	1.35	17.34	19.70	738	827
1200	30.81	31.49	31.93	32.49	32.50	1.55	21.53	21.08	462	735
1300	33.02	33.57	33.90	34.38	34.40	1.63	22.07	21.96	253	550
1400	34.89	35.48	35.94	36.46	36.43	1.48	20.82	22.93	478	698
1500	36.75	37.31	37.66	38.08	38.00	1.42	22.77	23.18	195	443
1600	37.65	37.98	38.25	38.58	38.44	1.22	22.42	22.48	64	251
1700	37.69	38.01	38.25	38.54	38.37	1.51	18.27	21.55	56	194

INCIDENT ENERGY = 0.15590E+08 JOULES
STORED ENERGY = 0.78639E+07 JOULES
WITHDRAWN ENERGY = 0.0 JOULES
COLLECTION EFF. = 0.504
AVG FLOWRATE = 0.0 CU M/SEC

COLLECTOR A, 5/27/83, NO MIXING, NO DRAW

TEST STARTING AT 7:00
TEST DURATION = 10 HOURS
INITIAL TEMP = 21.5 C
FINAL TEMP = 40.6 C

HOUR ENDING	MEASURED TANK TEMPERATURES T5 (C)	T4 (C)	T3 (C)	T2 (C)	T1 (C)	WIND VEL (M/S)	SKY TEMP (C)	AMB TEMP (C)	IRRAD BEAM (W/SQ M)	IRRAD TOTL (W/SQ M)
800	21.13	21.51	21.68	22.38	22.82	1.34	0.01	10.27	633	282
900	21.49	22.22	22.98	24.20	25.27	1.57	0.01	12.28	720	505
1000	22.70	23.87	25.03	26.50	28.02	1.49	0.01	15.07	720	679
1100	24.65	26.02	27.46	29.03	30.81	1.00	0.01	16.70	593	781
1200	27.11	28.61	30.22	31.97	33.80	1.50	0.01	17.26	704	900
1300	29.74	31.36	33.08	34.91	36.74	1.15	0.01	18.83	795	924
1400	32.09	34.05	35.77	37.62	39.62	1.61	0.01	20.01	777	858
1500	33.81	36.12	38.02	39.84	42.06	1.76	0.01	21.08	761	732
1600	35.04	37.55	39.57	41.52	43.94	1.79	0.01	22.09	723	553
1700	35.69	38.55	40.51	42.47	45.01	2.55	0.01	21.87	617	337

INCIDENT ENERGY = 0.19962E+08 JOULES
STORED ENERGY = 0.87269E+07 JOULES
WITHDRAWN ENERGY = 0.0 JOULES
COLLECTION EFF. = 0.437
AVG FLOWRATE = 0.0 CU M/SEC

COLLECTOR A, 5/28/83, NO MIXING, NO DRAW

TEST STARTING AT 7:00
TEST DURATION = 10 HOURS
INITIAL TEMP = 22.0 C
FINAL TEMP = 31.2 C

HOUR ENDING	MEASURED TANK TEMPERATURES T5 (C)	T4 (C)	T3 (C)	T2 (C)	T1 (C)	WIND VEL (M/S)	SKY TEMP (C)	AMB TEMP (C)	IRRAD BEAM (W/SQ M)	IRRAD TOTL (W/SQ M)
800	21.65	21.63	22.09	22.53	22.63	0.61	10.59	13.29	136	211
900	21.96	22.08	23.09	24.03	24.77	0.67	13.35	16.44	387	455
1000	23.05	24.35	25.12	26.35	27.54	0.73	17.90	18.92	384	621
1100	25.06	26.73	27.81	29.24	30.80	0.76	20.82	21.10	394	745
1200	27.08	28.95	30.11	31.63	33.39	0.84	22.77	22.46	39	437
1300	27.98	29.89	31.05	32.58	34.40	0.81	23.13	21.98	1	231
1400	28.24	30.06	31.15	32.60	34.44	1.03	22.77	20.94	1	160
1500	28.38	30.23	31.35	32.69	34.43	1.33	22.95	20.90	3	226
1600	28.61	30.54	31.64	32.94	34.50	1.10	22.77	20.81	1	172
1700	28.44	30.40	31.50	32.71	34.13	0.83	22.60	20.38	1	73

INCIDENT ENERGY = 0.10150E+08 JOULES
STORED ENERGY = 0.42110E+07 JOULES
WITHDRAWN ENERGY = 0.0 JOULES
COLLECTION EFF. = 0.415
AVG FLOWRATE = 0.0 CU M/SEC

COLLECTOR A, 5/31/83, NO MIXING, NO DRAW

TEST STARTING AT 7:00
TEST DURATION = 10 HOURS
INITIAL TEMP = 22.5 C
FINAL TEMP = 32.0 C

HOUR ENDING	MEASURED TANK TEMPERATURES T5 (C)	T4 (C)	T3 (C)	T2 (C)	T1 (C)	WIND VEL (M/S)	SKY TEMP (C)	AMB TEMP (C)	IRRAD BEAM (W/SQ M)	IRRAD TOTL (W/SQ M)
800	22.34	22.86	22.88	23.63	23.87	0.95	11.19	15.19	471	282
900	23.09	23.87	24.29	25.38	26.14	0.68	15.84	17.38	281	427
1000	24.10	25.05	25.76	26.94	27.94	1.46	19.19	17.72	1	267
1100	24.57	25.57	26.32	27.50	28.53	1.41	19.73	17.81	1	292
1200	25.36	26.60	27.38	28.58	29.57	1.65	21.00	18.45	12	376
1300	26.06	27.28	28.14	29.32	30.35	2.49	20.46	17.86	2	300
1400	26.40	27.66	28.53	29.70	30.72	2.40	21.00	18.11	3	290
1500	26.98	28.45	29.39	30.55	31.52	2.87	20.28	18.81	92	403
1600	27.62	29.51	30.39	31.72	32.85	2.83	18.27	19.76	434	504
1700	28.48	30.75	31.71	33.12	34.52	3.37	14.51	19.70	512	325

INCIDENT ENERGY = 0.10562E+08 JOULES
STORED ENERGY = 0.43471E+07 JOULES
WITHDRAWN ENERGY = 0.0 JOULES
COLLECTION EFF. = 0.412
AVG FLOWRATE = 0.0 CU M/SEC

COLLECTOR B, 4/16/83, NO MIXING, NO DRAW

TEST STARTING AT 7:00
TEST DURATION = 10 HOURS
INITIAL TEMP = 21.3 C
FINAL TEMP = 49.7 C

HOUR ENDING	TANK TEMP. (C) CALCULATED ENDING	CALCULATED AVG	MEAS AVG	IRRADIANCE TOTAL (W/SQ M)	IRRADIANCE BEAM (W/SQ M)	AMB TEMP (C)	SKY TEMP (C)	WIND VEL (M/S)
800	22.16	21.73	20.78	333.0	546.0	1.3	-9.4	4.4
900	24.42	23.31	21.92	583.0	690.0	2.6	-6.7	5.2
1000	28.02	26.20	24.61	800.0	761.0	4.1	-4.1	5.5
1100	32.53	30.27	28.73	951.0	790.0	5.5	1.1	4.6
1200	37.43	34.97	33.65	1026.0	798.0	7.0	3.3	4.2
1300	42.26	39.82	38.69	1023.0	793.0	8.7	4.4	4.4
1400	46.55	44.36	43.36	938.0	775.0	10.1	3.8	4.3
1500	49.82	48.68	47.04	781.0	734.0	10.1	2.7	5.1
1600	51.69	50.76	49.17	566.0	662.0	10.3	1.1	4.5
1700	52.10	51.90	49.78	319.0	535.0	10.3	0.0	3.6

INCIDENT ENERGY	=	0.34711E+08	JOULES
STORED ENERGY	=	0.12611E+08	JOULES
WITHDRAWN ENERGY	=	0.0	JOULES
COLLECTION EFF.	=	0.363	
AVG FLOWRATE	=	0.0	CU M/SEC
AVG ULC	=	-0.35671	W/(SQ M * C)
AVG (TCALC-TA)/I	=	0.04127	C/(W/SQ M)

COLLECTOR B, 4/21/83, NO MIXING, NO DRAW

TEST STARTING AT 8:00
TEST DURATION = 8 HOURS
INITIAL TEMP = 10.8 C
FINAL TEMP = 35.1 C

HOUR ENDING	TANK TEMP. (C) CALCULATED ENDING	TANK TEMP. (C) CALCULATED AVG	TANK TEMP. (C) MEAS AVG	IRRADIANCE TOTAL (W/SQ M)	IRRADIANCE BEAM (W/SQ M)	AMB TEMP (C)	SKY TEMP (C)	WIND VEL (M/S)
900	13.14	11.96	11.62	561.0	693.0	5.2	-5.3	5.0
1000	16.78	14.94	14.71	770.0	746.0	7.1	-0.6	4.7
1100	21.29	19.02	18.93	919.0	759.0	8.6	3.3	4.5
1200	25.42	23.35	24.24	860.0	560.0	10.3	6.5	4.9
1300	26.64	25.89	26.71	318.0	5.0	9.7	7.6	4.4
1400	29.72	28.18	28.29	684.0	383.0	11.1	6.5	4.1
1500	33.12	31.41	31.88	766.0	694.0	12.6	4.4	4.6
1600	35.21	34.12	34.45	557.0	648.0	13.0	2.9	4.1

INCIDENT ENERGY = 0.25772E+08 JOULES
STORED ENERGY = 0.10845E+08 JOULES
WITHDRAWN ENERGY = 0.0 JOULES
COLLECTION EFF. = 0.421
AVG FLOWRATE = 0.0 CU M/SEC
AVG ULC = -2.87248 W/(SQ M * C)
AVG (TCALC-TA)/I = 0.02044 C/(W/SQ M)

COLLECTOR B, 4/22/83, NO MIXING, NO DRAW

TEST STARTING AT 8:00
TEST DURATION = 8 HOURS
INITIAL TEMP = 11.2 C
FINAL TEMP = 38.8 C

HOUR ENDING	TANK TEMP. (C) CALCULATED ENDING	TANK TEMP. (C) CALCULATED AVG	TANK TEMP. (C) MEAS AVG	IRRADIANCE TOTAL (W/SQ M)	IRRADIANCE BEAM (W/SQ M)	AMB TEMP (C)	SKY TEMP (C)	WIND VEL (M/S)
900	13.47	12.32	12.21	525.0	450.0	7.4	3.8	1.1
1000	16.28	14.84	14.80	609.0	185.0	11.7	10.6	1.4
1100	20.75	18.47	18.96	915.0	550.0	12.8	12.6	1.8
1200	25.67	23.18	24.22	977.0	734.0	14.7	11.8	1.9
1300	30.68	28.15	29.53	1008.0	736.0	15.8	14.5	1.8
1400	35.30	32.98	34.72	968.0	688.0	16.9	16.0	2.2
1500	37.02	36.24	38.19	430.0	182.0	15.5	14.1	2.4
1600	38.06	37.54	38.92	294.0	28.0	16.0	15.8	2.1

INCIDENT ENERGY	=	0.27152E+08	JOULES
STORED ENERGY	=	0.12307E+08	JOULES
WITHDRAWN ENERGY	=	0.0	JOULES
COLLECTION EFF.	=	0.453	
AVG FLOWRATE	=	0.0	CU M/SEC
AVG ULC	=	-6.19403	W/(SQ M * C)
AVG (TCALC-TA)/I	=	0.01622	C/(W/SQ M)

COLLECTOR B, 4/25/83, NO MIXING, NO DRAW

TEST STARTING AT 11:00
TEST DURATION = 5 HOURS
INITIAL TEMP = 26.8 C
FINAL TEMP = 45.8 C

HOUR ENDING	TANK TEMP. (C) CALCULATED ENDING	CALCULATED AVG	MEAS AVG	IRRADIANCE TOTAL (W/SQ M)	IRRADIANCE BEAM (W/SQ M)	AMB TEMP (C)	SKY TEMP (C)	WIND VEL (M/S)
1200	31.55	29.17	29.27	1006.0	785.0	7.1	1.1	6.4
1300	36.26	33.90	34.51	1005.0	784.0	9.3	2.9	6.0
1400	40.45	38.36	39.42	922.0	758.0	11.3	3.8	5.7
1500	43.67	41.99	43.18	769.0	698.0	12.5	3.3	5.6
1600	45.60	44.64	45.32	565.0	632.0	12.8	2.2	6.5

INCIDENT ENERGY = 0.20234E+08 JOULES
STORED ENERGY = 0.84344E+07 JOULES
WITHDRAWN ENERGY = 0.0 JOULES
COLLECTION EFF. = 0.417
AVG FLOWRATE = 0.0 CU M/SEC
AVG ULC = -0.86830 W/(SQ M * C)
AVG (TCALC-TA)/I = 0.03165 C/(W/SQ M)

COLLECTOR B, 4/26/83, NO MIXING, NOON DRAW

TEST STARTING AT 7:00
TEST DURATION = 10 HOURS
INITIAL TEMP = 19.6 C
FINAL TEMP = 36.6 C

DRAW STARTING AT 1200 AND LASTING 2. MINUTES
DRAW MASS = 45.2 KG
DRAW TEMP = 36.5 C
MAIN TEMP = 11.8 C

HOUR ENDING	TANK TEMP. (C) CALCULATED ENDING	CALCULATED AVG	MEAS AVG	IRRADIANCE TOTAL (W/SQ M)	IRRADIANCE BEAM (W/SQ M)	AMB TEMP (C)	SKY TEMP (C)	WIND VEL (M/S)
800	20.43	20.01	19.84	313.0	558.0	12.3	1.1	3.2
900	22.62	21.51	21.33	541.0	656.0	13.9	5.0	3.4
1000	26.08	24.33	24.23	746.0	719.0	15.9	8.6	3.6
1100	30.39	28.21	28.46	895.0	753.0	18.0	12.0	4.3
1200	35.18	32.77	33.52	981.0	778.0	19.8	14.7	4.5
1300	31.73	29.49	28.07	949.0	725.0	20.7	15.5	4.6
1400	36.07	33.89	32.39	904.0	758.0	21.9	15.5	4.5
1500	39.46	37.76	35.76	757.0	743.0	22.6	14.7	3.8
1600	41.52	40.50	37.18	553.0	686.0	22.2	13.2	4.6
1700	42.18	41.85	37.00	324.0	598.0	21.9	12.0	4.4

AVG DRAW TEMP: CALC = 30.9 MEAS = 36.5

INCIDENT ENERGY = 0.33018E+08 JOULES
STORED ENERGY = 0.75713E+07 JOULES
WITHDRAWN ENERGY = 0.46745E+07 JOULES
COLLECTION EFF. = 0.371
AVG FLOWRATE = 0.0 CU M/SEC
AVG ULC = -3.10039 W/(SQ M * C)
AVG (TCALC-TA)/I = 0.01742 C/(W/SQ M)

COLLECTOR B, 4/27/83, NO MIXING, NO DRAW

TEST STARTING AT 9:00
TEST DURATION = 6 HOURS
INITIAL TEMP = 17.6 C
FINAL TEMP = 43.9 C

HOUR ENDING	TANK TEMP. (C) CALCULATED ENDING	TANK TEMP. (C) CALCULATED AVG	TANK TEMP. (C) MEAS AVG	IRRADIANCE TOTAL (W/SQ M)	IRRADIANCE BEAM (W/SQ M)	AMB TEMP (C)	SKY TEMP (C)	WIND VEL (M/S)
1000	20.91	19.50	19.27	726.0	710.0	20.0	14.5	2.0
1100	22.80	22.69	23.76	873.0	728.0	22.6	17.9	2.3
1200	27.74	24.94	28.92	953.0	762.0	23.9	20.1	2.4
1300	32.60	30.11	34.17	959.0	770.0	25.3	21.0	2.6
1400	36.92	34.74	39.06	880.0	753.0	26.4	21.5	2.5
1500	40.30	38.60	42.85	742.0	735.0	26.4	20.1	3.1

INCIDENT ENERGY = 0.24340E+08 JOULES
STORED ENERGY = 0.11701E+08 JOULES
WITHDRAWN ENERGY = 0.0 JOULES
COLLECTION EFF. = 0.481
AVG FLOWRATE = 0.0 CU M/SEC
AVG ULC = 275.34595 W/(SQ M * C)
AVG (TCALC-TA)/I = 0.00507 C/(W/SQ M)

COLLECTOR B, 4/28/83, NO MIXING NOON DRAW

TEST STARTING AT 7:00
TEST DURATION = 7 HOURS
INITIAL TEMP = 14.1 C
FINAL TEMP = 33.0 C

DRAW STARTING AT 1200 AND LASTING 2. MINUTES
DRAW MASS = 45.7 KG
DRAW TEMP = 32.9 C
MAIN TEMP = 13.0 C

HOUR ENDING	TANK TEMP. (C) CALCULATED ENDING	CALCULATED AVG	MEAS AVG	IRRADIANCE TOTAL (W/SQ M)	IRRADIANCE BEAM (W/SQ M)	AMB TEMP (C)	SKY TEMP (C)	WIND VEL (M/S)
800	14.94	14.55	14.45	304.0	565.0	14.8	6.5	0.6
900	17.18	16.10	16.06	527.0	663.0	18.0	11.6	1.2
1000	20.75	19.05	19.13	728.0	719.0	21.4	16.4	1.6
1100	24.26	23.71	23.57	878.0	756.0	23.7	19.2	1.6
1200	29.15	26.32	28.81	957.0	767.0	25.5	21.5	2.2
1300	28.10	26.15	25.87	943.0	729.0	26.9	22.8	2.6
1400	32.48	30.15	30.90	878.0	709.0	28.2	22.8	2.5

AVG DRAW TEMP: CALC = 26.2 MEAS = 32.9

INCIDENT ENERGY = 0.24729E+08 JOULES
STORED ENERGY = 0.84327E+07 JOULES
WITHDRAWN ENERGY = 0.38076E+07 JOULES
COLLECTION EFF. = 0.495
AVG FLOWRATE = 0.0 CU M/SEC
AVG ULC = 91.08936 W/(SQ M * C)
AVG (TCALC-TA)/I = -0.00048 C/(W/SQ M)

COLLECTOR B, 5/5/83, MIXING, NO DRAW

TEST STARTING AT 7:00
TEST DURATION = 10 HOURS
INITIAL TEMP = 19.2 C
FINAL TEMP = 47.4 C

HOUR ENDING	TANK TEMP. (C) CALCULATED ENDING	CALCULATED AVG	MEAS AVG	IRRADIANCE TOTAL (W/SQ M)	IRRADIANCE BEAM (W/SQ M)	AMB TEMP (C)	SKY TEMP (C)	WIND VEL (M/S)
800	19.88	19.60	19.60	278.0	395.0	11.3	-1.1	2.7
900	21.77	20.82	21.09	489.0	474.0	12.4	-1.1	4.4
1000	24.88	23.32	23.80	705.0	593.0	13.7	1.1	4.9
1100	29.03	26.94	27.73	887.0	706.0	14.4	10.0	5.3
1200	33.56	31.28	32.44	958.0	714.0	15.6	12.4	4.5
1300	38.07	35.81	37.17	961.0	731.0	17.0	13.2	4.4
1400	42.08	40.06	41.50	888.0	717.0	17.8	13.2	4.9
1500	45.17	43.62	44.81	745.0	694.0	18.0	12.6	5.2
1600	47.02	46.06	46.79	549.0	653.0	17.9	10.8	4.6
1700	47.37	47.19	47.39	321.0	555.0	17.2	9.2	4.3

INCIDENT ENERGY = 0.32155E+08 JOULES
STORED ENERGY = 0.12533E+08 JOULES
WITHDRAWN ENERGY = 0.0 JOULES
COLLECTION EFF. = 0.390
AVG FLOWRATE = 0.90584E-05 CU M/SEC
AVG ULC = -1.61722 W/(SQ M * C)
AVG (TCALC-TA)/I = 0.02648 C/(W/SQ M)

COLLECTOR B, 5/6/83, MIXING, NO DRAW

TEST STARTING AT 7:00
TEST DURATION = 10 HOURS
INITIAL TEMP = 21.4 C
FINAL TEMP = 52.3 C

HOUR ENDING	TANK TEMP. (C) CALCULATED ENDING	CALCULATED AVG	MEAS AVG	IRRADIANCE TOTAL (W/SQ M)	IRRADIANCE BEAM (W/SQ M)	AMB TEMP (C)	SKY TEMP (C)	WIND VEL (M/S)
800	21.95	21.67	21.84	311.0	609.0	8.7	-1.6	0.5
900	23.98	22.96	23.48	536.0	712.0	12.1	3.3	0.6
1000	27.30	25.63	26.56	729.0	757.0	15.3	8.6	0.6
1100	31.52	29.39	30.87	878.0	786.0	17.3	12.6	0.7
1200	36.13	33.81	35.83	951.0	786.0	19.6	13.9	0.7
1300	40.72	38.41	40.88	956.0	785.0	21.2	17.7	1.2
1400	44.81	42.75	45.48	881.0	772.0	22.9	17.7	1.0
1500	47.95	46.37	49.09	736.0	743.0	24.0	18.3	0.9
1600	49.82	48.89	51.30	539.0	688.0	24.3	17.7	0.8
1700	50.18	50.00	52.19	312.0	585.0	23.8	16.4	1.1

INCIDENT ENERGY = 0.32383E+08 JOULES
STORED ENERGY = 0.13714E+08 JOULES
WITHDRAWN ENERGY = 0.0 JOULES
COLLECTION EFF. = 0.424
AVG FLOWRATE = 0.16314E-04 CU M/SEC
AVG ULC = -1.97213 W/(SQ M * C)
AVG (TCALC-TA)/I = 0.02500 C/(W/SQ M)

INVESTIGATION OF STANDARD TEST PROCEDURES FOR INTEGRAL STORAGE SOLAR DOMESTIC HOT WATER SYSTEMS

by

Russell Charles Lindsay

(ABSTRACT)

All-day experimental tests were performed to determine the thermal performance of two commercial integral storage collectors for solar domestic hot water systems. These tests were performed under a variety of ambient conditions and irradiance levels, both with and without forced circulation and noontime hot water draws. An analytical model was developed to predict the thermal performance of one of the two systems tested and predicted performance was compared with experimental results. Experimental and analytical results indicate that thermal stratification has a mininal effect on the daily collection efficiency of integral storage collector, so that a standard test similar to ASHRAE Standard 93-77 might reasonably be used to obtain the performance characteristics of the collection element of these systems. The results of an ASHRAE 93-77 type test might then be used to obtain performance ratings under ASHRAE Standard 95 procedures using an in-line heat source. The results of the present investigation may be used to validate such an ASHRAE 95 test method.